



Elisa Zanuso Jiménez

**Strategies for enhanced enzymatic  
hydrolysis of lignocellulosic biomass**

**Universidade do Minho**  
Escola de Engenharia







**Universidade do Minho**

Escola de Engenharia

Elisa Zanuso Jiménez

**Strategies for enhanced enzymatic  
hydrolysis of lignocellulosic biomass**

Thesis submitted in fulfilment of the requirements for the  
degree of Ph.D. in Chemical and Biological Engineering

Work developed under supervision of:

**Prof. Doctor José António Couto Teixeira**

**Prof. Doctor Lucília Maria Alves Ribeiro Domingues**

**Prof. Doctor Héctor Arturo Ruíz Leza**

## **DIREITOS DE AUTOR E CONDIÇÕES DE UTILIZAÇÃO DO TRABALHO POR TERCEIROS**

Este é um trabalho académico que pode ser utilizado por terceiros desde que respeitadas as regras e boas práticas internacionalmente aceites, no que concerne aos direitos de autor e direitos conexos.

Assim, o presente trabalho pode ser utilizado nos termos previstos na licença abaixo indicada.

Caso o utilizador necessite de permissão para poder fazer um uso do trabalho em condições não previstas no licenciamento indicado, deverá contactar o autor, através do RepositóriUM da Universidade do Minho.

### **Licença concedida aos utilizadores deste trabalho**



**Atribuição-NãoComercial-SemDerivações**  
**CC BY-NC-ND**

<https://creativecommons.org/licenses/by-nc-nd/4.0/>

## **ACKNOWLEDGMENTS**

I wish to record my sense of gratitude and acknowledge the support of every single person I met and were involved during this path. Thanks for making the conclusion of my doctoral thesis possible.

To begin, I would like to express my profound thanks to my supervisors: Prof. José A. Teixeira for your trust, for the opportunity to develop my work under your supervision, and for always being opened to share your enormous knowledge. To Prof. Lucília Domingues for your excellent scientific guidance and for giving me support during rough times. And to Prof. Héctor A. Ruiz for your valuable support since I had the idea of starting a PhD, your scientific advice was much appreciated.

To my LF colleagues, thank you for making me feel welcomed since the day I arrived and for your collaboration and assistance along my time in there. My LBM colleagues thank you for your help and availability. Thank you all B.Factory and CEB colleagues for many enjoyable moments we shared.

I am so grateful for my colleagues who became my dear friends. Thank you for being an important part of my journey, for your advice, and for being there to hear me, support me, and make unforgettable memories. Obrigada!

A very special thanks to my friends around the world: Sara, Ale, Andrea, and Silvia. Although the distance and the time zone difference you were always there as my back up and relief.

Mi mas profundo agradecimiento es para mi familia. Mi papá Stefano, mi mamá Dora Elia, mi hermano Emanuele, ustedes son mi pilar, mi guia y mi norte. Gracias por su confianza ciega, apoyo, y su amor infinito. Alexandre, merci for being my determination and motivation, home is wherever we are together, you are my silver lining. Mis abuelos en el cielo y mis abuelas en la Tierra, questo è per voi.

I would like to acknowledge the Mexican Science and Technology Council - Energy Sustainability Fund of Secretary of Energy Mexico (CONACY-SENER) (CONACYT ID 639021/495314) for the PhD fellowship granted, as well as the University of Minho, School of Engineering, and the Centre of Biological Engineering.

## **STATEMENT OF INTEGRITY**

I hereby declare having conducted this academic work with integrity. I confirm that I have not used plagiarism or any form of undue use of information or falsification of results along the process leading to its elaboration.

I further declare that I have fully acknowledged the Code of Ethical Conduct of the University of Minho.

## RESUMO

### Estratégias para a melhoria da hidrólise enzimática de biomassa lignocelulósica

A mitigação das alterações climáticas, a produção sustentável de combustíveis e materiais, e o alarmante aquecimento global estão a impulsionar investigadores, indústrias e governos a dirigirem-se para uma transição obrigatória de combustíveis fósseis para biomassa renovável. Neste contexto, as biorefinerías desempenham um papel importante na bioconversão de biomassa renovável, tal como materiais lignocelulósicos, através de uma série de processos (plataformas bioquímicas e termoquímicas) que resultam em combustíveis e produtos químicos. A plataforma de açúcares na biorefinería, onde são utilizadas enzimas ou produtos químicos, é uma escolha viável para obter unidades elementares (*building blocks*) de açúcares para futuros processos de fermentação.

A imobilização de enzimas e o desenho de reatores são domínios críticos que melhoram a utilização de enzimas utilizadas na hidrólise de biomassa lignocelulósica. Neste âmbito, um *cocktail* de celulasas foram imobilizadas em nanopartículas magnéticas revestidas de quitosano. O sistema desenvolvido foi capaz de ser reutilizado até 13 ciclos, utilizando carboximetilcelulose como substrato representando um incremento de 8.2 vezes de glucose obtida por massa de enzima utilizada. O desafio e a importância de testar celulase imobilizada em a biomassa lignocelulosica levou à utilização do caroço de milho como biomassa modelo para avaliar a eficiência do sistema proposto. O caroço de milho pré-tratado hidrotermicamente – fração rica em conteúdo de celulose – foi utilizado como substrato [carga de sólidos de 5% (p/v)] para avaliar o potencial de hidrólise da celulase imobilizada, obtendo-se 22 g/L de glucose que corresponde a um rendimento de conversão de 65%. Além disso, o projeto do reator deve ultrapassar as principais restrições do processo de hidrólise enzimática com carga de sólidos elevada que engloba a deficiente transferência de massa e calor, condições reológicas desafiantes e a inibição enzimática. Assim, uma segunda estratégia abordada neste trabalho foi a utilização do reator de fluxo oscilatório, conhecido pela sua capacidade de mistura. A avaliação atingiu uma carga máxima de caroço de milho pré-tratado hidrotermicamente de 18% (p/v) e, nestas condições desafiantes de cargas sólidas elevadas, resultou numa concentração de glucose de 100 g/L, representando um rendimento de sacarificação de 81% em 20 h. Posteriormente, foram estudadas estratégias de *fed-batch* atingindo cargas sólidas de 25% (p/v) e rendimento de sacarificação de 97%.

O desenvolvimento de um sistema de imobilização de enzima eficiente e o uso inovador do reator de fluxo oscilatório são os dois resultados principais desta tese que se destinava a contribuir nos desafios que tornam a hidrólise enzimática de materiais lignocelulósicos um passo crítico na transição a uma bioeconomia.

**Palavras-chave:** biomassa lignocelulósica, biorefinería, imobilização de celulase, reator de fluxo oscilatório

## **ABSTRACT**

### **Strategies for enhanced enzymatic hydrolysis of lignocellulosic biomass**

Climate change mitigation, sustainable fuels and materials production, and alarming global warming are driving forces for researchers, industries, and governments to head into a mandatory fossil fuel transition to renewable biomass. Here, biorefineries play an important role to biotransform renewable biomass, such as lignocellulosic materials, through a series of processes (biochemical and thermochemical platforms) into biofuels and chemicals. The sugar platform in biorefinery, where enzymes or chemicals are used, is a feasible choice to obtain building block sugars for further fermentation processes.

Enzyme immobilization and bioreactor design are critical domains which improve the use of enzymes used for hydrolysis of lignocellulosic biomass. Under this scope, a cellulase cocktail was immobilized into chitosan-coated magnetic nanoparticles. The developed system could be reused up to 13 cycles, using carboxymethyl cellulose as substrate representing an 8.2-fold increase in glucose produced per mass of enzyme compared. The challenge and importance of testing immobilized cellulase against lignocellulosic biomass led to the use of corn cob as model biomass for evaluating the efficiency of the system proposed. The hydrothermally pretreated corn cob - solid rich in cellulose content - was employed as substrate [5% (w/v) solid loading] to evaluate the hydrolysis potential of the immobilized cellulase, being obtained 22 g/L of glucose which corresponds to 65% conversion yield. Further, bioreactor design should overcome the major restraints of the enzymatic hydrolysis process at high solid loadings which in general encompass poor mass and heat transfer, challenging rheological conditions, and enzyme inhibition. Thus, a second strategy tackled the novel use of oscillatory flow reactor, known for its improved mixing. A maximum batch loading of hydrothermally pretreated corn cob of 18% (w/v) was assessed and, under these challenging conditions, a glucose concentration of 100 g/L was achieved representing a saccharification yield of 81% in 20 h. Then, fed-batch strategies were studied being possible with solid loadings as high as of 25% (w/v) to obtain a saccharification yield of 97%.

The development of an efficient enzyme 's immobilization system and the use of an innovative oscillatory flow reactor are the two main outcomes of this thesis that aimed at contributing to some of the challenges of enzymatic hydrolysis of lignocellulosic materials that hinder the transition to a biobased economy.

**Keywords:** cellulase immobilization, biorefinery, lignocellulosic biomass, oscillatory flow reactor



## TABLE OF CONTENTS

ACKNOWLEDGMENTS .....	iii
STATEMENT OF INTEGRITY .....	iv
RESUMO .....	v
ABSTRACT.....	vi
LIST OF FIGURES .....	x
LIST OF TABLES .....	xii
LIST OF ABBREVIATIONS AND ACRONYMS .....	xiii
SCIENTIFIC OUTPUT .....	xv
<b>CHAPTER I</b> .....	1
1.1 MOTIVATION .....	2
1.2 THESIS OUTLINE.....	3
1.3 REFERENCES.....	4
<b>CHAPTER II</b> .....	5
2.1 RENEWABLE RESOURCES FOR A BIOBASED ECONOMY TRANSITION.....	6
2.1.1 Biorefinery based on lignocellulosic biomass.....	7
2.2 PROCESS BIOCONVERSION AND LIGNOCELLULOSIC ENZYMES.....	11
2.2.1 Enzymatic hydrolysis at high solid loadings .....	12
2.2.2 Key enzymes in lignocellulosic biorefineries .....	12
2.2.2.1 Characteristics of the cellulases enzymes .....	12
2.2.2.2 Characteristics of the hemicellulases enzymes.....	14
2.2.2.3 Characteristics of the ligninases enzymes .....	14
2.2.2.4 Auxiliary enzymes.....	14
2.3 ENZYME IMMOBILIZATION .....	15
2.3.1 Immobilization techniques .....	17
2.3.2 Enzyme support classification and novel supports .....	18
2.4 LIGNOCELLULOSIC ENZYMES IMMOBILIZATION: ADVANTAGES AND LIMITATIONS .....	19
2.4.1 Reducing inhibition.....	19
2.4.2 Enhancing enzyme temperature and pH stability.....	20
2.4.3 Immobilized enzymes reusability and operation under continuous regime.....	21
2.4.4 Mass transfer limitations .....	25
2.5 BIOREACTORS TECHNOLOGY FOR ENZYMATIC HYDROLYSIS .....	26
2.5.1 Bioreactors for immobilized enzyme complex.....	26
2.5.1.1 Magnetic-based bioreactors .....	28
2.5.1.2 Non-magnetic based bioreactors.....	29

2.5.2 Oscillatory flow bioreactors .....	31
2.6 REFERENCES .....	32
<b>CHAPTER III</b> .....	45
ABSTRACT.....	46
3.1 INTRODUCTION .....	47
3.2 EXPERIMENTAL METHODS.....	49
3.2.1 Chitosan coating and glutaraldehyde activation .....	49
3.2.2 Cellulase cocktail immobilization.....	49
3.2.3 Physico-chemical characterization of MNP .....	50
3.2.3.1 FTIR-ATR characterization.....	50
3.2.3.2 Microscopic morphology.....	50
3.2.4 Biological characterization of the immobilized cellulase cocktail.....	50
3.2.4.1 Binding efficiency .....	50
3.2.4.2 Enzyme activity determination and acetic acid tolerance .....	50
3.2.5 Storage stability and reusability of immobilized cellulase cocktail .....	51
3.2.6 Hydrothermal pretreatment of corn cob .....	51
3.2.7 Enzymatic saccharification of hydrothermally pretreated corn cob .....	52
3.2.8 Statistical analyses .....	53
3.3 RESULTS AND DISCUSSION .....	53
3.3.1 Cellulase cocktail immobilization.....	53
3.3.2 FITR-ATR characterization .....	54
3.3.3 Microscopic morphology .....	55
3.3.4 Binding efficiency, enzyme activity, and acetic acid tolerance .....	56
3.3.5 Storage stability.....	58
3.3.6 Reusability of immobilized cellulase .....	59
3.3.7 Enzymatic saccharification of pretreated corn cob using immobilization as strategy .....	61
3.4 CONCLUSIONS .....	64
3.5 REFERENCES .....	65
<b>CHAPTER IV</b> .....	71
ABSTRACT.....	72
4.1 INTRODUCTION .....	73
4.2 EXPERIMENTAL METHODS.....	76
4.2.1 Hydrothermal pretreatment of corn cob .....	76
4.2.2 Oscillatory flow reactor bioreactor configuration for enzymatic hydrolysis .....	76
4.2.3 Analytical methods .....	77

4.2.4 Enzymatic hydrolysis .....	78
4.2.5 Preliminary experiments in OFR.....	78
4.2.6 Experimental design .....	79
4.2.7 Fed-batch strategy for enzymatic hydrolysis.....	79
4.3 RESULTS AND DISCUSSION .....	79
4.3.1 Chemical composition of untreated and hydrothermally pretreated corn cob.....	79
4.3.2 Preliminary experiments .....	80
4.3.3 OFR configuration for enzymatic hydrolysis .....	81
4.3.4 Enzymatic hydrolysis at low enzyme load in OFR.....	83
4.3.5 Fed-batch strategy in OFR.....	85
4.4 CONCLUSIONS .....	87
4.5 REFERENCES .....	88
<b>CHAPTER V</b> .....	93
5.1 CONCLUSIONS .....	94
5.2 FUTURE PERSPECTIVES.....	95
5.3 REFERENCES.....	96

## LIST OF FIGURES

### CHAPTER 2

Figure 2.1. Biofuel energy production. Total biofuel production is measured in terawatt-hour (TWh) per year. Biofuel production includes both bioethanol and biodiesel. (Open Access, Our World in Data, Ritchie et al., 2020)..... 6

Figure 2.2. Environmental issues related to fossil fuel reliance and the biorefinery process as part of bioeconomy..... 8

Figure 2.3. Representation of lignocellulosic biomass biotransformation and products..... 9

Figure 2.4. Pretreatment technologies classification and examples. .... 10

Figure 2.5. Simplified scheme of cellulases synergic action to degrade cellulose. (R: Reducing ends, NR: non-reducing ends) ..... 13

Figure 2.6. Enzyme immobilization techniques with their advantages and limitations..... 17

Figure 2.7. Different reactor configuration for enzymatic hydrolysis. .... 27

Figure 2.8. Summary of oscillatory flow reactor key features ..... 31

### CHAPTER 3

Figure 3.1. Schematic representation of the methodology followed in this chapter, characterization techniques used and the enzymatic hydrolysis. .... 49

Figure 3.2. Schematic representation of cellulase immobilization using chitosan as coating agent and  $\text{Fe}_3\text{O}_4$  as magnetic support. .... 54

Figure 3.3. FTIR-ATR spectra a) free enzyme, b) chitosan, c) enzyme loaded on chitosan coated  $\text{Fe}_3\text{O}_4$ , d)  $\text{Fe}_3\text{O}_4$  chitosan coated, e)  $\text{Fe}_3\text{O}_4$ ..... 55

Figure 3.4. Spectroscopy images a) bare  $\text{Fe}_3\text{O}_4$ , b)  $\text{Fe}_3\text{O}_4$  coated with chitosan, c, d) enzyme loaded on chitosan coated  $\text{Fe}_3\text{O}_4$ ; TEM (a, b, c) SEM (d)..... 56

Figure 3.5. Chitosan coated magnetic nanoparticle saturation assay. Enzyme was added in 10, 50 and 100  $\text{mg}_{\text{enzyme}}$  and the enzyme loading, and binding efficiency were calculated. Enzyme loading is represented by bars, and the binding efficiency is represented by the continuous line. .... 57

Figure 3.6. Glucose production using MNP at different enzyme loadings. The hydrolysis was performed at  $50^\circ\text{C}$ , during 1 h using CMC 1% (w/v) as substrate in 0.1 M citrate buffer at pH 4.8..... 58

Figure 3.7. Reusability of cellulase immobilized on chitosan coated $Fe_3O_4$ nanoparticles. The yield represents the mg of glucose produced per g of substrate (CMC) and the bars represent the number of cycles performed.....	60
Figure 3.8. Enzymatic hydrolysis kinetic. Glucose production (a) and saccharification yield (b) of pretreated corn cob at a solid loading of 5% (w/v). ■ free enzyme, ● immobilized enzyme.....	62
Figure 3.9. Reusability of immobilized cellulase using hydrothermally pretreated corn con at 1% (w/v) after 48 h.....	64
<b>CHAPTER 4</b>	
Figure 4.1 Schematic representation of vortices created inside OFR. Rings and arrows were added for visualization of the angles phase. Gray) beginning of the cycle; blue) before flow reversing; black) after flow reversing. (Adapted and modified from [Reis et al., 2005]). .....	75
Figure 4.2. Schematic representation of the OFR used in this work. 1) oscillatory device and chamber; 2) heating fluid inlet; 3) heating fluid outlet, 4) sampling port, 5) baffles with smooth periodic constrictions, 6) solids inlet.....	77
Figure 4.3. Preliminary enzymatic hydrolysis assay using 5% (w/v) hydrothermally pretreated corn cob during 24 h, at 50°C at different oscillatory conditions of amplitude and frequency.....	80
Figure 4.4 Glucose production comparison in OFR using wet and dry substrate at 18% (w/v) and 20 FPU/mL. Wet solids (dotted line) dry solids (continuous line).....	81
Figure 4.5. Main effect plot for glucose (g/L) showing the positive impact of frequency and amplitude on the process. ....	85
Figure 4.6. Fed-batch kinetic in OFR (blue, continued line) and flask (gray, dotted line) using 25% (w/v) hydrothermally pretreated corn cob.....	87
Figure 4.7. Glucose production (a) and conversion (b) of HSEH kinetics in OFR by fed batch strategy. FB1 (■ blue), FB2(● gray), FB3 (▲ green).....	87

## **LIST OF TABLES**

### **CHAPTER 2**

Table 2. 1 Immobilized enzymes to obtain added value products and their applications .....	16
Table 2.2 Immobilized enzyme reusability examples applied in the hydrolysis of lignocellulosic biomass and carboxymethyl cellulose (CMC).....	23

### **CHAPTER 3**

Table 3.1 Overview of reported activity and yield of cellulase immobilized on different supports	60
Table 3.2 Saccharification rate of pretreated corn cob hydrolysis with 5% (w/v) loading using free and immobilized cellulase cocktail .....	63

### **CHAPTER 4**

Table 4.1 HSEH fed-batch mode conditions.....	79
Table 4.2 Different bioreactor configuration for HSEH.....	83
Table 4.3 OFR frequency and amplitude experimental conditions and corresponding, glucose production, and saccharification yield for 18% solid loading (w/v).....	84

## LIST OF ABBREVIATIONS AND ACRONYMS

2G	Second generation
3D	Three-Dimensional
ANOVA	Analysis of Variance
CDH	Cellobiose Dehydrogenase
CLEAs	Cross-Linking Enzyme Aggregates
CMC	Carboxymethyl Cellulose
COVID-19	Coronavirus Disease of 2019
$d$	Diameter
$d_o$	Baffle internal diameter
$\rho$	Density
DES	Deep Eutectic Solvents
DNS	3,5-dinitrosalicylic acid
DP	Degree of Polymerization
DW	Dry Weight
EC	Enzyme Commission number
$f$	Frequency
FB	Fed-batch strategy
Fe <sub>3</sub> O <sub>4</sub>	Iron(II,III) Oxide
FPU	Filter Paper Units
FTIR-ATR	Fourier Transform Infrared Spectroscopy - Attenuated Total Reflection
GA	Glutaraldehyde
GHG	Green House Gases
GWI	Global Warming Impact
HPLC	High-Performance Liquid Chromatography
HRR	Horizontally Rotated Bioreactor
HSEH	High Solids Enzymatic Hydrolysis
IL	Ionic Liquids
IR	Refractive Index
$L$	Baffle spacing
LCM	Lignocellulosic materials
LPMO	Lytic Polysaccharide Monoxygenases

$\mu$	Viscosity
MBR	Membrane Bioreactors
MNP	Magnetic Nanoparticles
N/D	Not Defined
NREL	National Renewable Energy Laboratory
OBR	Oscillatory Baffled Reactor
OFR	Oscillatory Flow Reactor
$R_o$	Severity Factor
$Re_o$	Oscillatory Reynolds Number
SEM	Scanning Electron Microscopy
$St$	Strouhal Number
STBR	Stirred Tank Bioreactor
STR	Stirred Tank Reactor
TEM	Transmission Electron Microscopy
UI	International Units
v/v	Volume per Volume
VSTR	Vertical Stirred Tank Bioreactor
w/v	Weight per Volume
$x_o$	Amplitude
XOS	Xylooligosaccharides



## SCIENTIFIC OUTPUT

According to the 2<sup>nd</sup> paragraph of the article 8 of the Portuguese Decree-Law no. 388/70, the scientific outputs of this thesis are listed below.

The results presented in this thesis have been partially published elsewhere.

### Peer reviewed journal articles:

Zanuso, E., Ruiz, H.A., Domingues, L., Teixeira, J.A. 2022. Oscillatory flow bioreactor operating at high solids loading for enzymatic hydrolysis of lignocellulosic biomass. *Submitted for publication*

Zanuso, E., Ruiz, H.A., Domingues, L., Teixeira, J.A. 2022. Magnetic nanoparticles as support for cellulase immobilization strategy for enzymatic hydrolysis using hydrothermally pretreated corn cob biomass. *BioEnergy Research*. <https://doi.org/10.1007/s12155-021-10384-z>

Zanuso, E., Gomes, D., Ruiz, H.A., Teixeira, J.A., Domingues, L. 2021. Enzyme immobilization as a strategy towards efficient and sustainable lignocellulosic biomass conversion into chemicals and biofuels: current status and perspectives. *Sustainable Energy & Fuels*. 5, 4233. doi:10.1039/d1se00747e

Gomes, D., Cunha, J., Zanuso, E., Teixeira, J., Domingues, L. 2021. Strategies towards reduction of cellulases consumption: debottlenecking the economics of lignocellulosics valorization process- *Polysaccharides*, 2, 287-310. <https://doi.org/10.3390/polysaccharides2020020>

# **CHAPTER I**

---

Motivation and outline

## 1.1 MOTIVATION

It can be said that 150 years ago, one expert was needed to solve a problem. But today, thanks to the high extent of information, problems got more sophisticated. So, in order to solve a problem, different experts' should work together. Problem-solving nowadays can be only achieved by inter-disciplinary synergy. Yet, in nature, synergy has always been the rule of progress. At molecular level, the same happens when multiple carbohydrate-active enzymes collectively work to degrade polymers.

In a world where, on one hand, greenhouse gasses emission should be dramatically reduced but, on the other hand, population is expected to reach 9.7 billion by 2050 (United Nations, 2022), the challenge is clear: the world needs more energy with less (ideally, zero) environmental impact. Some countries are developing strategies and implementing programs related to the use of renewable energies. Thus, bioeconomy is the established path to shifting resources from fossil to an economy based on renewable biological ones. Policy measures that some countries have adopted for a bioeconomy transition includes public research and development findings, infrastructure investments, tax initiatives, startup support, private capital, standards for biobased products, education support, international collaboration, among other countries specific policies (International Advisory Council on Global Bioeconomy, 2020).

To achieve this transition, the implementation of biorefineries as process facilities to sustainable convert biomass into a wide spectrum of bioenergy and biochemicals comes as a solution to detach from the traditional petroleum refinery. Biomass biorefining is the promising route, specifically from lignocellulosic resources. A key platform of the process is the sugar platform. In advanced biorefineries of lignocellulosic biomass, sugars (as glucose) are obtained after fractionation through the pretreatment followed by the enzymatic hydrolysis processes. The importance of the sugar supply relies on the capacity of being used as substrate to produce chemical building blocks, fuels, fine chemicals, food, and animal feed through fermentation pathways (de Jong, et al., 2020).

Enzymatic cellulose hydrolysis - saccharification - is a complex step on the biorefinery process. It is considered as a bottleneck in the economic valorization of lignocellulosic materials due to the high enzyme prices. To tackle the enzymatic saccharification obstacle, several strategies have been studied as enzyme reutilization, high solid loadings operations, consolidated processes, or the use of more efficient cellulolytic organisms. However, during the enzymatic hydrolysis process there are many interactions to consider, thus making the process more sophisticated.

Considering the sugar platform from lignocellulosic biomass through enhanced enzymatic hydrolysis processes is of great interest for industrialization and novel solutions are still on demand, the approach of this thesis focuses on strategies to develop and enhance the enzymatic saccharification process. Thus, the focus of this work was on two key process intensification technologies:

- 1) the use of magnetic nanoparticles as support for enzyme immobilization, the immobilization mechanism, and the application of the immobilized biocatalyst for lignocellulosic saccharification;
- 2) the assessment of a novel oscillatory flow reactor integrated with smooth constrictions to operate at high solid loadings and the fed-batch strategy to reach up to 25% (w/v) solid loading.

### **1.2 THESIS OUTLINE**

This thesis presents the main results obtained from the research activity undertaken mainly at CEB – Centre of Biological Engineering, University of Minho, Braga, Portugal under the supervision of Professor José A. Teixeira, Professor Lucília Domingues from University of Minho, and Professor Héctor A. Ruiz from Autonomous University of Coahuila.

Based on the aim of this project, this thesis is organized as follows:

In Chapter I is presented the motivation and outline of this work.

Chapter II presents an introduction of the current biorefinery perspectives. Following by a revision of immobilization techniques and with emphasis on cellulase immobilization in nano size supports. Also, the perspective of bioreactors for enzymatic hydrolysis is presented, focusing on the use of oscillatory flow reactors.

The cellulase cocktail immobilization onto magnetic nanoparticles is addressed in Chapter III, detailing the immobilization mechanism, challenges of the process and their application for hydrolyzing lignocellulosic biomass.

In Chapter IV, the transversal utilization of oscillatory flow bioreactor for enzymatic hydrolysis of lignocellulosic biomass operating at high solids loading and using fed-batch strategy is reported.

Finally, Chapter V provides the conclusions of this thesis and perspectives of relevant topics derived from this work that would be interesting to address in the future.

### **1.3 REFERENCES**

- de Jong, E., Stichnothe, H., Bell, G., Jørgensen, H, 2020. IEA Bioenergy Task 42 - Bio-based chemicals: A 2020 update. IEA Bioenergy, Paris, France, ISBN 978-1-910154-69-4.
- International Advisory Council on Global Bioeconomy, 2020. Global bioeconomy policy report (IV): A decade of bioeconomy policy development around the world. Available at [https://gbs2020.net/wp-content/uploads/2020/11/GBS-2020\\_Global-Bioeconomy-Policy-Report\\_IV\\_web.pdf](https://gbs2020.net/wp-content/uploads/2020/11/GBS-2020_Global-Bioeconomy-Policy-Report_IV_web.pdf).
- United Nations, Department of Economic and Social Affairs, Population Division, 2022. World population prospects 2022: Summary of results. UN DESA/POP/2022/TR/NO.3.

## CHAPTER II

---

### General introduction

**This chapter is partially based on the following review papers:**

Zanuso, E., Gomes, D., Ruiz, H.A., Teixeira, J.A., Domingues, L. 2021. Enzyme immobilization as a strategy towards efficient and sustainable lignocellulosic biomass conversion into chemicals and biofuels: current status and perspectives. *Sustainable Energy & Fuels*. 5, 4233. doi:10.1039/d1se00747e

Gomes, D., Cunha, J., Zanuso, E., Teixeira, J., Domingues, L. 2021. Strategies towards reduction of cellulases consumption: debottlenecking the economics of lignocellulosics valorization process-*Polysaccharides*, 2, 287-310. <https://doi.org/10.3390/polysaccharides2020020>

## 2.1 RENEWABLE RESOURCES FOR A BIOBASED ECONOMY TRANSITION

The urgent need to reduce GHG (Greenhouse Gases) emissions is a trend the world is following. Urbanization, industrialization, and trade openness are identified as factors that impact the environment by increasing the energy consumption and the CO<sub>2</sub> emissions (Hussain et al., 2020). Additionally, the environmental concerns on energy security, the promotion of sustainable technologies application and governmental regulations aim to a bio-based economic model to produce alternative products for a fossil fuel dependency detachment. For example, the European Union climate energy target for 2050 is to reach 80-95% GHG reduction versus 1990 by applying 55-75% shares of renewable energy (IHS Markit, 2018). Figure 2.1 shows the biofuel growth where an increase since 2005 is noticeable due to policies development in emerging economies. The slight decrease in 2020 is mainly resulting from the COVID-19 pandemic lower fuel demand, however it is expected to recover in 2022 as the fuel demand will restore (OECD/FAO, 2021).

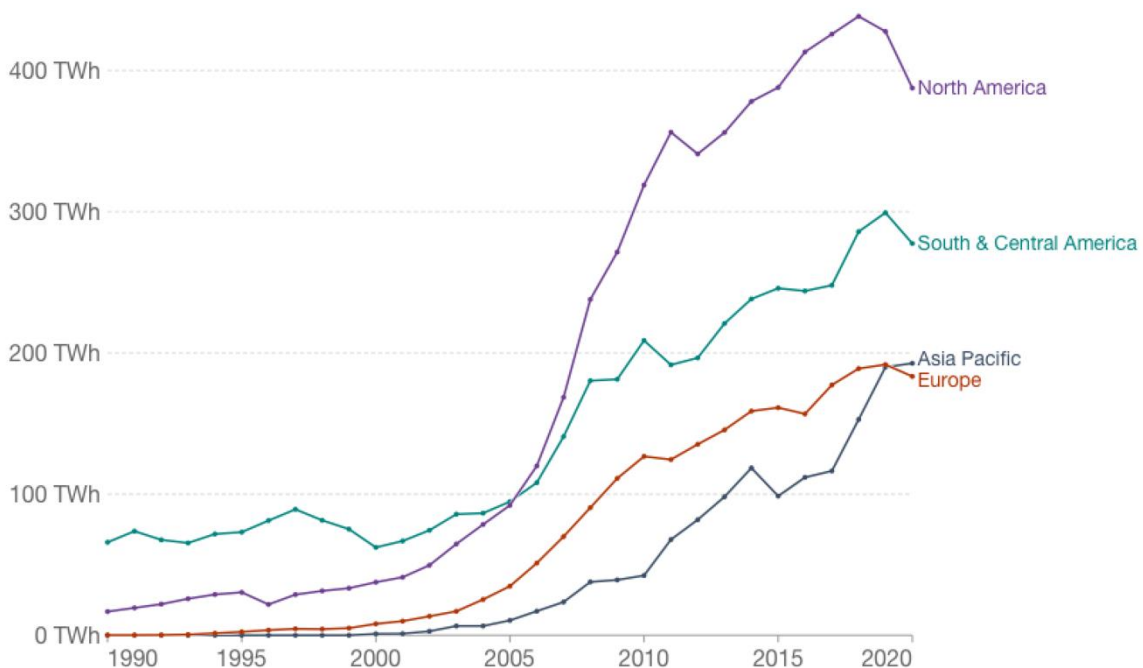


**Figure 2.1.** Biofuel energy production. Total biofuel production is measured in terawatt-hour (TWh) per year. Biofuel production includes both bioethanol and biodiesel. (Open Access, Our World in Data, Ritchie et al., 2020).

The current world ethanol production is led by United States of America with a total of 190 operating ethanol biorefineries. These facilities manufacture 54% of the global ethanol output, where 94% of the production comes from corn starch (Renewable Fuels Association, 2020). The second largest ethanol producer is Brazil, manufacturing 30% of the world's ethanol output mainly from sugarcane (Karp et al., 2021). Concerning biorefineries in Europe, 803 facilities were identified in 2018. Interestingly, 177 of

those facilities are integrated biorefineries that combine the production of energy and bio-based products. Also, it is worth mentioning that the most used feedstock in the European Union comes from agricultural residues (Parisi, 2018). However, the path to phase out fossil fuels is still on its early stages. In most countries transport energy comes 95% from fossil fuel where only 4% - 6% or less comes from renewable shares (Pelkmans, 2021). These percentages show how in global terms the use of liquid biofuels is in early stages and major steps are needed to achieve the transition.

Bioeconomy refers to the use of renewable resources to produce food, energy, and chemicals, particularly from biomass feedstocks. Renewable resources used as feedstock in a bioprocess are carbon source biomasses as algal biomass, food wastes, industrial wastes, lignocellulosic biomass, etc. (Aparicio et al., 2021; Cristóbal et al., 2018; Gomes et al., 2016; Pinheiro et al., 2019). Towards a successful bioeconomy transition, biotechnological processes have been studied and developed, involving the use of biocatalysts to produce, modify or improve any product. The biotechnology potential to specifically produce bio-based fuels, chemicals, and fine chemicals, largely contributes to the definition of the biorefinery concept, consisting of the overall conversion of the different lignocellulosic fractions (cellulose, hemicellulose, and lignin) into high-added value products (pharmaceutical, bioactive compounds), biofuels (solid, liquid and gaseous), and chemicals (polymers, adhesives).

### **2.1.1 Biorefinery based on lignocellulosic biomass**

Lignocellulosic materials (LCM) are the most abundant renewable resources with an annual worldwide production estimated in 170 million metric tons, yet only 5% is used due to their recalcitrance (Zhang et al., 2019). Common LCM includes softwoods and hardwoods, such as eucalyptus, pine, and paulownia, as well as agricultural residues, namely sugarcane bagasse, wheat straw, oat straw, agave bagasse, corn residues (cob and stover), rice straw, vine pruning residues, and coconut residues (Aguilar et al., 2018a; Baptista et al., 2020; Gomes et al., 2021; Gonçalves et al., 2014; Jesus et al., 2022, 2017; Pontes et al., 2018). Overall, LCM are mainly composed by cellulose (30 – 50%), hemicellulose (20 – 30%) and lignin (10 – 30%) on dry basis, among other minimum components depending on the feedstock. The exact composition is biomass specific and depends on its origin, growth, and harvest conditions, or even on the previous processes undertaken in the case of residues. Biorefineries based on LCM are typically classified according to the process used to transform and convert the biomass in two main platforms: the thermochemical and the biochemical platform (Figure 2.2). The thermochemical platform



relies on processes such as pyrolysis, combustion, thermal liquefaction, and gasification. This platform is mostly used to obtain syngas, bio-oil, and biochar (Pang, 2019).

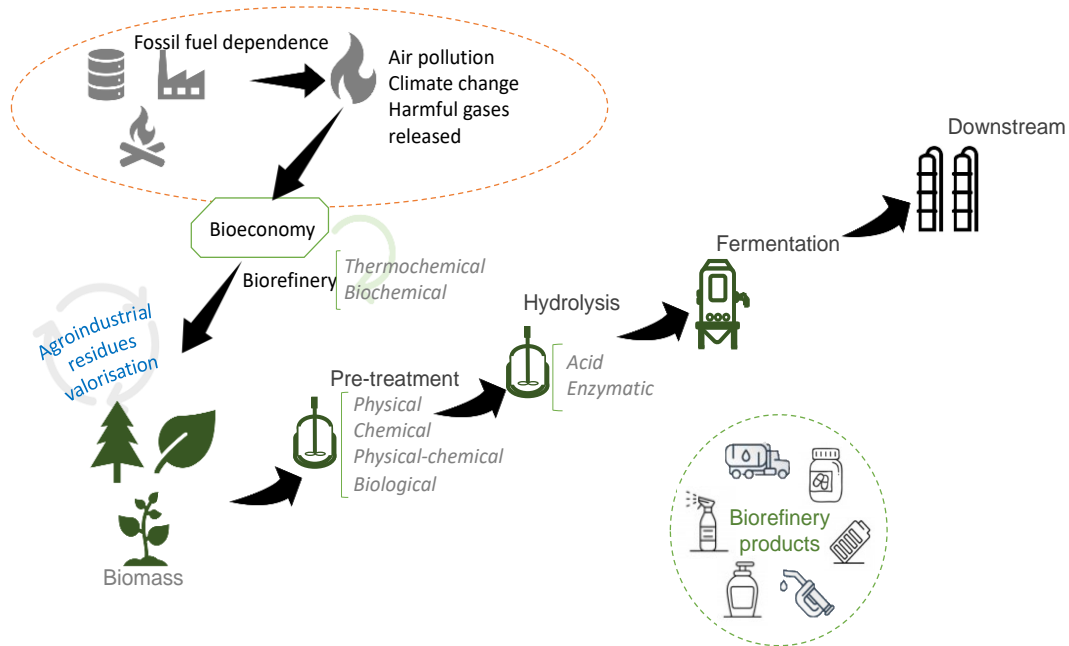


**Figure 2.2.** Environmental issues related to fossil fuel reliance and the biorefinery process as part of bioeconomy.

On the other hand, the biochemical platform uses biocatalysts and microorganisms to transform the biomass through processes such as enzymatic hydrolysis, fermentation, and digestion, thus taking place at milder conditions compared to the thermochemical platform (Aguirre-Fierro et al., 2019; Kumar et al., 2019; Ruiz et al., 2020). The wide variety of products, as shown in Figure 2.3, that can be obtained under the biochemical platform include biofuels, biopolymers, platform chemicals, pharmaceuticals, among others (Pino et al., 2020).

Biofuel's production has been the major promoter on the development and consolidation of biorefineries. Ethanol is the most important engine biofuel in the transportation sector obtained from renewable biomasses, but it can also have several other applications, namely in healthcare, fuel cells and manufacturing (Liu et al., 2019; Zheng et al., 2020). Concerns on the use of edible crops for energy production led to a shift for the use of agro-industrial residues as raw material, noted as second generation biorefineries or cellulosic biorefineries with significant advances in the microbial conversion process in the latest years (Cunha et al., 2020; Hassan et al., 2019).

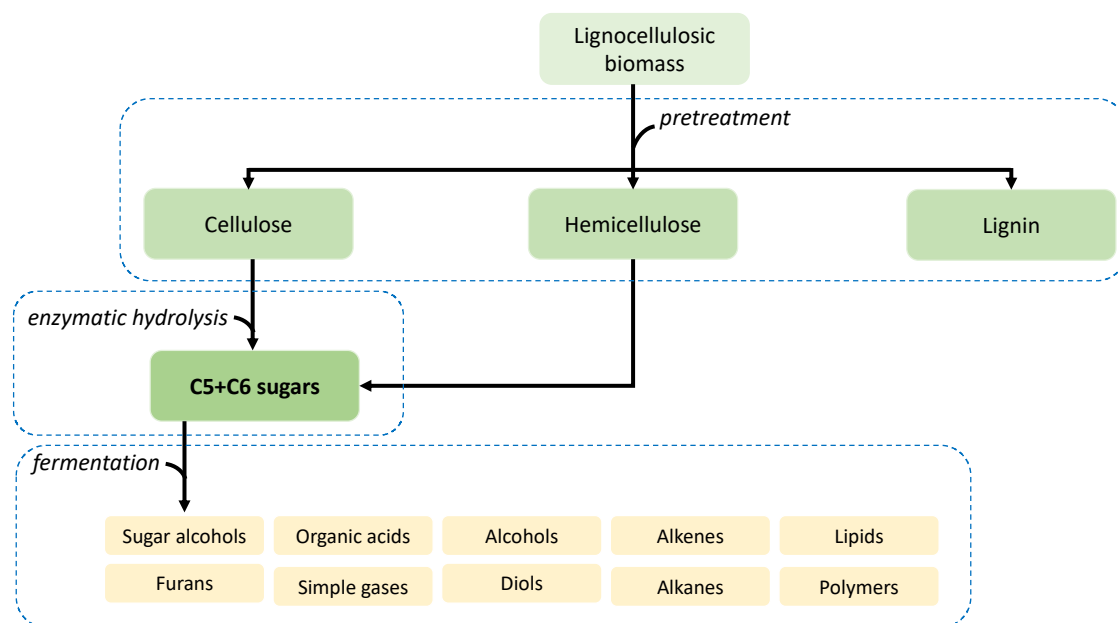


**Figure 2.3.** Representation of lignocellulosic biomass biotransformation and products.

Despite the use of LCM in second generation (2G) biorefineries being well documented, research on this area is still ongoing as there are barriers, both technical and economical, that remain as the impediment to a low-cost bioconversion process. The process for the conversion of LCM typically consists in: *i)* milling, *ii)* solid (biomass) pretreatment step, followed by *iii)* enzymatic hydrolysis to release fermentable sugars, then *iv)* fermentation and, *v)* product recovery (Zabed et al., 2017).

The three main components of LCM are cellulose, hemicellulose, and lignin. Cellulose is the most abundant biopolymer worldwide constituted by glucose monomers (D-glucose) linked by  $\beta$ -(1,4)-glycosidic bonds. Naturally, it is presented in both crystalline and amorphous form, and it has a higher degree of polymerization (DP) compared to hemicellulose, considered to reach up to 7000-15000 D-glucose units (Brunner, 2014). The second most abundant component of LCM is hemicellulose. Hemicellulose is formed by both five and six carbon monosaccharides, and due to its amorphous structure, it can easily dissolve in water at temperatures above 180 °C (Chen et al., 2017). The role of lignin in plants is to provide microbial protection and structural support. Lignin is composed by phenyl propane units connected through ether and carbon-carbon bonds and contain phenolic compounds that can be upgraded to value-added chemicals (Paone et al., 2019).

The recalcitrant structure of LCM is one of the obstacles for an effective biotransformation. Therefore, pretreatment is a decisive first step for fractionation, but also for a chemical and structural

alteration (Ruiz et al., 2020). The purpose of this step is to break down the LCM recalcitrance structure, where lignin and hemicellulose form a physical barrier and cellulose crystallinity is very compact in highly ordered regions, thus blocking the access of enzymes to cellulose. Also, a pretreatment challenge is to modify the structural composition of the LCM while the production of derived inhibitory compounds is minimized (Cunha et al., 2019). Pretreatments are typically divided on physical, chemical, physico-chemical, and biological. Figure 2.4 exemplifies the different types of pretreatments. Hydrothermal pretreatment is a technology that is gaining popularity due to the promising results that can be obtained and the fact that water is the only solvent used, thus it is considered a green technology. Hydrothermal pretreatment is the combination of physic conditions as elevated temperature and high pressions, and chemical conditions as water ionization, that modify the LCM structure by solubilizing the hemicellulose, removing lignin, decreasing cellulose crystallinity, and increasing cellulose pore size to facilitate the enzyme access (Zanuso et al., 2017).

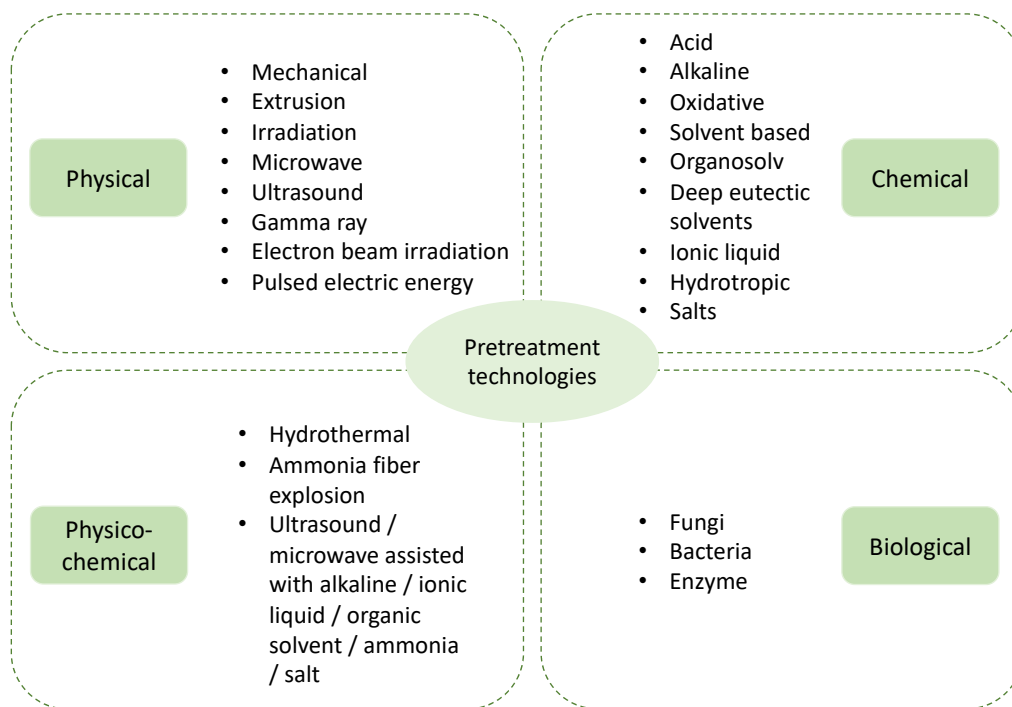


**Figure 2.4.** Pretreatment technologies classification and examples.

Water is used as the only solvent during the hydrothermal pretreatment, this helps reduce the environmental impact of the process. Also, compared with acid/alkaline pretreatments, it presents the advantage of less equipment corrosion. The role of temperature and pressure on the hydrothermal pretreatment is crucial as the water properties change due to the sub and super critical operation (Ruiz

et al., 2021). The temperature operation range is between 150 and 230 °C and a pressure range of 4.8 – 28 bar (approx.). These conditions promote the water to dissociate into H<sup>+</sup> and OH<sup>-</sup> which acidifies the medium. The acidic conditions benefit the carbohydrates degradation (Ruiz et al., 2020; Sarker et al., 2021). Consequently, carbohydrates are extracted (from hemicellulosic phase) and fractionated, and two phases are obtained, where hemicellulose is solubilized and depolymerized into the liquid phase and a solid-rich in cellulose and lignin can be collected and used as substrate for further bioconversion.

## **2.2 PROCESS BIOCONVERSION AND LIGNOCELLULOSIC ENZYMES**

Established on the fact that hydrolysis is a crucial step on the biorefinery process, its importance to produce monomers and oligomers from the polysaccharides obtained during the pretreatment is a topic widely studied. The cellulose hydrolysis can be accomplished via either enzymatic or acid hydrolysis. However, the ability of acids to degrade sugars has some drawbacks compared with an enzymatic hydrolysis. For example, during an acid hydrolysis, furan by-products are formed from the degradation of glucose which are considered as inhibitors for the fermentation (Billès et al., 2017; Cunha et al., 2019). Besides, acid hydrolysis requires higher equipment maintenance due to corrosion plus additional cost for correct waste disposal, where enzymes are biodegradable and operate at milder conditions, thus lower energy consumption is assumed (Aditya et al., 2016; Barbosa et al., 2020).

Enzymatic hydrolysis is used to hydrolyze and depolymerize polysaccharides obtained from the pretreated LCM (cellulose and hemicellulose) into sugars for further conversion into a range of by-products, such as fine chemicals, added value products and fuels (Costa et al., 2020). Numerous factors affect the efficiency of the enzymatic hydrolysis such as the inhibition of the enzyme by end-products, its thermal stability, pH, but also substrate related factors namely the cellulose crystallinity and the accessibility of the enzyme to cellulose (Sun et al., 2016; Zoghiami and Paës, 2019). Regarding the process of LCM enzymatic hydrolysis there is also the challenge of the insoluble solid substrate. Usually, for enzymatic hydrolysis of pretreated solids loading strategies vary between 5 – 10% (w/v), but an increase to at least 12-15% (w/v) has the potential to improve glucose production hence increasing the economic viability of the process (Pino et al., 2018). In addition, high enzyme costs and low stability demands constant research on operational strategies to achieve a viable lignocellulosic industrial process using these biocatalysts (Aguilar et al., 2018b).

### **2.2.1 Enzymatic hydrolysis at high solid loadings**

Enzymatic hydrolysis at high solid loading has been considered as a strategy to improve the process economics by attaining higher product concentrations and reduce input energy (Weiss et al., 2019). High solid refers to a loading range of 15% – 30% (w/v) however, increasing the loading is not a straightforward operation as other complications come to arise. When operating at high solids loading, one of the preeminent complications is the low amount of free water which trigger other obstacles. These co-related obstacles due to the water availability constrain include mixing problems (thus the inability for the enzyme to reach the substrate), heterogenous heat distribution, and high slurry viscosity (Battista et al., 2018; Shiva et al., 2022).

Commonly, the upper limit to achieve a proper mixing in enzymatic hydrolysis is between 12% - 15% (w/v) as sufficient enzyme-substrate contact can be assured. At higher solid loading, the viscosity increases, the mixing becomes poor, and dead zones are created (no mixing areas) leading to the decrease of conversion yields (Weiss et al., 2019). Another obstacle when operating at high solid loading is the increased production of enzyme inhibitors (Kristensen et al., 2009). To reduce these complications, different approaches have been studied as fed-batch operation to reduce viscosity, bioreactor design to improve mass and heat transfer, and rheological characterizations to understand slurry behavior (Afedzi et al., 2022; Battista et al., 2019; Geng et al., 2015; Lu et al., 2021; Pino et al., 2018).

### **2.2.2 Key enzymes in lignocellulosic biorefineries**

The quest to improve the lignocellulosic biomass hydrolysis is still ongoing. However, the research to understand the action mechanism, is the basis to achieve a reduction in operation costs. This section focuses on the characteristics of three key lignocellulosic enzyme complexes, namely, cellulases, hemicellulases, and ligninases. Furthermore, enzymes as lytic polysaccharide monooxygenases and cellobiose dehydrogenases have been drawing attention recently, hence a section on these auxiliary enzymes is also comprised.

#### **2.2.2.1 Characteristics of the cellulases enzymes**

Cellulases are a complex system of mainly three groups of enzymes: endo-(1,4)- $\beta$ -D-glucanase (EC 3.2.1.4), exo-(1,4)- $\beta$ -D-glucanase (EC 3.2.1.91), and  $\beta$ -glucosidase (EC 3.2.1.21) (Payne et al., 2015). These enzymes work coactively to convert cellulose into fermentable monomeric sugars by hydrolyzing

their glycosidic bonds, a schematic representation is shown in Figure 2.5. Endoglucanases act randomly (and preferably) in the amorphous regions of cellulose releasing new reducing/non-reducing ends and oligomers of different length. Exo-glucanases (cellobiohydrolases) hydrolyze the reducing and non-reducing ends to release cellobiose, a reducing disaccharide consisting in two molecules of glucose. Finally,  $\beta$ -glucosidases act on cellobiose to produce soluble glucose monomers (Barbosa et al., 2020). Nowadays, *Trichoderma reesei* is one of the most employed microorganisms in the production of commercial enzymes (Gomes et al., 2015). These cellulolytic cocktails are highly selective and require low energy inputs as their optimum operational conditions are mild; cellulases optimum temperature and pH are between 40-55 °C and 4.5-6, respectively. However, the use of cellulolytic enzymes for second generation biofuels production is still considered expensive (20-30% of the total cost of 2G ethanol production) despite being a more environmentally friendly hydrolysis process compared, for example, with sulfuric acid hydrolysis which involves drawbacks as corrosion and glucose degradation (Saini et al., 2018).

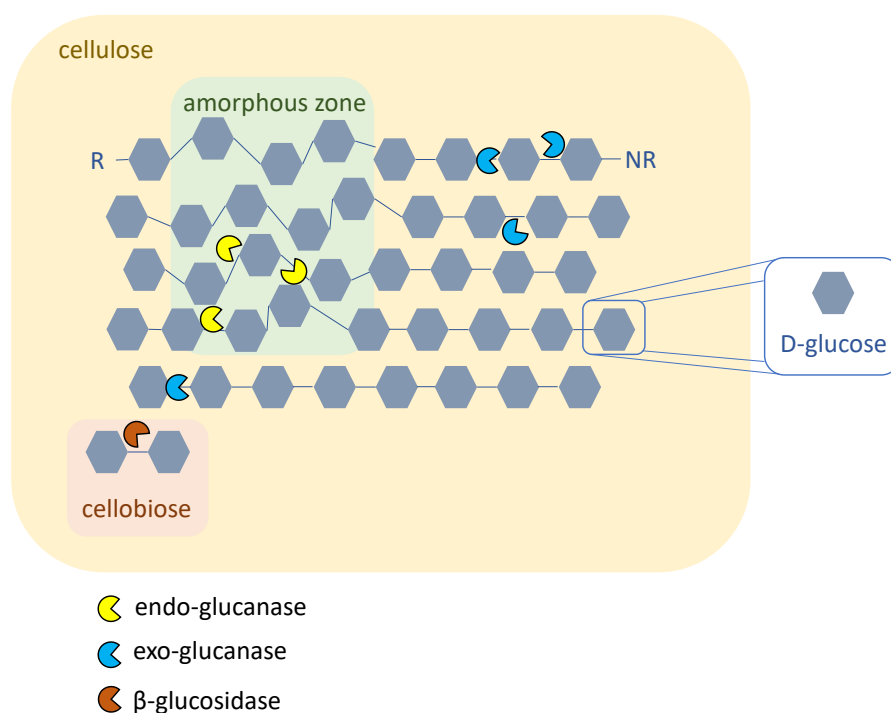


**Figure 2.5.** Simplified scheme of cellulases synergic action to degrade cellulose. (R: Reducing ends, NR: non-reducing ends).

### **2.2.2.2 Characteristics of the hemicellulases enzymes**

Hemicellulases comprise different enzymes that synergistically work to degrade hemicellulose. The global mechanism involves the degradation of xylan to oligomers by xylanases (EC 3.2.1.8), and then to xylose by  $\beta$ -xylosidases (EC 3.2.1.37).  $\beta$ -mannosidase (EC 3.2.1.25) and arabinofuranosidases (EC 3.2.1.55), as well as other hemicellulases, complement the degradation of the main chain of xylan (Fang and Qu, 2018; Zhang et al., 2019). These enzymes are widely used in different areas as food and beverages processing, pulp paper bleaching, wastewater treatment and lignocellulosics bioconversion (Jampala et al., 2017).

### **2.2.2.3 Characteristics of the ligninases enzymes**

Ligninases consist mainly in laccases (EC 1.10.3.2), lignin peroxidases (EC 1.11.1.14), manganese peroxidases (EC 1.11.1.13), and versatile peroxidase (EC 1.11.1.16) enzymes that work synergistically to hydrolyze both phenolic and non-phenolic lignin units (Zhang et al., 2019). Laccases are enzymes classified as multicopper oxidases, mostly from fungal origin but also produced by bacteria and found in plants. These enzymes catalyze the oxidation of phenolic compounds by reducing molecular oxygen into water as by-product. Laccases are considered a “green tool” used in various biotechnological processes as bioremediation, textile industry, pulp and paper industry, food technology and lignocellulosic delignification (Rodríguez-Couto, 2018). Specifically for lignocellulosic biomass, laccases are attractive since they act in lignin-rich substrates modifying the surface morphology of the LCM by degrading the lignin, thus, obtaining a lignin-free porous material with enhanced cellulose accessibility for cellulases (Avanthi and Banerjee, 2016). Laccases can reach yields up to 80-90% delignification without the use of hazardous chemicals (Mayolo-Deloisa et al., 2020). However, the large-scale use of laccases has been limited due to different factors such as a low redox potential, dependence on substrate chemistry and enzyme inhibition (Kumar and Chandra, 2020).

### **2.2.2.4 Auxiliary enzymes**

In recent years, a new mechanism was introduced with the discovery of the lytic polysaccharide monoxygenases (LPMO) (EC 1.14.99.54, EC 1.14.99.56, EC 1.14.99.-) and cellobiose dehydrogenase (CDH) (EC 1.1.99.18). These enzymes have been reclassified to the family of auxiliary activities (AA10), same family as the ligninases, as redox enzymes that act in conjunction with carbohydrate-active enzymes (Levasseur et al., 2013). LPMO have the potential to cleave and decrystallize the crystalline cellulose, thus

increasing the substrate accessibility for cellulases to act and CDH oxidize cellobiose and other cello-oligosaccharides and potentialize the action of the LPMO acting as electron donor (Bischof et al., 2016). The potential of these enzymes is still of great opportunity for research and improve the enzymatic hydrolysis process.

### **2.3 ENZYME IMMOBILIZATION**

Enzymes are replacing processes where hazardous chemicals are used since they are greener, more specific, and less pollutant. As the cost of these green biocatalysts remains high on lignocellulosic conversion, studies on its reduction are essential (Gomes et al., 2018; Ramesh et al., 2020). In this sense, immobilization has been used as an alternative and promising approach to reduce enzyme costs. To illustrate the application of enzyme immobilization to produce a variety of high-added value compounds, Table 2.1 shows, for example, bioactive compounds produced by immobilized cellulase on different supports able to hydrolyze substrates as orange peel, onion skin extract, olive oil leaf extract, among others. Different supports and immobilization techniques facilitate the separation of enzymes from the medium, leading to an enzyme-free product (or minimizing enzyme contamination in the product), efficient recovery, robust enzyme systems, and long-term operational stability (Gomes et al., 2018; Sheldon and Woodley, 2018).

Enzyme immobilization has been studied for more than 40 years, but recent developments on novel materials for enzyme supports, like nanomaterials, engineering surfaces and 3D printed supports, led to a revival of this topic. These new materials are in constant development to extend their immobilization efficiency, by providing highly porous structures, ultra-high surface areas, magnetic properties, stability and extended lifetime (Sigurdardóttir et al., 2018). Also, the development of new techniques due to advances in organic chemistry and molecular biology bring efficient and site-specific immobilization of enzymes into supports (Homaei et al., 2013).



**Table 2. 1** Immobilized enzymes to obtain added value products and their applications.

<b>Immobilized enzyme system</b>	<b>Substrate</b>	<b>Product</b>	<b>Applications</b>	<b>Reference</b>
Xylanase and $\beta$ -xylosidase co-immobilized on chitosan	Oat spelt xylan	Xylobiose	Pharmaceutical industry - Beneficial effect on intestinal microbial flora	Maalej-Achouri et al., 2009
Cellulase, pectinase and hemicellulase immobilized on alginate	Flaxseeds	Flaxseed oil	Food industry – Oil with nutritional value	Long et al., 2011
Cellulase and pectinase immobilized on iron oxide magnetic nanoparticles	Orange peel	Carotenoidic pigments	Pharmaceutical industry – Bioactive compound	Kumar et al., 2016
Hybrid nanoflower of manganese phosphate and L-arabinose isomerase	D-galactose	D-tagatose	Food and pharmaceutical industry – sugar with low energy content	Rai et al., 2018
Cellulase immobilized on magnetic nanoparticles	Onion skin extract	Quercetin	Pharmaceutical and food industry – Bioactive compound	Kumar et al., 2019
Cellulase and glucose oxidase co-immobilized on graphene oxide	CMC	Gluconic acid	Food, pharmaceutical, detergent and textile industry – Mild acidulant	Zhang et al., 2019
Cellulase immobilized on porous ceramic beads	Oleuropein from olive leaf extract	Hydroxytyrosol	Pharmaceutical industry - Bioactive compound	Liu et al., 2020
Laccase immobilized on chitosan coated $\text{Fe}_3\text{O}_4/\text{SiO}_2$	Sweet sorghum stover	Delignified biomass for biohydrogen production	Biofuel	Shanmugam et al., 2020
Xylanase immobilized on calcium alginate 3D printed support	Corn cob	Xylooligosaccharides	Food and pharmaceutical industry – prebiotic	Jiang et al., 2020

### 2.3.1 Immobilization techniques

Immobilization techniques are mainly divided in four groups, depending on how the enzymes interact with the support or with each other: adsorption, covalent bonding, entrapment/encapsulation, and cross-linking, as shown in Figure 2.6. Adsorption is considered a simple low-cost technique. Here, an enzyme solution is in contact with the support for a certain period where bonds such as dipole-dipole, Van der Waals forces and electrostatic interactions are formed. Main drawbacks of this method include the weakness of the bonds and the potential of enzyme leakage when conditions of the media such as pH, temperature or polarity are changed (Nguyen and Kim, 2017).

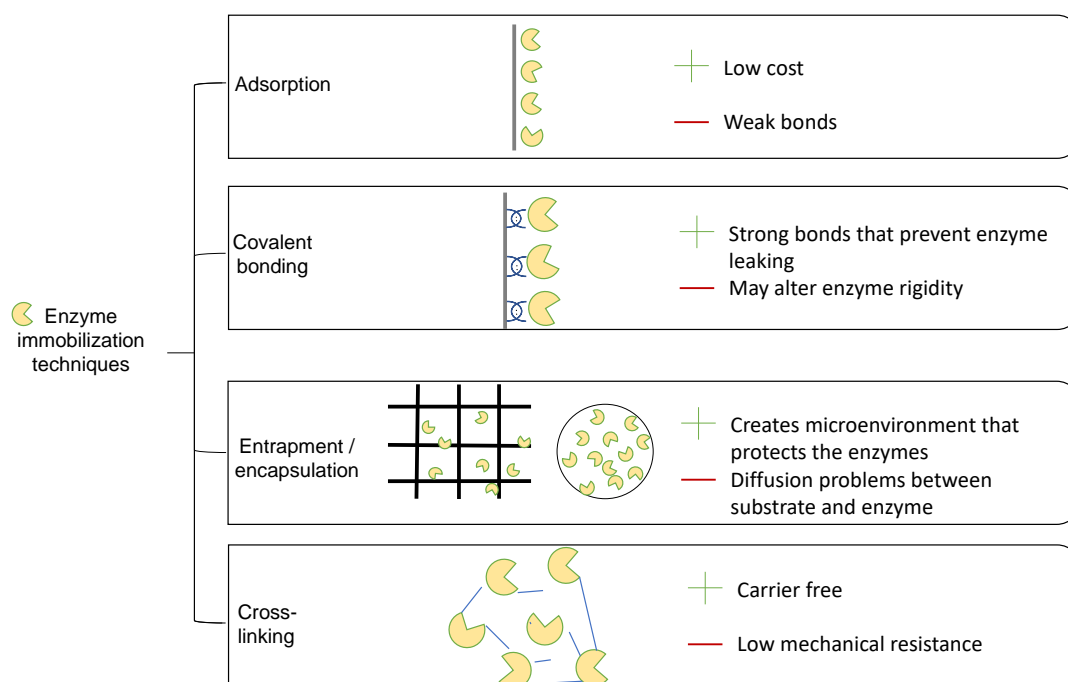


**Figure 2.6.** Enzyme immobilization techniques with their advantages and limitations

Covalent bonding is widely used for enzyme immobilization as it improves enzyme stability, and the formed bonds are strong enough to prevent enzyme leakage (Papadopoulou et al., 2019). Covalent immobilization include amide, ether, thioether, and carbamate bonds. This procedure generally includes an initial support activation to provide hydroxyl groups on its surface, which reacts with the enzyme nucleophiles. Glutaraldehyde is commonly used since it provides a longer space between the support and enzyme. Enzymes might get bonded via the essential amino acids for the catalytic activity, leading to a decrease in the catalytic activity. On the other hand, a correct orientation can increase the stability of the immobilized enzyme compared with its free form (Romero-Fernández and Paradisi, 2020; Tan et al., 2018). The number of covalent bonds that can be formed depend on the concentration of aldehyde

groups on the support and on the concentration of amine groups found at the enzyme surface (Maalej-Achouri et al., 2009).

Immobilization via entrapment consists in the inclusion of the enzyme into a carrier. Entrapment differs from encapsulation as encapsulation is the containment or separation of the enzyme from the media by a porous and permeable organic/inorganic polymer (Chapman and Stenzel, 2019; Romero-Fernández and Paradisi, 2020). Encapsulation creates a microenvironment that protect the enzymes against harsh environments, such as those found in lignocellulose hydrolysates due to the presence of inhibitors. Within the encapsulation technique exist the so-called single enzyme-nanoparticle immobilization, consisting in the modification of the enzyme surface to synthesize a thin polymer layer which covers individually each enzyme (Hegedus and Nagy, 2015). This polymer layer, while improving the thermal and solvent stability of the enzyme, does not hinder its activity neither the diffusion between the substrate and the enzyme. This is useful even when large substrates as cellulose are used, since the layer can be adjusted in terms of thickness and porosity (Chapman and Stenzel, 2019; Hegedüs et al., 2012).

Lastly, among the different types of immobilizations there is also the cross-linking technique. This technique is considered a carrier-free technique as it consists in the formation of enzyme aggregates, known as cross-linking enzyme aggregates (CLEAs). In this technique, each enzyme acts as support to each other by forming molecular bonds between the enzymes. However, cross-linking is not considered a viable alternative for industrial processes as CLEAs are not mechanical resistant and their recovery is complicated (Ravindran and Jaiswal, 2019).

### **2.3.2 Enzyme support classification and novel supports**

Most of the immobilization techniques involve the use of a support. Supports are mainly divided in organic and inorganic materials. Classic categories involve metal oxides, minerals and carbon materials for the inorganic area, and polymers, either synthetic or biopolymers, for the organic category. Common inorganic materials include silica and oxides as titanium, iron, aluminum, and gold. These materials own interesting properties such as mechanical resistance, high and porous surface area, and enable a stable enzyme-support complex (Zdarta et al., 2018). On the other hand, the most used organic supports comprise chitosan, a polyaminosaccharide, that possess functional groups which facilitate the binding to the enzyme, alginate, and agarose due to their ability of gelation, carrageenan, collagen and polyacrylamide, among others (Eş, et al., 2015; Verma et al., 2020).

Organic and inorganic materials have been extensively studied for a variety of enzymes support and are selected based on the specific application and the properties that benefit the process. Still, novel technologies and methodologies are constantly emerging, leading to the development of novel supports, tailor-made, for the requirements of each process. For instance, 3D printers have been used to manufacture supports with specific properties such as shape and porosity, to enhance the immobilization strategy (Kazenwadel et al., 2016; Schmiege et al., 2019; Ye et al., 2019). Another example refers to the so-called smart materials, specifically the stimuli responsive materials, which alter their properties when exposed to certain conditions such as changes in temperature and pH. Among different properties that can be altered are volume, weight, hydrophilicity, and porosity (Duan and Zhang, 2017). Further interesting support is biochar, a product from the pyrolysis process (thermochemical platform) presenting a high porosity and surface area, making it attractive for enzyme immobilization. To facilitate biochar recovery, it can be combined with magnetic particles, and by applying an external magnetic field the biochar can be recovered. Moreover, biochar is a low-cost material since it can be produced from lignocellulosic biomass, thus, contributing to the biorefinery concept (Mo et al., 2020). Likewise, graphene oxide has been used as a promising support for enzyme immobilization due to the vast functional groups and large surface area and, since graphene oxide can be magnetizable, it can facilitate its recovery for reuse (Paz-Cedeno et al., 2021).

### **2.4 LIGNOCELLULOSIC ENZYMES IMMOBILIZATION: ADVANTAGES AND LIMITATIONS**

Enzyme immobilization has been a research topic in many areas as pharmaceutical, food industry and biofuels. However, cellulases present added challenges due to the substrate configuration and the process itself where the product can be an inhibitor factor for the cellulases complex. This part focuses on the advantages and limitations immobilized cellulases despite many cellulase immobilization reports do not test their biocatalyst with lignocellulosic biomass, rather authors test their immobilized complex with synthetic cellulose as Avicel or carboxymethyl cellulose (CMC).

#### **2.4.1 Reducing inhibition**

Cellulolytic enzymes face inhibition due to multiple compounds formed from the degradation of LCM during pretreatment: glucose, cellobiose, mannose, xylose, oligosaccharides, furans, phenolic compounds, and organic acids (Andrić et al., 2010; Berlin et al., 2006; Romani et al., 2014). Despite

their low concentrations in pretreated biomass, mannose and xylose inhibit exo-glucanases by reducing their productive binding to the cellulose surface, also tannins and gallic acid (originated from lignin degradation) inhibit  $\beta$ -glucosidase by causing its deactivation (Kim et al., 2011; Zhai et al., 2018). Immobilization has proved to overcome some of these inhibition effects by preventing inhibitors to bind to the active site of the enzyme. This increased resistance to inhibitors may be attributed to the steric hindrance of the covalent immobilization of the enzyme into the support (Qi et al., 2018). For instance, Qi et al. (2018) compared the cellulase activity of free and immobilized enzymes on a magnetic core-shell metal-organic support in the presence of 5 g/L of inhibitors (formic acid, furfural, and vanillin). The authors found that the residual activity of the immobilized cellulases was 16.8% and 21.5% higher than the free enzymes in the presence of formic acid and vanillin, respectively, but no significant differences were observed in the case of furfural. In another study, Kumar et al. (2017) used alkali-pretreated paddy straw as substrate and observed that immobilized holocellulases (cellulases and hemicellulases) on magnetic nanoparticles complexes had better performance than free enzymes after 24 h of hydrolysis, possibly because the activity of the free enzymes decreased due to a feedback inhibition by end products. This increase of tolerance when enzymes are immobilized is also advantageous, for example, to hydrolyze LCM pretreated with ionic liquids (IL) or with deep eutectic solvents (DES) as enzyme inhibitory effects of IL/DES components have been reported and to avoid an additional washing step of the material (Romani et al., 2020; Tantayotai et al., 2019). As an example, Xu et al. (2016) immobilized cellulases on PEGylated graphene oxide nanosheets and compared them with free cellulases in the hydrolysis of rice straw pretreated with IL in a final concentration of 15% (w/v) of the IL. During the first 4 h of hydrolysis, the immobilized enzymes were able to hydrolyze 64% of the substrate, where the free enzymes only achieved 5% of cellulose conversion. In another study using sugarcane bagasse and wheat straw pretreated with IL (substrate was not washed), cellulases immobilized on magnetic nanoparticles achieved a 3-fold higher hydrolysis yield as compared with free enzymes (Grewal et al., 2017).

#### **2.4.2 Enhancing enzyme temperature and pH stability**

Cellulases activity is highly sensitive to temperature with an optimum temperature between 40-55°C (Costa et al., 2020). Operation at low temperatures leads to slower reactions and to an increased risk of microbial contaminations; on the other hand, temperatures above the optimal lead to a decrease of activity and possible irreversible enzyme denaturation (Gomes et al., 2015). For industrial lignocellulosic processes, thermal stability of cellulolytic enzymes is relevant as high temperature facilitates biomass decomposition and the enzyme handling (Payne et al., 2015). One of the most

common advantages shown by immobilized cellulases is an increase in their thermal stability. For example, after 120 min of hydrolysis, cellulases immobilized on multiwalled carbon nanotubes showed 2 times more sugars released than the free cellulases, at 70°C (Ahmad and Khare, 2018). In another study, cellulases immobilized on silica core-shell magnetic nanoparticles lost 4% of their activity after 4 h at 65°C, while 71% of activity loss was observed for the free enzymes (Khorshidi et al., 2016). Also, for cellulases immobilized on chitosan coated Fe<sub>3</sub>O<sub>4</sub> nanoparticles the residual activity remained at 81.9%, whereas for the free enzymes only 63.9% of the activity remained after 6 h at 60 °C (Tan et al., 2018). The loss of activity on immobilized enzymes hence seems to occur in a slower rate comparing to the free systems. This increase on thermal stability is attributed to the rigid structure of the enzyme due to the covalent and hydrogen bonds formed after immobilization to the support.

Another advantage of immobilized cellulases is the stability gain in a wide range of pH. The protonation of functional groups of the enzyme can either favor the catalytic activity or break it down when one essential group is protonated (Bisswanger, 2014). For instance, at pH higher than 5.0, cellulase has a decrease on the activity that may be attributed to the stretching and degeneration of the active center due to electrostatic repulsion between ionic groups of the enzyme in alkaline media (Miao et al., 2016). This loss in activity is usually less drastic after immobilization and might be attributed to the microenvironment that surrounds the enzymes, changing the ionization state of their functional groups and the formation of new intermolecular interactions between the amino acid chains and the support (Dinçer and Telefoncu, 2007; Khoshnevisan et al., 2011; Muthuvelu et al., 2020; Qi et al., 2018). For example, Wang et al. (2018) reported that cellulases immobilized on styren/maleic anhydride copolymer nanoparticles were able to maintain 80% of their activity at pH 8.0 against only 16% by the free form. A recent study from Muthuvelu et al. (2020) also showed that immobilized laccases on copper ferrite magnetic nanoparticles and ferrite magnetic nanoparticles resisted the harsh range of pH tested (pH range 3.0-9.0) better than its free form even showing a slightly higher activity. For lignocellulosics hydrolysis, enzyme stability at low pH values is particularly relevant as, for example, autohydrolysis liquors are usually acidic, thus, a more stable enzyme would be beneficial to avoid extra washing or neutralizing steps.

### **2.4.3 Immobilized enzymes reusability and operation under continuous regime**

An immediate advantage of immobilization is the ability to easily recover and reuse enzymes, while also enabling an enzyme-free product recovery and a reduced end-product inhibition when operating in continuous mode. This latter feature is particularly useful for large scale applications as it can lower the overall process cost (Zdarta et al., 2018). The ability to reuse an immobilized enzyme is determined

by the residual activity after several batches or hours, in case of continuous operation, as shown in Table 2.2. For example,  $\beta$ -glucosidases immobilized on magnetic chitosan microspheres were reused during 8 batches of pretreated corn straw saccharification and maintained 84.4% of their original activity after the last batch (Zheng et al., 2013). Zang et al. (2014) covalently immobilized cellulases onto chitosan coated  $\text{Fe}_3\text{O}_4$  particles and used them to hydrolyze 1% (w/v) carboxymethyl cellulose (CMC) for 24 h during several batches. After 10 batches it was observed that the activity decreased with the number of batches, yet 50% remained after the last batch. Here, the utilization of magnetic supports brings the additional benefit of the easiness of cellulases recovery since the catalyst can be directly separated with an external magnetic field from the products. In other study using cellulases immobilized on plastic polymer beads of polystyrene, polypropylene, and polyethylene it was also demonstrated their reusability by 8 repeated batches in the hydrolysis of CMC, where the activity loss reported was between 3 - 7% of its initial activity (Ahirwar et al., 2017). In some cases, the hydrolysis of lignocellulosic biomass showed higher yields when free enzymes were used, however, free enzymes face difficulties for its recovery and reuse, thus it is an important disadvantage compared with immobilized systems (Saha et al., 2019). Although this inferior performance by the nanohybrid it should be acknowledged that it can be easily recovered and reused.

Moreover, immobilized enzymes facilitate the implementation of processes operating in a continuous regime by maintaining enzymes stability for longer periods and reducing enzyme losses. At large scale, continuous operation is an efficient strategy to improve processes enabling an improved mass and heat transfer, reduced variability, a simpler down streaming and, specifically for enzymatic hydrolysis processes, a reduction of end-product inhibition since the products are constantly being removed (Lindeque and Woodley, 2019; Thompson et al., 2019). For instance, Romero-Fernández et al. (2018) immobilized xylanases on a methacrylic polymer-based support and used them for the continuous hydrolysis of xylan corncob to produce xylooligosaccharides in a packed-bed reactor. Immobilized xylanases enabled process intensification by operating at flow rates high enough to have short residence time which favor the production of xylooligosaccharides and increase the specific productivity of XOS compared with the batch reactor. In a report by Cárdenas-Fernández et al. (2018)  $\alpha$ -L-arabinofuranosidases were immobilized on an epoxy-functionalized resin and performed the continuous hydrolysis of sugar beet pectin on a packed bed reactor; after 173 h of continuous operation the overall reaction yield was maintained at 79%.

**Table 2.2** Immobilized enzyme reusability examples applied in the hydrolysis of lignocellulosic biomass and carboxymethyl cellulose (CMC).

Support	Enzyme	Substrate	Reuses/ Cycles	Retained activity	Reference
Magnetic chitosan microspheres	$\beta$ -glucosidase	Pretreated corn straw	8 cycles 32 h each	84.4% after last cycle	Zheng et al., 2013
Silica functionalized gold nanoparticle	Cellulase from <i>Trichoderma reesei</i>	Bamboo chopsticks powder	4 cycles of 2 days each	84.14% after first cycle	Cheng and Chang, 2013
Calcium alginate entrapment	$\beta$ -glucosidase	Hydrothermally pretreated barley straw	1 cycle of 72 h	n/d	Tsai and Meyer, 2014
Silica sol-gel	Celulase (Cellucast 1.5 L)	Microcrystalline pretreated with IL	9 cycles of 8 h each	30% after the last cycle	Ungurean et al., 2014
Fe <sub>3</sub> O <sub>4</sub> @silica core-shell nanoparticles	Cellulase from <i>Aspergillus niger</i> (Sigma-Aldrich)	CMC	10 cycles of 60 min each	30% of initial activity after 6th cycle	Khorshidi et al., 2016
Magnetic nanoparticles	Cellulase from <i>Trichoderma reesei</i>	IL pretreated wheat straw and sugarcane bagasse	2 cycles	63% hydrolysis yield for both biomass in the second cycle	Grewal et al., 2017
Iron oxide magnetic nanoparticles	Cellulase from <i>Alternaria alternata</i>	Sugarcane bagasse powder pretreated with acid	3 cycles of 24 h each	68 and 52% cellulose to glucose conversion after second and 3rd cycle	Ingle et al., 2017
Fe <sub>3</sub> O <sub>4</sub> magnetic nanoparticles	Cellulase from <i>Trichoderma reesei</i> (Sigma)	Pretreated bamboo powder	4 cycles of 24 h each	63 and 38% hydrolysis activity after second and 4th cycle	Jia et al., 2017
Chitosan-coated magnetic nanoparticles	Cellulase from <i>Trichoderma reesei</i> (Cellucast 1.5 L)	CMC	18 cycles	Maintained 80% of its activity for 15 cycles	Sánchez-Ramírez et al., 2017
Multiwall carbon nanotube	Cellulase from <i>Aspergillus niger</i>	CMC	10 cycles	75% after sixth cycle	Ahmad and Khare, 2018



**Table 2.2** continued

<b>Support</b>	<b>Enzyme</b>	<b>Substrate</b>	<b>Reuses/ Cycles</b>	<b>Retained activity</b>	<b>Reference</b>
Polyurea microspheres	Cellulase from <i>Aspergillus niger</i>	CMC	8 cycles of 1 h each	75% of initial activity maintained after 8 cycles	Sui et al., 2019
Chitosan coated magnetic graphene	Cellulase from <i>Trichoderma reesei</i>	CMC	8 cycles	49% of its initial activity after 8th cycle	Asar et al., 2020
Activated magnetic nanoparticle	Cellulase	CMC	10 cycles	30% after 10th cycle	Abraham and Puri, 2020
Graphene oxide reinforced hydrogels	Cellulase (PersiCel1)	CMC	6 cycles	51% activity after four cycles	Ariaeenejad et al., 2020
Magnetic nanoparticles	Cellulase from <i>A. fumigatus</i>	Pretreated rice straw	4 cycles	78.6 % and 50.34% after second and 4th cycle	Kaur et al., 2020
Magnetic nanoparticles from bacteria mediated synthesis	Cellulase from <i>Trichoderma viride</i>	CMC	3 cycles of 1 h each	80% after 3rd cycle	Desai and Pawar, 2020
Magnetic graphene oxide	Cellulase (Cellic CTec2)	Pretreated sugarcane bagasse	10 cycles of 24 h each	72% after first cycle and stable from 6-9th cycle at 27%.	Paz-Cedeno et al., 2021

#### 2.4.4 Mass transfer limitations

Specifically for the case of LCM enzymatic hydrolysis, mass transfer becomes an issue as cellulose is a large polymeric substrate and high solid loads are needed for a viable process (Minteer, 2016). Therefore, enzyme immobilization via entrapment or encapsulation may not be a suitable strategy due to the limited accessibility of the LCM (range size 0.1-5  $\mu\text{m}$  in diameter) to pass through the membrane pores ( $\sim 200$  nm for alginate beads). In fact, in a previous study from Ungurean et al. (2014) the authors demonstrated the possibility of hydrolyzing poplar biomass, previously pretreated with IL, using cellulases immobilized onto a sol-gel but observed a lower saccharification using the immobilized cellulases compared to the free enzymes, possibly due to the resistance of the substrate (with a high molecular weight) to pass through the pores of the silica sol-gel matrix. A recent study from Jiang et al. (2020) reported the immobilization of xylanases in calcium microspheres using 3D printing technology to produce xylooligosaccharides from corn cob. The authors observed that after 4 h of reaction, free xylanases had a faster reaction rate than the immobilized enzymes, attributing this result to the limited diffusion of the substrate causing mass transfer resistance. Nonetheless, at the end of the reaction after 72 h, the xylooligosaccharides production was greater with the immobilized xylanases, laying on the fact that free xylanases were unstable over time.

A major limitation found on studies addressing cellulases immobilization is that most of them use synthetic cellulose, such as microcrystalline cellulose or carboxymethyl cellulose, as substrate to test the immobilization systems, with only few performed with pretreated LCM as substrate. The use of microcrystalline cellulose enables an easier mass transfer when comparing with using real LCM substrates, since it has a uniform particle size in the range of 20 – 200  $\mu\text{m}$ . Jia et al. (2017) studied the hydrolysis of pretreated bamboo powder (177  $\mu\text{m}$ ) using magnetic cross linked cellulase aggregates and various concentrations of pretreated solid. The highest hydrolysis yield was achieved when a low biomass concentration (0.075%, w/v) was used, reaching 44% of conversion with free enzymes and only 21% with the immobilized cellulases. This limitation was attributed to the poor diffusivity of the cross linked cellulase aggregates and to the fact that bamboo is hard to hydrolyze due to its rigid structure. Similarly, Ingle et al. (2017) studied the hydrolysis of sugarcane bagasse powder, pretreated with acid, employing immobilized cellulases on iron oxide magnetic nanoparticles at different temperatures (27, 40, 50 and 60  $^{\circ}\text{C}$ ) and performed three consecutive cycles of 24 h. At 40 $^{\circ}\text{C}$  they achieved a cellulose to glucose conversion rate of 72%, 68% and 52% for each cycle, respectively. However, comparing the first cycle with the free enzymes system, the conversion achieved was higher for the free cellulases. Porous materials

provide larger superficial area for enzymes to be immobilized, however, when enzymes are immobilized on a porous material, the porous design and size must be related with the enzyme molecular size to optimize the adsorption capability (Chen et al., 2017). Also, the inner part of the pore creates a microenvironment different from the surface that affects the flexibility of the enzyme (Mo et al., 2020). To overcome these effects on enzyme immobilization, Mo et al. (2020) suggested supports with a large specific area and improved open pore structure to provide more sites for enzyme immobilization. An open porous structure, besides providing more area for the enzyme to absorb, also facilitate the substrate to reach the enzyme.

### **2.5 BIOREACTORS TECHNOLOGY FOR ENZYMATIC HYDROLYSIS**

Reactor selection for the enzymatic hydrolysis step can be a strategy to enhance the process. Traditional reactors as stirred tank bioreactor (STBR), horizontal tubular bioreactor, airlift bioreactor, among others, had been used for the enzymatic hydrolysis process, sometimes with improvements on impellers or energy consumption. The constant development on both enzymes and reactors has brought alternative bioreactor strategies, these includes magnetically stabilized bioreactors or the application of novel reactors as oscillatory flow reactors. However, the core challenge is still the complexity of the enzymatic hydrolysis process.

#### **2.5.1 Bioreactors for immobilized enzyme complex**

While immobilization has for long been used on an industrial context (either for microorganisms or enzymes), the immobilization of cellulases for the hydrolysis of lignocellulosic materials represents though a new and especial challenge. The utilization of insoluble solids imposes serious limitations over the immobilization techniques as particles dimensions hinders an efficient penetration through low-diffusion systems, such as encapsulated enzymes (Jørgensen and Pinelo, 2017). Additionally, the fact that some of these materials have a low density and, in some cases, a high water-retention capacity usually results on high viscosity suspensions, which may lead to rheological issues and mixture problems (Koppram et al., 2014). These and other issues not only raise important challenges in the selection of the immobilization technique but will also dictate the design of industrial-scale reactors for their implementation.

Industrial scale cellulases immobilization may be applied under two distinct main paradigms. The first one refers to operating under a batch regime, being the enzymes recovered at the end of the batch and recovered/recycled into a new batch, resembling the traditional recycling of yeast cells usually conducted on brewing or bioethanol industries (these, however, do not rely on immobilization); this is the approach most frequently studied on literature (Berbegal et al., 2019; Genisheva et al., 2014; Pires et al., 2012). On the other hand, continuous regime operation, allows not only to reduce enzymes consumption but also a constant product removal, reducing possible effects of end-product inhibition. The latter one will naturally be more challenging as the catalyst needs to be continuously contained inside the reactor, which implies selective enzyme retention, as shown in Figure 2.7. Because of the aspects mentioned above, studies specifically addressing the enzymatic hydrolysis of lignocellulosic residues with immobilized cellulases on a reactor are almost inexistent; few works exist referring to the utilization of CMC (Abraham et al., 2014; Gebreyohannes et al., 2018; Melander et al., 2005; Sui et al., 2019) but these does not pose the challenges of traditional LCM. Here is important to clarify that the utilization of membrane bioreactors (MBR), which mainly intends to selectively retain enzymes, refers to a distinct concept of enzymes retention, and not immobilization.

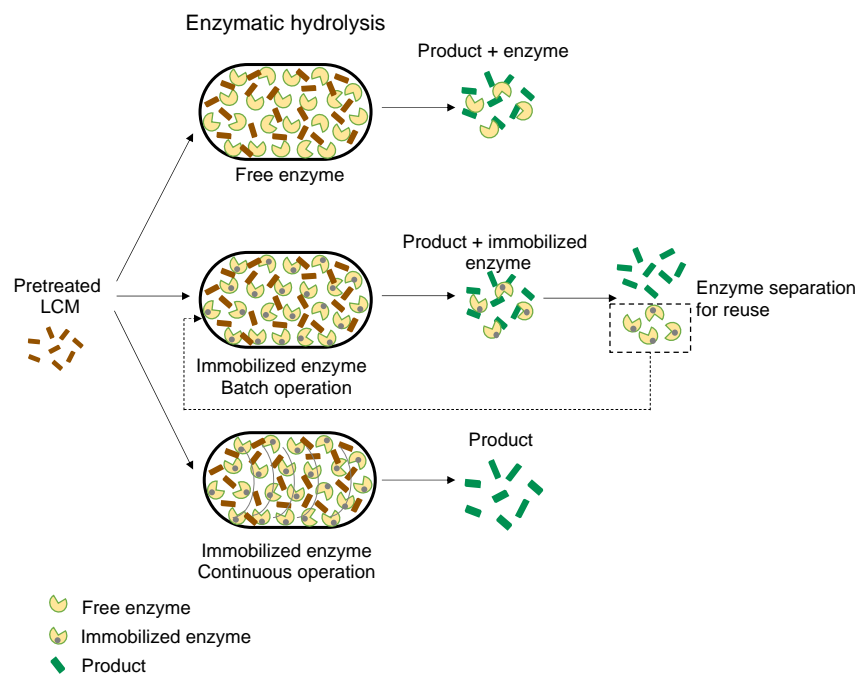


**Figure 2.7.** Different reactor strategy for enzymatic hydrolysis.

### 2.5.1.1 Magnetic-based bioreactors

The utilization of magnetic supports for enzyme immobilization enables the easiest and most direct way to recover enzymes. Using a traditional stirred tank reactor on a batch regime, and assuming a very favourable scenario where the solid is completely hydrolysed (which would imply total solubilisation), the enzyme-support complex may even sediment if their density allows it (for example,  $\text{Fe}_3\text{O}_4$  nanoparticles density is 4.8-5.1 g/mL), being the final medium easily removed from a superior withdraw point. This, however, seems to not correspond to the traditional incomplete hydrolysis of LCM, with ranging levels of unconverted holocellulose and other “inert” components, such as ash and lignin (Gomes et al., 2016). Using the solid sediment on this case would lead to a build-in of lignin during the process, with a consequent increase of the mixture viscosity and non-productive binding of cellulases. However, the application of an external magnetic field at the end of the process can effectively separate the enzymes from the final medium, but also from the spent solid (Roth et al., 2016).

Under a different paradigm, the operation on a continuous regime brings additional challenges. To maintain steady levels of enzyme activity over time, a proper magnetic field is required during operation, which will avoid cellulases “wash-out” by counteracting the drag force of the bed. The most studied reactor design in this context is a magnetic fluidized-bed reactor. With the suitable application of a magnetic field along the reactor it is possible to exert some control over the velocity of the bed, while avoiding considerable pressure drops associated to packed-bed reactors (Sada et al., 1981). This type of equipment was recently reported by Cui et al. (2018), where the authors immobilized cellulases on  $\text{Fe}_3\text{O}_4$  describing their operation on a new magnetic three-phase fluidized bed reactor. The magnetic fluidized bed was achieved through Helmholtz coils placed along the extension of the bed column; complementing the fluidized bed, the output stream was processed through an ultrafiltration unit, enabling to recirculate both solids and “washed” cellulases back to the reactor. The authors observed that the type of magnetic field was determinant for the activity of the immobilized enzyme with a pulsed field enabling the highest levels of activity during operation (23.3 UI/g), which was obtained for a given intensity of the magnetic field (1.5 kA/m). Referring to a similar reactor design, Al-Qodah et al. (2015) addressed an interesting aspect concerning the characteristic of the magnetic support. According to the authors, the high minimum fluidization velocities usually required for high-density magnetic supports are not compatible to the low rates of biological reactions, such as those conducted by enzymes, hence requiring superior residence times. Therefore, the authors studied the utilization of different low-density magnetic supports for cells immobilization on magnetically stabilized beds. Hydrodynamic tests confirmed that these innovative

supports had lower minimum fluidization velocities, which means a higher residence time, and attained a higher expanded bed.

### **2.5.1.2 Non-magnetic based bioreactors**

The utilization of non-magnetic immobilization supports brings new challenges to the reactor design. The retention of enzymes within the system boundaries would necessarily require either a barrier to avoid their escape (e.g., membrane), their binding to a physical surface, their containment in a given space, or a combination of these.

Regarding the employment of a barrier and in what refers to one of the few studies employing real LCM, Cheng and Chang (2013) developed a system for the continuous hydrolysis of waste bamboo chopsticks with cellulases immobilized on silica functionalized gold nanoparticles. The equipment was constituted by a common stirred tank reactor where fresh substrate was continuously fed while a volume of media was being removed by a port with a filter/sieve attached, which according to the authors seems to avoid the loss of silica-immobilized enzymes. As previously mentioned, this concept must be distinguished from the exclusive utilization of membrane systems without immobilization; those require a finest filtration, usually achieved with membranes with a 10-30 kDa cut-off. Another example of membranes-immobilization synergism refers to the work of Nguyen et al. (2015) where the authors prepared cellulase aggregates, which they posteriorly trapped inside PES membranes to continuously hydrolyse CMC while retaining cellulase aggregates. According to the authors, for values of feeding flow equal or below to 0.1 mL/min the membrane was able to retain 86% of enzymes aggregates. Moreover, the continuous withdraw of the product avoid the enzyme inhibition, thus, increasing the process efficiency compared with a batch operation.

On a different approach, immobilized enzymes can be also contained using a packed-bed reactor where the catalyst is packed on a specific part of the reactor while the substrate solution passes through the bed. This particular configuration presents specific advantages when working with an immobilized biocatalyst since it avoids the possible damage caused by mechanical mixing, it can be easily scaled-up and is suitable for continuous operation (Cárdenas-Fernández et al., 2018). Even though packed bed-reactor represents one of the most used reactor designs in chemical engineering, or even for biological processes, it presents however some important limitations. The most obvious in the context of LCM hydrolysis is that is not suitable for media with suspended solids, as solids can easily accumulate at the front of the bed, leading to its blockage and consequent higher pressure drops (Karube et al., 1977). In

fact, studies referring to the utilization of cellulases/hemicellulases immobilized on a packed-bed reactor and using suspended solids are very scarce. For example, an early study by Venardos et al. (1980) reported the immobilization of  $\beta$ -glucosidase on a packed bed reactor but the substrate used was a cellobiose solution. Liu et al. (2020) described the utilization of Cellic CTec2 immobilized on a packed-bed reactor for the hydrolysis of oleuropein in olive leaf extracts. Overall, the authors obtained a good maintenance of process efficiency during 20 consecutive batches with a substrate concentration of 20 g/L of leaf extract. On a recent study by Romero-Fernández et al. (2018) the authors implemented a continuous process of xylan hydrolysis into XOS by a xylanase immobilized on a packed-bed reactor, however, the substrate solutions corresponded to a 4% solution of purified xylan from corncob. Worth also to mention the rise of new reactor configurations such as the rotating bed reactor (Pithani et al., 2019); these, however, have still been poorly studied in the context of solids hydrolysis using immobilized catalyst.

One last reactor configuration in the immobilized catalyst condition is the traditional fluidized bed-reactor in which the immobilized enzymes are “eluted” by the flow of liquid, forming an expanded bed. In a context of solids hydrolysis, this should represent a more viable option since solid particles have a higher mobility through the bed, avoiding the blockage of the bed. On the other hand, this superior mobility can also lead to a higher catalyst loss when operating on continuous mode; immobilization on larger particles supports (e.g., alginate beads) would be beneficial for this reactor configuration, but these low-diffusion materials are normally incompatible with the conversion of insoluble solids. As for the packed-bed reactor, despite the wide utilization of this reactor configuration for many decades now, their utilization on the hydrolysis of real LCM has almost not been studied so far. One of the few studies employing a cellulosic substrate refers to an early work by Karube et al. (1977) on the hydrolysis of Avicel by cellulases immobilized on a fluidized bed reactor. The fluidized bed was composed by cellulases entrapped on collagen beads, while the substrate was a 0.33% Avicel solution. Comparatively to the free cellulases, immobilized enzymes presented a more constant but also a slightly inferior hydrolysis rate in the first 100 h, possibly explained by some mass transfer limitations resulting from enzymes entrapment. For superior hydrolysis times the immobilized system became more interesting as the hydrolysis rate remained constant, while it considerably decreased for the free cellulases.

### 2.5.2 Oscillatory flow bioreactors

Oscillatory flow reactor (OFR) is a type of reactor configuration that consist in a tube with equally spaced plates or baffles were a superimposed oscillatory motion that cause specific flow patterns which relate to an increase of heat and mass transfer efficiency (Stonestreet and Harvey, 2002). Considering the features this type reactor offers (Figure 2.8), it has been used in a wide type of operations such as fine chemicals, wastewater treatments, pharmaceuticals, and biological operations. The OFR design is mostly equipped with a heating jacket and an oscillatory device. OFR becomes interesting for industrial continuous operations as the net flow rate is independent of the mixing, thus longer residence time can be attained at lower flow rates and compact designs (Bianchi et al., 2020).

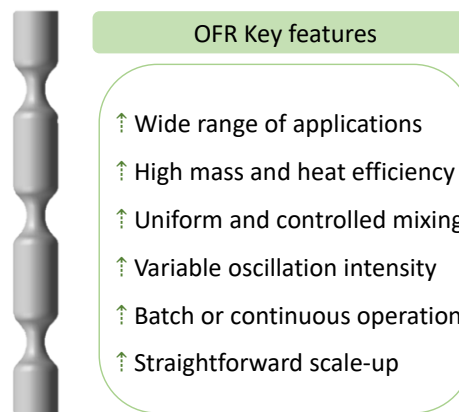


**Figure 2.8.** Summary of oscillatory flow reactor key features

The specific flow patterns that occur when oscillation is applied in OFRs creates vortices which improve the radial and axial mixing. These motion inside the reactor assure a well-mixed regions between each baffle ensuing the behavior to relate to a series of stirred tank reactors (Masngut et al., 2010). OFR variables that affect the radial mixing are the oscillation frequency ( $f$ ), amplitude ( $x_0$ ), reactor diameter ( $d$ ), baffle spacing ( $L$ ), baffle internal diameter ( $d_b$ ), and the fluid's rheological properties (Reis et al., 2005). The intensity mixing is commonly dictated by the oscillatory Reynolds number ( $Re_0$ ) and the Strouhal number ( $St$ ) which can be used as primary parameters reference (Sern et al., 2012). The mixing intensity on the tube is described by the oscillatory Reynold number defined as the equation (eq. 2.1):

$$Re_0 = \frac{2\pi f x_0 d \rho}{\mu} \quad \text{eq. 2.1}$$



Where  $\rho$  is the solution density and  $\mu$  is the viscosity of the solution. The  $Re_c$  is used to define the mixing intensity in the OFR. The Strouhal number describes the effective propagation of the vortices through the oscillation amplitude and the tube diameter and is defined as the following equation (eq. 2.2):

$$St = \frac{d}{4\pi x_0} \quad \text{eq. 2.2}$$

Regarding the use of OFR in bioprocesses, it represents an interesting reactor configuration compared to traditional reactor configurations. An example regarding the improved mass transfer in OFR is an early proof-of-concept study realized by Reis et al. (2006) where they reported an increase on *S. cerevisiae* biomass growth of 83% compared with a STBR and 214% when compared to shake flask. They related the increment in biomass growth to the enhanced mass transfer achieved in the reactor. Another highlighted advantage in OFR is the low and uniform shear rates which is beneficial as some enzymes and microorganisms are shear-sensitive due to their relative fragility and possible inhibition by high shear rates (Afedzi et al., 2022; Da Silva et al., 2020). Reports can be found where higher ethanol production was achieved in OFR compared with stirred tanks and the improved performance is associated to the shear reduction for both the enzymes and yeasts (Ikwebe and Harvey, 2020, 2015). Furthermore, as the dynamic parameters that dictate the behavior of the axial and radial mixing are based on the Reynolds and Strouhal number, and both numbers are dimensionless, the scale-up becomes easier by maintaining those parameters and the geometric features of the reactor (the relation of baffle spacing and open area) constant (Ahmed et al., 2017; Bianchi et al., 2020). Despite the straightforward scale up OFR offers, there are some constraints when using this reactor strategy. Regarding the design, the scale-up can cause pressure drops due to frictional losses and long reactor lengths needed (up to meters) (Abbott et al., 2013). Withal, there is still nowadays some knowledge-gaps as most of the research dedicated to OFR focuses on single-phase systems and the optimal operation conditions may not fulfill more complex systems operations, hence, the appropriate flow conditions must be adapted to the application, characteristics and objective of the process (Avila et al., 2021).

## 2.6 REFERENCES

- Abbott, M.S.R., Harvey, A.P., Valente Perez, G., Theodorou, M.K., 2013. Biological processing in oscillatory baffled reactors: Operation, advantages and potential. *Interface Focus* 3. <https://doi.org/10.1098/rsfs.2012.0036>
- Abraham, R.E., Puri, M., 2020. Commercial application of lignocellulose-degrading enzymes in a

- biorefinery, in: Arora, N.K., Mishra, J., Mishra, V. (Eds.), *Microbial Enzymes: Roles and Applications in Industries*. Springer Singapore, Singapore, pp. 287–301. [https://doi.org/10.1007/978-981-15-1710-5\\_11](https://doi.org/10.1007/978-981-15-1710-5_11)
- Abraham, R.E., Verma, M.L., Barrow, C.J., Puri, M., 2014. Suitability of magnetic nanoparticle immobilised cellulases in enhancing enzymatic saccharification of pretreated hemp biomass. *Biotechnol. Biofuels* 7, 90. <https://doi.org/https://doi.org/10.1186/1754-6834-7-90>
- Aditiya, H.B., Mahlia, T.M.I., Chong, W.T., Nur, H., Sebayang, A.H., 2016. Second generation bioethanol production: A critical review. *Renew. Sustain. Energy Rev.* 66, 631–653. <https://doi.org/10.1016/j.rser.2016.07.015>
- Afedzi, A.E.K., Rattanaporn, K., Parakulsuksatid, P., 2022. Impeller selection for mixing high-solids lignocellulosic biomass in stirred tank bioreactor for ethanol production. *Bioresour. Technol. Reports* 17, 100935. <https://doi.org/10.1016/j.biteb.2021.100935>
- Aguilar, D.L., Rodríguez-Jasso, R.M., Zanuso, E., de Rodríguez, D.J., Amaya-Delgado, L., Sanchez, A., Ruiz, H.A., 2018a. Scale-up and evaluation of hydrothermal pretreatment in isothermal and non-isothermal regimen for bioethanol production using agave bagasse. *Bioresour. Technol.* 263, 112–119. <https://doi.org/10.1016/j.biortech.2018.04.100>
- Aguilar, Daniela L., Rodríguez-Jasso, R.M., Zanuso, E., Lara-Flores, A.A., Aguilar, C.N., Sanchez, A., Ruiz, H.A., 2018b. Operational strategies for enzymatic hydrolysis in a biorefinery, in: Kumar, S., Sani, R. (Eds.), *Biorefining of biomass to biofuels. Biofuel and Biorefinery Technologies*. pp. 223–248. [https://doi.org/10.1007/978-3-319-67678-4\\_10](https://doi.org/10.1007/978-3-319-67678-4_10)
- Aguirre-Fierro, A., Pino, M., Zanuso, E., Londoño Hernández, L., Nájera, A., Torres, A., Aguilar, C., Rodríguez-Jasso, R., Robledo, A., Ruiz, H., 2019. Biochemical and thermochemical platforms for bioproducts and biofuels in terms of biorefinery, in: *Advances in Food Bioproducts and Bioprocessing*. pp. 145–192. <https://doi.org/10.1201/9780429331817-8>
- Ahirwar, R., Sharma, J.G., Nahar, P., Kumar, S., 2017. Immobilization studies of cellulase on three engineered polymer surfaces. *Biocatal. Agric. Biotechnol.* 11, 248–251. <https://doi.org/10.1016/j.bcab.2017.07.014>
- Ahmad, R., Khare, S.K., 2018. Immobilization of *Aspergillus niger* cellulase on multiwall carbon nanotubes for cellulose hydrolysis. *Bioresour. Technol.* 252, 72–75. <https://doi.org/10.1016/j.biortech.2017.12.082>
- Ahmed, S.M.R., Phan, A.N., Harvey, A.P., 2017. Scale-up of oscillatory helical baffled reactors based on residence time distribution. *Chem. Eng. Technol.* 40, 907–914. <https://doi.org/10.1002/ceat.201600480>
- Al-Qodah, Z., Al-Shannag, M., Assirey, E., Orfali, W., Bani-Melhem, K., Alananbeh, K., Bouqellah, N., 2015. Characteristics of a novel low density cell-immobilized magnetic supports in liquid magnetically stabilized beds. *Biochem. Eng. J.* 97, 40–49. <https://doi.org/10.1016/j.bej.2015.01.004>
- Andrić, P., Meyer, A.S., Jensen, P.A., Dam-Johansen, K., 2010. Reactor design for minimizing product inhibition during enzymatic lignocellulose hydrolysis: I. Significance and mechanism of cellobiose and glucose inhibition on cellulolytic enzymes. *Biotechnol. Adv.* 28, 308–324. <https://doi.org/10.1016/j.biotechadv.2010.01.003>
- Aparicio, E., Rodríguez-Jasso, R.M., Pinales-Márquez, C.D., Loredó-Treviño, A., Robledo-Olivo, A., Aguilar, C.N., Kostas, E.T., Ruiz, Héctor A. Loredó-trevi, A., 2021. High-pressure technology for *Sargassum*

- spp biomass pretreatment and fractionation in the third generation of bioethanol production. *Bioresour. Technol.* 329. <https://doi.org/10.1016/j.biortech.2021.124935>
- Ariaeenejad, S., Motamedi, E., Hosseini Salekdeh, G., 2020. Stable cellulase immobilized on graphene oxide@CMC-g-poly(AMPS-co-AAm) hydrogel for enhanced enzymatic hydrolysis of lignocellulosic biomass. *Carbohydr. Polym.* 230, 115661. <https://doi.org/10.1016/j.carbpol.2019.115661>
- Asar, M.F., Ahmad, N., Husain, Q., 2020. Chitosan modified Fe<sub>3</sub>O<sub>4</sub>/graphene oxide nanocomposite as a support for high yield and stable immobilization of cellulase: its application in the saccharification of microcrystalline cellulose. *Prep. Biochem. Biotechnol.* 50, 460–467. <https://doi.org/10.1080/10826068.2019.1706562>
- Avanthi, A., Banerjee, R., 2016. A strategic laccase mediated lignin degradation of lignocellulosic feedstocks for ethanol production. *Ind. Crops Prod.* 92, 174–185. <https://doi.org/10.1016/j.indcrop.2016.08.009>
- Avila, M., Kawas, B., Fletcher, D.F., Poux, M., Xuereb, C., Aubin, J., 2021. Design, performance characterization and applications of continuous oscillatory baffled reactors. *Chem. Eng. Process. - Process Intensif.* 108718. <https://doi.org/10.1016/j.cep.2021.108718>
- Baptista, S.L., Carvalho, L.C., Romani, A., Domingues, L., 2020. Development of a sustainable bioprocess based on green technologies for xylitol production from corn cob. *Ind. Crops Prod.* 156, 112867. <https://doi.org/10.1016/j.indcrop.2020.112867>
- Barbosa, F.C., Silvello, M.A., Goldbeck, R., 2020. Cellulase and oxidative enzymes: new approaches, challenges and perspectives on cellulose degradation for bioethanol production. *Biotechnol. Lett.* 42, 875–884. <https://doi.org/10.1007/s10529-020-02875-4>
- Battista, F., Gomez Almendros, M., Rousset, R., Boivineau, S., Bouillon, P.A., 2018. Enzymatic hydrolysis at high dry matter content: The influence of the substrates' physical properties and of loading strategies on mixing and energetic consumption. *Bioresour. Technol.* 250, 191–196. <https://doi.org/10.1016/j.biortech.2017.11.049>
- Battista, F., Gomez Almendros, M., Rousset, R., Bouillon, P.A., 2019. Enzymatic hydrolysis at high lignocellulosic content: Optimization of the mixing system geometry and of a fed-batch strategy to increase glucose concentration. *Renew. Energy* 131, 152–158. <https://doi.org/10.1016/j.renene.2018.07.038>
- Berbegal, C., Polo, L., García-Esparza, M.J., Lizama, V., Ferrer, S., Pardo, I., 2019. Immobilisation of yeasts on oak chips or cellulose powder for use in bottle-fermented sparkling wine. *Food Microbiol.* 78, 25–37. <https://doi.org/10.1016/j.fm.2018.09.016>
- Berlin, A., Balakshin, M., Gilkes, N., Kadla, J., Maximenko, V., Kubo, S., Saddler, J., 2006. Inhibition of cellulase, xylanase and  $\beta$ -glucosidase activities by softwood lignin preparations. *J. Biotechnol.* 125, 198–209. <https://doi.org/10.1016/j.jbiotec.2006.02.021>
- Bianchi, P., Williams, J.D., Kappe, C.O., 2020. Oscillatory flow reactors for synthetic chemistry applications. *J. Flow Chem.* 10, 475–490. <https://doi.org/10.1007/s41981-020-00105-6>
- Billès, E., Coma, V., Peruch, F., Grelier, S., 2017. Water-soluble cellulose oligomer production by chemical and enzymatic synthesis: a mini-review. *Polym. Int.* 66, 1227–1236. <https://doi.org/10.1002/pi.5398>
- Bisswanger, H., 2014. Enzyme assays. *Perspect. Sci.* 1, 41–55. <https://doi.org/10.1016/j.pisc.2014.02.005>

- Brunner, G., 2014. Processing of biomass with hydrothermal and supercritical water, in: *Supercritical Fluid Science and Technology*. pp. 395–509. <https://doi.org/10.1016/B978-0-444-59413-6.00008-X>
- Cárdenas-Fernández, M., Hamley-Bennett, C., Leak, D.J., Lye, G.J., 2018. Continuous enzymatic hydrolysis of sugar beet pectin and L-arabinose recovery within an integrated biorefinery. *Bioresour. Technol.* 269, 195–202. <https://doi.org/10.1016/j.biortech.2018.08.069>
- Chapman, R., Stenzel, M.H., 2019. All wrapped up: stabilization of enzymes within single enzyme nanoparticles. *J. Am. Chem. Soc.* 141, 143–150. <https://doi.org/10.1021/jacs.8b10338>
- Chen, B., Qiu, J., Mo, H., Yu, Y., Ito, K., Sakai, E., Feng, H., 2017. Synthesis of mesoporous silica with different pore sizes for cellulase immobilization: pure physical adsorption. *New J. Chem.* 41, 9338–9345. <https://doi.org/10.1039/c7nj00441a>
- Chen, J., Yuan, Z., Zanuso, E., Trajano, H.L., 2017. Response of biomass species to hydrothermal pretreatment, in: Ruiz, H., Hedegaard Thomsen, M., Trajano, H. (Eds.), *Hydrothermal Processing in Biorefineries*. Springer, Cham, Switzerland, pp. 95–140. [https://doi.org/10.1007/978-3-319-56457-9\\_4](https://doi.org/10.1007/978-3-319-56457-9_4)
- Cheng, C., Chang, K.C., 2013. Development of immobilized cellulase through functionalized gold nanoparticles for glucose production by continuous hydrolysis of waste bamboo chopsticks. *Enzyme Microb. Technol.* 53, 444–451. <https://doi.org/10.1016/j.enzmictec.2013.09.010>
- Costa, J.R., Tonon, R. V, Cabral, L., Gottschalk, L., Pastrana, L., Pintado, M.E., 2020. Valorization of agricultural lignocellulosic plant by-products through enzymatic and enzyme-assisted extraction of high-added value compounds: a review. *ACS Sustain. Chem. Eng.* <https://doi.org/10.1021/acssuschemeng.0c02087>
- Cristóbal, J., Caldeira, C., Corrado, S., Sala, S., 2018. Techno-economic and profitability analysis of food waste biorefineries at European level. *Bioresour. Technol.* 259, 244–252. <https://doi.org/10.1016/j.biortech.2018.03.016>
- Cui, J., Li, L., Kou, L., Rong, H., Li, B., Zhang, X., 2018. Comparing immobilized cellulase activity in a magnetic three-phase fluidized bed reactor under three types of magnetic field. *Ind. Eng. Chem. Res.* 57, 10841–10850. <https://doi.org/10.1021/acs.iecr.8b02195>
- Cunha, J.T., Romani, A., Costa, C.E., Sá-Correia, I., Domingues, L., 2019. Molecular and physiological basis of *Saccharomyces cerevisiae* tolerance to adverse lignocellulose-based process conditions. *Appl. Microbiol. Biotechnol.* 103, 159–175.
- Cunha, J.T., Soares, P.O., Baptista, S.L., Costa, C.E., Domingues, L., 2020. Engineered *Saccharomyces cerevisiae* for lignocellulosic valorization: a review and perspectives on bioethanol production. *Bioengineered* 11, 883–903. <https://doi.org/10.1080/21655979.2020.1801178>
- Da Silva, A.S.A., Espinheira, R.P., Teixeira, R.S.S., De Souza, M.F., Ferreira-Leitão, V., Bon, E.P.S., 2020. Constraints and advances in high-solids enzymatic hydrolysis of lignocellulosic biomass: A critical review. *Biotechnol. Biofuels* 13, 1–28. <https://doi.org/10.1186/s13068-020-01697-w>
- Desai, M.P., Pawar, K.D., 2020. Immobilization of cellulase on iron tolerant *Pseudomonas stutzeri* biosynthesized photocatalytically active magnetic nanoparticles for increased thermal stability. *Mater. Sci. Eng. C* 106, 110169. <https://doi.org/10.1016/j.msec.2019.110169>
- Dinçer, A., Telefoncu, A., 2007. Improving the stability of cellulase by immobilization on modified polyvinyl alcohol coated chitosan beads. *J. Mol. Catal. B Enzym.* 45, 10–14. <https://doi.org/10.1016/j.molcatb.2006.10.005>

- Duan, J.J., Zhang, L.N., 2017. Robust and smart hydrogels based on natural polymers. *Chinese J. Polym. Sci. English Ed.* 35, 1165–1180. <https://doi.org/10.1007/s10118-017-1983-9>
- Es, I., Gonçalves Viera, J.D., Corrêa Amaral, A., 2015. Principles, techniques, and applications of biocatalyst immobilization for industrial application. *Appl. Environ. Microbiol.* 99, 2065–2082. <https://doi.org/10.1007/s00253-015-6390-y>
- Fang, Xu, Qu, Yinbo, 2018. Fungal cellulolytic enzymes: Microbial production and application, in: Fang, X, Qu, Y (Eds.), *Fungal Cellulolytic Enzymes*. pp. 267–282. <https://doi.org/10.1007/978-981-13-0749-2>
- Gebreyohannes, A.Y., Dharmjeet, M., Swusten, T., Mertens, M., Verspreet, J., Verbiest, T., Courtin, C.M., Vankelecom, I.F.J., 2018. Simultaneous glucose production from cellulose and fouling reduction using a magnetic responsive membrane reactor with superparamagnetic nanoparticles carrying cellulolytic enzymes. *Bioresour. Technol.* 263, 532–540. <https://doi.org/10.1016/j.biortech.2018.05.002>
- Geng, W., Jin, Y., Jameel, H., Park, S., 2015. Strategies to achieve high-solids enzymatic hydrolysis of dilute-acid pretreated corn stover. *Bioresour. Technol.* 187, 43–48. <https://doi.org/https://doi.org/10.1016/j.biortech.2015.03.067>
- Genisheva, Z., Mota, A., Mussatto, S.I., Oliveira, J.M., Teixeira, J.A., 2014. Integrated continuous winemaking process involving sequential alcoholic and malolactic fermentations with immobilized cells. *Process Biochem.* 49, 1–9. <https://doi.org/10.1016/j.procbio.2013.10.005>
- Gomes, D., Domingues, L., Gama, M., 2016. Valorizing recycled paper sludge by a bioethanol production process with cellulase recycling. *Bioresour. Technol.* 216, 637–644. <https://doi.org/10.1016/j.biortech.2016.06.004>
- Gomes, D., Gama, M., Domingues, L., 2018. Determinants on an efficient cellulase recycling process for the production of bioethanol from recycled paper sludge under high solid loadings. *Biotechnol. Biofuels* 11, 1–12. <https://doi.org/10.1186/s13068-018-1103-2>
- Gomes, D., Rodrigues, A.C., Domingues, L., Gama, M., 2015. Cellulase recycling in biorefineries—is it possible? *Appl. Microbiol. Biotechnol.* 99, 4131–4143. <https://doi.org/10.1007/s00253-015-6535-z>
- Gomes, D.G., Michelin, M., Romani, A., Domingues, L., Teixeira, J.A., 2021. Co-production of biofuels and value-added compounds from industrial *Eucalyptus globulus* bark residues using hydrothermal treatment. *Fuel* 285, 119265. <https://doi.org/10.1016/j.fuel.2020.119265>
- Gomes, D.G., Serna-Loaiza, S., Cardona, C.A., Gama, M., Domingues, L., 2018. Insights into the economic viability of cellulases recycling on bioethanol production from recycled paper sludge. *Bioresour. Technol.* 267, 347–355. <https://doi.org/10.1016/j.biortech.2018.07.056>
- Gonçalves, F.A., Ruiz, H.A., Nogueira, C.D.C., Santos, E.S. Dos, Teixeira, J.A., De Macedo, G.R., 2014. Comparison of delignified coconuts waste and cactus for fuel-ethanol production by the simultaneous and semi-simultaneous saccharification and fermentation strategies. *Fuel* 131, 66–76. <https://doi.org/10.1016/j.fuel.2014.04.021>
- Grewal, J., Ahmad, R., Khare, S.K., 2017. Development of cellulase-nanoconjugates with enhanced ionic liquid and thermal stability for in situ lignocellulose saccharification. *Bioresour. Technol.* 242, 236–243. <https://doi.org/10.1016/j.biortech.2017.04.007>
- Hassan, S.S., Williams, G.A., Jaiswal, A.K., 2019. Moving towards the second generation of lignocellulosic biorefineries in the EU: Drivers, challenges, and opportunities. *Renew. Sustain. Energy Rev.* 101,

- 590–599. <https://doi.org/10.1016/j.rser.2018.11.041>
- Hegedüs, I., Hancsók, J., Nagy, E., 2012. Stabilization of the cellulase enzyme complex as enzyme nanoparticle. *Appl. Biochem. Biotechnol.* 168, 1372–1383. <https://doi.org/10.1007/s12010-012-9863-9>
- Hegedus, I., Nagy, E., 2015. Stabilization of activity of cellulase and hemicellulase enzymes by covering with polyacrylamide layer. *Chem. Eng. Process. Process Intensif.* 95, 143–150. <https://doi.org/10.1016/j.cep.2015.06.005>
- Homaei, A.A., Sariri, R., Vianello, F., Stevanato, R., 2013. Enzyme immobilization: an update. *J. Biol. Chem.* 6, 185–205. <https://doi.org/10.1007/s12154-013-0102-9>
- Hussain, J., Khan, A., Zhou, K., 2020. The impact of natural resource depletion on energy use and CO<sub>2</sub> emission in Belt & Road Initiative countries: A cross-country analysis. *Energy* 199, 117409. <https://doi.org/https://doi.org/10.1016/j.energy.2020.117409>
- Ikwebe, J., Harvey, A.P., 2020. Fuel ethanol production from cassava (*Manihot esculenta* Crantz) in an oscillatory baffled reactor. *Biofuels* 11, 451–457. <https://doi.org/10.1080/17597269.2017.1370886>
- Ikwebe, J., Harvey, A.P., 2015. Enzymatic saccharification of cellulose: A study of mixing and agitation in an oscillatory baffled reactor and a stirred tank reactor. *Biofuels* 6, 203–208. <https://doi.org/10.1080/17597269.2015.1078560>
- Ingle, A.P., Rathod, J., Pandit, R., Silverio da Silva, S., Rai, M., 2017. Comparative evaluation of free and immobilized cellulase for enzymatic hydrolysis of lignocellulosic biomass for sustainable bioethanol production. *Cellulose* 24, 5529–5540. <https://doi.org/10.1007/s10570-017-1517-1>
- Jampala, P., Preethi, M., Ramanujam, S., Harish, B.S., Uppuluri, K.B., Anbazhagan, V., 2017. Immobilization of levan-xylanase nanohybrid on an alginate bead improves xylanase stability at wide pH and temperature. *Int. J. Biol. Macromol.* 95, 843–849. <https://doi.org/10.1016/j.ijbiomac.2016.12.012>
- Jesus, M., Romani, A., Mata, F., Domingues, L., 2022. Current options in the valorisation of vine pruning residue for the production of biofuels, biopolymers, antioxidants, and bio-composites following the concept of biorefinery: A review. *Polymers*. 14. <https://doi.org/10.3390/polym14091640>
- Jesus, M.S., Romani, A., Genisheva, Z., Teixeira, J.A., Domingues, L., 2017. Integral valorization of vine pruning residue by sequential autohydrolysis stages. *J. Clean. Prod.* 168, 74–86. <https://doi.org/10.1016/j.jclepro.2017.08.230>
- Jia, J., Zhang, W., Yang, Z., Yang, X., Wang, N., Yu, X., 2017. Novel magnetic cross-linked cellulase aggregates with a potential application in lignocellulosic biomass bioconversion. *Molecules* 22, 269. <https://doi.org/10.3390/molecules22020269>
- Jiang, W., Pei, R., Zhou, S.F., 2020. 3D-printed xylanase within biocompatible polymers as excellent catalyst for lignocellulose degradation. *Chem. Eng. J.* 400, 125920. <https://doi.org/10.1016/j.cej.2020.125920>
- Jørgensen, H., Pinelo, M., 2017. Enzyme recycling in lignocellulosic biorefineries. *Biofuels, Bioprod. Biorefining* 11, 150–167. <https://doi.org/10.1002/bbb.1724>
- Karp, S.G., Medina, J.D.C., Letti, L.A.J., Woiciechowski, A.L., de Carvalho, J.C., Schmitt, C.C., de Oliveira Penha, R., Kumlehn, G.S., Soccol, C.R., 2021. Bioeconomy and biofuels: the case of sugarcane ethanol in Brazil. *Biofuels, Bioprod. Biorefining* 15, 899–912. <https://doi.org/10.1002/bbb.2195>

- Karube, I., Tanaka, S., Shirai, T., Suzuki, S., 1977. Hydrolysis of cellulose in a cellulase-bead fluidized bed reactor. *Biotechnol. Bioeng.* 19, 1183–1191. <https://doi.org/10.1002/bit.260190808>
- Kaur, P., Taggar, M.S., Kalia, A., 2020. Characterization of magnetic nanoparticle–immobilized cellulases for enzymatic saccharification of rice straw. *Biomass Convers. Biorefinery* 11, 955–969. <https://doi.org/10.1007/s13399-020-00628-x>
- Kazenwadel, F., Biegert, E., Wohlgemuth, J., Wagner, H., Franzreb, M., 2016. A 3D-printed modular reactor setup including temperature and pH control for the compartmentalized implementation of enzyme cascades. *Eng. Life Sci.* 16, 560–567. <https://doi.org/10.1002/elsc.201600007>
- Khorshidi, K.J., Lenjannezhadian, H., Jamalana, M., Zeinali, M., 2016. Preparation and characterization of nanomagnetic cross-linked cellulase aggregates for cellulose bioconversion. *J. Chem. Technol. Biotechnol.* 91, 539–546. <https://doi.org/10.1002/jctb.4615>
- Khoshnevisan, K., Bordbar, A.-K., Zare, D., Davoodi, D., Noruzi, M., Barkhi, M., Tabatabaei, M., 2011. Immobilization of cellulase enzyme on superparamagnetic nanoparticles and determination of its activity and stability. *Chem. Eng. J.* 171, 669–673. <https://doi.org/10.1016/j.cej.2011.04.039>
- Kim, Y., Ximenes, E., Mosier, N.S., Ladisch, M.R., 2011. Soluble inhibitors/deactivators of cellulase enzymes from lignocellulosic biomass. *Enzyme Microb. Technol.* 48, 408–415. <https://doi.org/10.1016/j.enzmictec.2011.01.007>
- Koppram, R., Tomás-Pejó, E., Xiros, C., Olsson, L., 2014. Lignocellulosic ethanol production at high-gravity: Challenges and perspectives. *Trends Biotechnol.* 32, 46–53. <https://doi.org/10.1016/j.tibtech.2013.10.003>
- Kristensen, J.B., Felby, C., Jørgensen, H., 2009. Yield-determining factors in high-solids enzymatic hydrolysis of lignocellulose. *Biotechnol. Biofuels* 2, 1–10. <https://doi.org/10.1186/1754-6834-2-11>
- Kumar, A., Chandra, R., 2020. Ligninolytic enzymes and its mechanisms for degradation of lignocellulosic waste in environment. *Heliyon* 6, e03170. <https://doi.org/10.1016/j.heliyon.2020.e03170>
- Kumar, A., Singh, S., Tiwari, R., Goel, R., Nain, L., 2017. Immobilization of indigenous holocellulase on iron oxide (Fe<sub>2</sub>O<sub>3</sub>) nanoparticles enhanced hydrolysis of alkali pretreated paddy straw. *Int. J. Biol. Macromol.* 96, 538–549. <https://doi.org/10.1016/j.ijbiomac.2016.11.109>
- Kumar, G., Dharmaraja, J., Arvindnarayan, S., Shoban, S., Bakonyi, P., Dattatray Saratale, G., Nemestóthy, N., Bélafi-Bakó, K., Yoon, J.-J., Kim, S.-H., 2019. A comprehensive review on thermochemical, biological, biochemical and hybrid conversion methods of bio-derived lignocellulosic molecules into renewable fuels. *Fuel* 251, 352–367. <https://doi.org/10.1016/j.fuel.2019.04.049>
- Kumar, S., Morya, V., Gadhavi, J., Vishnoi, A., Singh, J., Datta, B., 2019. Investigation of nanoparticle immobilized cellulase: nanoparticle identity, linker length and polyphenol hydrolysis. *Heliyon* 5, e01702. <https://doi.org/10.1016/j.heliyon.2019.e01702>
- Kumar, S., Sharma, P., Ratrey, P., Datta, B., 2016. Reusable nanobiocatalysts for the efficient extraction of pigments from orange peel. *J. Food Sci. Technol.* 53, 3013–3019. <https://doi.org/10.1007/s13197-016-2272-2>
- Levasseur, A., Drula, E., Lombard, V., Coutinho, P.M., Henrissat, B., 2013. Expansion of the enzymatic repertoire of the CAZy database to integrate auxiliary redox enzymes. *Biotechnol. Biofuels* 6, 1–14. <https://doi.org/10.1186/1754-6834-6-41>

- Lindeque, R.M., Woodley, J.M., 2019. Reactor selection for effective continuous biocatalytic production of pharmaceuticals. *Catalysts* 9, 262. <https://doi.org/10.3390/catal9030262>
- Liu, M., Yong, Q., Lian, Z., Huang, C., Yu, S., 2020. Continuous bioconversion of oleuropein from olive leaf extract to produce the bioactive product hydroxytyrosol using carrier-immobilized enzyme. *Appl. Biochem. Biotechnol.* 190, 148–165. <https://doi.org/10.1007/s12010-019-03081-3>
- Liu, Y., Bai, C., Liu, Q., Xu, Q., Qian, Z., Peng, Q., Yu, J., Xu, M., Zhou, X., Zhang, Y., Cai, M., 2019. Engineered ethanol-driven biosynthetic system for improving production of acetyl-CoA derived drugs in Crabtree-negative yeast. *Metab. Eng.* 54, 275–284. <https://doi.org/10.1016/j.ymben.2019.05.001>
- Long, J., Fu, Y., Zu, Y., Li, J., Wang, W., Gu, C., Luo, M., 2011. Ultrasound-assisted extraction of flaxseed oil using immobilized enzymes. *Bioresour. Technol.* 102, 9991–9996. <https://doi.org/https://doi.org/10.1016/j.biortech.2011.07.104>
- Lu, M., He, D., Li, J., Han, L., Xiao, W., 2021. Rheological characterization of ball-milled corn stover with different fragmentation scales at high-solids loading. *Ind. Crops Prod.* 167, 113517. <https://doi.org/10.1016/j.indcrop.2021.113517>
- Maalej-Achouri, I., Guerfali, M., Gargouri, A., Belghith, H., 2009. Production of xylo-oligosaccharides from agro-industrial residues using immobilized *Talaromyces thermophilus* xylanase. *J. Mol. Catal. B Enzym.* 59, 145–152. <https://doi.org/10.1016/j.molcatb.2009.02.003>
- Markit, I., 2018. London Energy Briefing. European power: En route for the energy transition.
- Masngut, N., Harvey, A.P., Ikwebe, J., 2010. Potential uses of oscillatory baffled reactors for biofuel production. *Biofuels* 1, 605–619. <https://doi.org/10.4155/bfs.10.38>
- Mayolo-Deloya, K., González-González, M., Rito-Palomares, M., 2020. Laccases in food industry: Bioprocessing, potential industrial and biotechnological applications. *Front. Bioeng. Biotechnol.* 8, 1–8. <https://doi.org/10.3389/fbioe.2020.00222>
- Melander, C., Bengtsson, M., Schagerlöf, H., Tjerneld, F., Laurell, T., Gorton, L., 2005. Investigation of micro-immobilised enzyme reactors containing endoglucanases for efficient hydrolysis of cellodextrins and cellulose derivatives. *Anal. Chim. Acta* 550, 182–190. <https://doi.org/10.1016/j.aca.2005.06.070>
- Miao, X., Pi, L., Fang, L., Wu, R., Xiong, C., 2016. Application and characterization of magnetic chitosan microspheres for enhanced immobilization of cellulase. *Biocatal. Biotransformation* 34, 272–282. <https://doi.org/10.1080/10242422.2016.1247830>
- Minteer, S.D., 2016. Cell-free biotechnologies, in: *Biotechnology for Biofuel Production and Optimization*. Elsevier B.V., pp. 433–448. <https://doi.org/10.1016/B978-0-444-63475-7.00016-9>
- Mo, H., Qiu, J., Yang, C., Zang, L., Sakai, E., 2020. Preparation and characterization of magnetic polyporous biochar for cellulase immobilization by physical adsorption. *Cellulose* 27, 4963–4973. <https://doi.org/10.1007/s10570-020-03125-6>
- Muthuvelu, K.S., Rajarathinam, R., Selvaraj, R.N., Rajendren, V.B., 2020. A novel method for improving laccase activity by immobilization onto copper ferrite nanoparticles for lignin degradation. *Int. J. Biol. Macromol.* 152, 1098–1107. <https://doi.org/10.1016/j.ijbiomac.2019.10.198>
- Nguyen, H.H., Kim, M., 2017. An overview of techniques in enzyme immobilization. *Appl. Sci. Converg. Technol.* 26, 157–163. <https://doi.org/10.5757/asct.2017.26.6.157>
- Nguyen, L.T., Neo, K.R.S., Yang, K.L., 2015. Continuous hydrolysis of carboxymethyl cellulose with



- cellulase aggregates trapped inside membranes. *Enzyme Microb. Technol.* 78, 34–39. <https://doi.org/10.1016/j.enzmictec.2015.06.005>
- OECD/FAO, 2021. OECD-FAO Agricultural Outlook 2021-2030. OECD Publishing, Paris. <https://doi.org/https://doi.org/10.1787/19428846-en>
- Pang, S., 2019. Advances in thermochemical conversion of woody biomass to energy, fuels and chemicals. *Biotechnol. Adv.* 37, 589–597. <https://doi.org/10.1016/j.biotechadv.2018.11.004>
- Paone, E., Tabanelli, T., Mauriello, F., 2019. The rise of lignin biorefinery. *Curr. Opin. Green Sustain. Chem.* 24, 1–6. <https://doi.org/10.1016/j.cogsc.2019.11.004>
- Papadopoulou, A., Zarafeta, D., Galanopoulou, A.P., Stamatis, H., 2019. Enhanced catalytic performance of *Trichoderma reesei* cellulase immobilized on magnetic hierarchical porous carbon nanoparticles. *Protein J.* 38, 640–648. <https://doi.org/10.1007/s10930-019-09869-w>
- Parisi, C., 2018. Biorefineries distribution in the EU. <https://doi.org/10.2760/126478>
- Payne, C.M., Knott, B.C., Mayes, H.B., Hansson, H., Himmel, M.E., Sandgren, M., Ståhlberg, J., Beckham, G.T., 2015. Fungal cellulases. *Chem. Rev.* 115, 1308–1448. <https://doi.org/10.1021/cr500351c>
- Paz-Cedeno, F.R., Carceller, J.M., Iborra, S., Donato, R.K., Godoy, A.P., Veloso de Paula, A., Monti, R., Corma, A., Masarin, F., 2021. Magnetic graphene oxide as a platform for the immobilization of cellulases and xylanases: Ultrastructural characterization and assessment of lignocellulosic biomass hydrolysis. *Renew. Energy* 164, 491–501. <https://doi.org/10.1016/j.renene.2020.09.059>
- Pelkmans, L., 2021. IEA Bioenergy countries' report.
- Pinheiro, T., Coelho, E., Romani, A., Domingues, L., 2019. Intensifying ethanol production from brewer's spent grain waste: Use of whole slurry at high solid loadings. *N. Biotechnol.* 53, 1–8. <https://doi.org/10.1016/j.nbt.2019.06.005>
- Pino, M.S., Pedraza Segura, L., Acosta, R., Vallejos, M.E., Zanuso, E., Rodríguez-Jasso, Rosa M. Toribio Cuaya, H., Larragoiti Kuri, J., Area, M.C., Nabarlantz, D., Ruiz, H.A., 2020. Biomass fractionation to bio-based products in terms of biorefinery concept, in: Nevárez-Moorillón, G.V., Prado-Barragán, A., Martínez-Hernández, J.L., Aguilar, C.N. (Eds.), *Food Microbiology and Biotechnology*. Academic Apple Press, pp. 395–427.
- Pino, M.S., Rodríguez-Jasso, R.M., Michelin, M., Flores-Gallegos, A.C., Morales-Rodríguez, R., Teixeira, J.A., Ruiz, H.A., 2018. Bioreactor design for enzymatic hydrolysis of biomass under the biorefinery concept. *Chem. Eng. J.* 347, 119–136. <https://doi.org/10.1016/j.cej.2018.04.057>
- Pires, E.J., Ruiz, H.A., Teixeira, J.A., Vicente, A.A., 2012. A new approach on brewer's spent grains treatment and potential use as lignocellulosic yeast cells carriers. *J. Agric. Food Chem.* 60, 5994–5999. <https://doi.org/10.1021/jf300299m>
- Pithani, S., Karlsson, S., Emtenäs, H., Öberg, C.T., 2019. Using spinchem rotating bed reactor technology for immobilized enzymatic reactions: A case study. *Org. Process Res. Dev.* 23, 1926–1931. <https://doi.org/10.1021/acs.oprd.9b00240>
- Pontes, R., Romani, A., Michelin, M., Domingues, L., Teixeira, J., Nunes, J., 2018. Comparative autohydrolysis study of two mixtures of forest and marginal land resources for co-production of biofuels and value-added compounds. *Renew. Energy* 128, 20–29. <https://doi.org/10.1016/j.renene.2018.05.055>
- Qi, B., Luo, J., Wan, Y., 2018. Immobilization of cellulase on a core-shell structured metal-organic

- framework composites: Better inhibitors tolerance and easier recycling. *Bioresour. Technol.* 268, 577–582. <https://doi.org/10.1016/j.biortech.2018.07.115>
- Rai, S.K., Narnoliya, L.K., Sangwan, R.S., Yadav, S.K., 2018. Self-assembled hybrid nanoflowers of manganese phosphate and *L*-arabinose isomerase: A stable and recyclable nanobiocatalyst for equilibrium level conversion of d-galactose to d-tagatose. *ACS Sustain. Chem. Eng.* 6, 6296–6304. <https://doi.org/10.1021/acssuschemeng.8b00091>
- Ramesh, A., Harani Devi, P., Chattopadhyay, S., Kavitha, M., 2020. Commercial applications of microbial enzymes, in: Arora, N.K., Mishra, J., Mishra, V. (Eds.), *Microbial Enzymes: Roles and Applications in Industries*. Springer Singapore, Singapore, pp. 137–184. [https://doi.org/10.1007/978-981-15-1710-5\\_6](https://doi.org/10.1007/978-981-15-1710-5_6)
- Ravindran, R., Jaiswal, A.K., 2019. Current advances in immobilization techniques of enzymes. *Enzym. Fuell Cells; Mater. Appl.* 44, 51–72.
- Reis, N., Gonçalves, C.N., Vicente, A.A., Teixeira, J.A., 2006. Proof-of-concept of a novel micro-bioreactor for fast development of industrial bioprocesses. *Wiley Interisci.* 744–753. <https://doi.org/10.1002/bit.21035>
- Reis, N., Harvey, A.P., Mackley, M.R., Vicente, A.A., Teixeira, J.A., 2005. Fluid mechanics and design aspects of a novel oscillatory flow screening mesoreactor. *Chem. Eng. Res. Des.* 83, 357–371. <https://doi.org/10.1205/cherd.03401>
- Renewable Fuels Association, 2020. Ethanol industry outlook [WWW Document]. URL <https://ethanolrfa.org/publications/outlook> (accessed 8.30.20).
- Ritchie, H., Roser, M., Rosado, P., 2020. Energy. Our World Data. <https://doi.org/https://ourworldindata.org/energy>
- Rodríguez-Couto, S., 2018. Solid-state fermentation for laccases production and their applications, in: *Current Developments in Biotechnology and Bioengineering*. pp. 211–234. <https://doi.org/10.1016/b978-0-444-63990-5.00011-6>
- Romaní, A., Morais, E.S., Soares, P.O., Freire, M.G., Freire, C.S.R., Silvestre, A.J.D., Domingues, L., 2020. Aqueous solutions of deep eutectic systems as reaction media for the saccharification and fermentation of hardwood xylan into xylitol. *Bioresour. Technol.* 311, 123524. <https://doi.org/10.1016/j.biortech.2020.123524>
- Romaní, A., Ruiz, H.A., Pereira, F.B., Domingues, L., Teixeira, J.A., 2014. Effect of hemicellulose liquid phase on the enzymatic hydrolysis of autohydrolyzed *Eucalyptus globulus* wood. *Biomass Convers. Biorefinery* 4, 77–86. <https://doi.org/10.1007/s13399-013-0093-3>
- Romero-Fernández, M., Moreno-Perez, S., H. Orrego, A., Martins de Oliveira, S., I. Santamaría, R., Díaz, M., Guisan, J.M., Rocha-Martin, J., 2018. Designing continuous flow reaction of xylan hydrolysis for xylooligosaccharides production in packed-bed reactors using xylanase immobilized on methacrylic polymer-based supports. *Bioresour. Technol.* 266, 249–258. <https://doi.org/10.1016/j.biortech.2018.06.070>
- Romero-Fernández, M., Paradisi, F., 2020. General overview on immobilization techniques of enzymes for biocatalysis, in: *Catalyst Immobilization*. John Wiley & Sons, Ltd, pp. 409–435. <https://doi.org/10.1002/9783527817290.ch12>
- Roth, H.C., Schwaminger, S.P., Peng, F., Berensmeier, S., 2016. Immobilization of cellulase on magnetic nanocarriers. *ChemistryOpen* 5, 183–187. <https://doi.org/10.1002/open.201600028>

- Ruiz, H.A., Conrad, M., Sun, S.-N., Sanchez, A., Rocha, G.J.M., Romani, A., Castro, E., Torres, A., Rodríguez-Jasso, R.M., Andrade, L.P., Smirnova, I., Sun, R.-C., Meyer, A.S., 2020. Engineering aspects of hydrothermal pretreatment: From batch to continuous operation, scale-up and pilot reactor under biorefinery concept. *Bioresour. Technol.* 299, 122685. <https://doi.org/10.1016/J.BIORTECH.2019.122685>
- Ruiz, H.A., Galbe, M., Garrote, G., Ramirez-Gutierrez, D.M., Ximenes, E., Sun, S.N., Lachos-Perez, D., Rodríguez-Jasso, R.M., Sun, R.C., Yang, B., Ladisch, M.R., 2021. Severity factor kinetic model as a strategic parameter of hydrothermal processing (steam explosion and liquid hot water) for biomass fractionation under biorefinery concept. *Bioresour. Technol.* 342. <https://doi.org/10.1016/j.biortech.2021.125961>
- Sada, E., Katoh, S., Shiozawa, M., Fukui, T., 1981. Performance of fluidized-bed reactors utilizing magnetic fields. *Biotechnol. Bioeng.* 23, 2561–2567. <https://doi.org/10.1002/bit.260231113>
- Saha, K., Verma, P., Sikder, J., Chakraborty, S., Curcio, S., 2019. Synthesis of chitosan-cellulase nanohybrid and immobilization on alginate beads for hydrolysis of ionic liquid pretreated sugarcane bagasse. *Renew. Energy* 133, 66–76. <https://doi.org/10.1016/j.renene.2018.10.014>
- Saini, A., Aggarwal, N.K., Yadav, A., 2018. Microbial cellulases: Role in second-generation ethanol production, in: *Microbial Bioprospecting for Sustainable Development*. pp. 167–187. [https://doi.org/10.1007/978-981-13-0053-0\\_8](https://doi.org/10.1007/978-981-13-0053-0_8)
- Sánchez-Ramírez, J., Martínez-Hernández, J.L., Segura-Ceniceros, P., López, G., Saade, H., Medina-Morales, M.A., Ramos-González, R., Aguilar, C.N., Ilyina, A., 2017. Cellulases immobilization on chitosan-coated magnetic nanoparticles: application for *Agave Atrovirens* lignocellulosic biomass hydrolysis. *Bioprocess Biosyst. Eng.* 40, 9–22. <https://doi.org/10.1007/s00449-016-1670-1>
- Sarker, T.R., Pattnaik, F., Nanda, S., Dalai, A.K., Meda, V., Naik, S., 2021. Hydrothermal pretreatment technologies for lignocellulosic biomass: A review of steam explosion and subcritical water hydrolysis. *Chemosphere* 284, 131372. <https://doi.org/10.1016/j.chemosphere.2021.131372>
- Schmieg, B., Döbber, J., Kirschhöfer, F., Pohl, M., Franzreb, M., 2019. Advantages of hydrogel-based 3D-printed enzyme reactors and their limitations for biocatalysis. *Front. Bioeng. Biotechnol.* 6, 211. <https://doi.org/10.3389/fbioe.2018.00211>
- Sern, W.K., Takriff, M.S., Kamarudin, S.K., Talib, M.Z.M., Hasan, N., 2012. Numerical simulation of fluid flow behaviour on scale up of oscillatory baffled column. *J. Eng. Sci. Technol.* 7, 119–130.
- Shanmugam, S., Krishnaswamy, S., Chandrababu, R., Veerabagu, U., Pugazhendhi, A., Mathimani, T., 2020. Optimal immobilization of *Trichoderma asperellum* laccase on polymer coated Fe<sub>3</sub>O<sub>4</sub>@SiO<sub>2</sub> nanoparticles for enhanced biohydrogen production from delignified lignocellulosic biomass. *Fuel* 273, 117777. <https://doi.org/10.1016/j.fuel.2020.117777>
- Sheldon, R.A., Woodley, J.M., 2018. Role of Biocatalysis in sustainable chemistry. *Chem. Rev.* 118, 801–838. <https://doi.org/10.1021/acs.chemrev.7b00203>
- Shiva, Climent Barba, F., Rodríguez-Jasso, R.M., Sukumaran, R.K., Ruiz, H.A., 2022. High-solids loading processing for an integrated lignocellulosic biorefinery: Effects of transport phenomena and rheology – A review. *Bioresour. Technol.* 127044. <https://doi.org/10.1016/j.biortech.2022.127044>
- Sigurdardóttir, S.B., Lehmann, J., Ovtar, S., Grivel, J.-C., Della Negra, M., Kaiser, A., Pinelo, M., 2018. Enzyme immobilization on inorganic surfaces for membrane reactor applications: mass transfer challenges, enzyme leakage and reuse of materials. *Adv. Synth. Catal.* 360, 2578–2607. <https://doi.org/10.1002/adsc.201800307>

- Stonestreet, P., Harvey, A.P., 2002. A mixing-based design methodology for continuous oscillatory flow reactors. *Chem. Eng. Res. Des.* 80, 31–44. <https://doi.org/10.1205/026387602753393204>
- Sui, Y., Cui, Y., Xia, G., Peng, X., Yuan, G., Sun, G., 2019. A facile route to preparation of immobilized cellulase on polyurea microspheres for improving catalytic activity and stability. *Process Biochem.* 87, 73–82. <https://doi.org/10.1016/j.procbio.2019.09.002>
- Sun, Shaoni, Sun, Shaolong, Cao, X., Sun, R., 2016. The role of pretreatment in improving the enzymatic hydrolysis of lignocellulosic materials. *Bioresour. Technol.* 199, 49–58. <https://doi.org/10.1016/j.biortech.2015.08.061>
- Tan, L., Tan, Z., Feng, H., Qiu, J., 2018. Cellulose as a template to fabricate a cellulase-immobilized composite with high bioactivity and reusability. *New J. Chem.* 42, 1665–1672. <https://doi.org/10.1039/C7NJ03271D>
- Tantayotai, P., Rattanaporn, K., Tapaamorndech, S., Cheenkachorn, K., Sriariyanun, M., 2019. Analysis of an ionic liquid and salt tolerant microbial consortium which is useful for enhancement of enzymatic hydrolysis and biogas production. *Waste and Biomass Valorization* 10, 1481–1491. <https://doi.org/10.1007/s12649-017-0186-5>
- Thompson, M.P., Peñafiel, I., Cosgrove, S.C., Turner, N.J., 2019. Biocatalysis using immobilized enzymes in continuous flow for the synthesis of fine chemicals. *Org. Process Res. Dev.* 23, 9–18. <https://doi.org/10.1021/acs.oprd.8b00305>
- Tsai, C.-T., Meyer, A.S., 2014. Enzymatic cellulose hydrolysis: Enzyme reusability and visualization of  $\beta$ -glucosidase immobilized in calcium alginate. *Molecules* 19, 19390–19406. <https://doi.org/10.3390/molecules191219390>
- Ungurean, M., Csanádi, Z., Gubicza, L., Péter, F., 2014. An integrated process of ionic liquid pretreatment and enzymatic hydrolysis of lignocellulosic biomass with immobilised cellulase. *BioResources* 9, 6100–6116. <https://doi.org/10.15376/biores.9.4.6100-6116>
- Venardos, D., Klei, H.E., Sundstrom, D.W., 1980. Conversion of cellobiose to glucose using immobilized  $\beta$ -glucosidase reactors. *Enzyme Microb. Technol.* 2, 112–116. [https://doi.org/10.1016/0141-0229\(80\)90065-4](https://doi.org/10.1016/0141-0229(80)90065-4)
- Verma, M.L., Kumar, S., Das, A., Randhawa, J.S., Chamundeeswari, M., 2020. Chitin and chitosan-based support materials for enzyme immobilization and biotechnological applications. *Environ. Chem. Lett.* 18, 315–323. <https://doi.org/10.1007/s10311-019-00942-5>
- Wang, Y., Chen, D., Wang, G., Zhao, C., Ma, Y., Yang, W., 2018. Immobilization of cellulase on styrene/maleic anhydride copolymer nanoparticles with improved stability against pH changes. *Chem. Eng. J.* 336, 152–159. <https://doi.org/10.1016/j.cej.2017.11.030>
- Weiss, N.D., Felby, C., Thygesen, L.G., 2019. Enzymatic hydrolysis is limited by biomass-water interactions at high-solids: Improved performance through substrate modifications. *Biotechnol. Biofuels* 12, 1–13. <https://doi.org/10.1186/s13068-018-1339-x>
- Xu, J., Sheng, Z., Wang, X., Liu, X., Xia, J., Xiong, P., He, B., 2016. Enhancement in ionic liquid tolerance of cellulase immobilized on PEGylated graphene oxide nanosheets: Application in saccharification of lignocellulose. *Bioresour. Technol.* 200, 1060–1064. <https://doi.org/10.1016/j.biortech.2015.10.070>
- Ye, J., Chu, T., Chu, J., Gao, B., He, B., 2019. A versatile approach for enzyme immobilization using chemically modified 3D-printed scaffolds. *ACS Sustain. Chem. Eng.* 7, 18048–18054. <https://doi.org/10.1021/acssuschemeng.9b04980>

- Zabed, H., Sahu, J.N., Suely, A., Boyce, A.N., Faruq, G., 2017. Bioethanol production from renewable sources: Current perspectives and technological progress. *Renew. Sustain. Energy Rev.* 71, 475–501. <https://doi.org/10.1016/j.rser.2016.12.076>
- Zang, L., Qiu, J., Wu, X., Zhang, W., Sakai, E., Wei, Y., 2014. Preparation of magnetic chitosan nanoparticles as support for cellulase immobilization. *Ind. Eng. Chem. Res.* 53, 3448–3454. <https://doi.org/10.1021/ie404072s>
- Zanuso, E., Lara-Flores, A.A., Aguilar, D.L., Velazquez-Lucio, J., Aguilar, C.N., Rodriguez-Jasso, R.M., Ruiz, H.A., 2017. Kinetic modeling, operational conditions, and biorefinery products from hemicellulose: Depolymerization and solubilization during hydrothermal processing, in: Ruiz, H., Hedegaard Thomsen, M., Trajano, H. (Eds.), *Hydrothermal Processing in Biorefineries*. [https://doi.org/10.1007/978-3-319-56457-9\\_5](https://doi.org/10.1007/978-3-319-56457-9_5)
- Zdarta, J., Meyer, A.S., Jesionowski, T., Pinelo, M., 2018. A general overview of support materials for enzyme immobilization: characteristics, properties, practical utility. *Catalyst* 8, 92. <https://doi.org/10.3390/catal8020092>
- Zhai, R., Hu, J., Saddler, J.N., 2018. The inhibition of hemicellulosic sugars on cellulose hydrolysis are highly dependant on the cellulase productive binding, processivity, and substrate surface charges. *Bioresour. Technol.* 258, 79–87. <https://doi.org/10.1016/j.biortech.2017.12.006>
- Zhang, F., Bunternngsook, B., Li, J.-X., Zhao, X.-Q., Champreda, V., Liu, C.-G., Bai, F.-W., 2019. Regulation and production of lignocellulolytic enzymes from *Trichoderma reesei* for biofuels production, in: Li, Y., Ge, X. (Eds.), *Advances in Bioenergy, Advances in Bioenergy*. Elsevier, pp. 79–119. <https://doi.org/https://doi.org/10.1016/bs.aibe.2019.03.001>
- Zhang, H., Hua, S.F., Zhang, L., 2019. Co-immobilization of cellulase and glucose oxidase on graphene oxide by covalent bonds: a biocatalytic system for one-pot conversion of gluconic acid from carboxymethyl cellulose. *J. Chem. Technol. Biotechnol.* 95, 1116–1125. <https://doi.org/10.1002/jctb.6296>
- Zhang, Y., He, H., Liu, Y., Wang, Y., Huo, F., Fan, M., Adidharma, H., Li, X., Zhang, S., 2019. Recent progress in theoretical and computational studies on the utilization of lignocellulosic materials. *Green Chem.* 21, 9–35. <https://doi.org/10.1039/c8gc02059k>
- Zheng, P., Wang, J., Lu, C., Xu, Y., Sun, Z., 2013. Immobilized  $\beta$ -glucosidase on magnetic chitosan microspheres for hydrolysis of straw cellulose. *Process Biochem.* 48, 683–687. <https://doi.org/10.1016/j.procbio.2013.02.027>
- Zheng, Y., Wan, X., Cheng, X., Cheng, K., Liu, Z., Dai, Z., 2020. Advanced catalytic materials for ethanol oxidation in direct ethanol fuel cells. *Catalysts* 10. <https://doi.org/10.3390/catal10020166>
- Zoghalmi, A., Paës, G., 2019. Lignocellulosic biomass: understanding recalcitrance and predicting hydrolysis. *Front. Chem.* 7, 874. <https://doi.org/10.3389/fchem.2019.00874>

## CHAPTER III

---

Cellulase immobilization on magnetic nanoparticles as strategy for enzymatic hydrolysis intensification using hydrothermally pretreated corn cob biomass

**The work reported on this chapter is published in:**

Zanuso, E., Ruiz, H.A., Domingues, L., Teixeira, J.A. 2022. Magnetic nanoparticles as support for cellulase immobilization strategy for enzymatic hydrolysis using hydrothermally pretreated corn cob biomass. *BioEnergy Research*. <https://doi.org/10.1007/s12155-021-10384-z>

**ABSTRACT**

Biorefinery comprise the application of processes and technologies to biotransform biomass efficiently and lessen the process cost. Enzymatic hydrolysis is a key process in the sugar platform to transform lignocellulosic biomass into monomeric and oligomeric sugars by using cellulolytic enzymes. A strategy to reduce cellulose costs is by immobilizing the enzymes which simplifies the biocatalyst recovery. For this strategy, the immobilization carrier plays a great role as it should fulfill the demands such as bonding availability, surface area, and magnetism / non-magnetism. This chapter is focused on the cellulase cocktail immobilization into chitosan-coated magnetic nanoparticles, which reached an immobilization of 65 mg<sub>protein</sub> per g of support. The biocatalyst was stable at 4 °C after 30 days maintaining 80% of the initial activity, and could be reused up to 13 cycles maintaining 48.8% of the initial activity. Also, pretreated corncob was used as the substrate to evaluate the hydrolysis potential of the immobilized cellulase and its reusability, thus, validating the capacity of immobilized cellulase cocktails to hydrolyze real lignocellulosic substrates, a step-forward to its implementation in lignocellulosic biorefineries, enzyme immobilization technology, and contributing to reduce the process cost.

### 3.1 INTRODUCTION

Biorefinery challenge to use biomass in a cost-effective manner through biological processes is a worldwide affair. One of the main challenges in lignocellulosic biorefineries (also known as second generation) is the enzymatic hydrolysis to fermentable sugars of the pretreated biomass (Gomes et al., 2021). This is a key step as the concentration of sugars obtained during the hydrolysis dictates the final ethanol production or alternative target compounds production (Baptista et al., 2021; Cunha et al., 2020b). Cellulases are a system of enzymes that work synergistically to hydrolyze the cellulose from pretreated lignocellulosic biomass (Pino et al., 2019; Ruiz et al., 2012). Hurdles of the enzymatic hydrolysis include the differentiate composition of feedstock and the instability and high price of the cellulolytic enzyme cocktail needed. Regardless of this, enzymatic hydrolysis is advantageous compared to acid hydrolysis as it is a low consumption energy process and causes no equipment corrosion (Barbosa et al., 2020).

Pretreatment facilitate to reduce the natural recalcitrant characteristic of lignocellulosic biomass by breaking down into its components (Kumar et al., 2020). In this sense, the integration of hydrothermal pretreatment, which involves the use of water under high temperature (150-230 °C) and pressure (approx. 4.8-28 bars), results in a pretreated lignocellulosic solid fraction - rich in cellulose - and the hemicellulose is depolymerized and solubilized on the liquid fraction (Chen et al., 2017; Zanuso et al., 2017). Hydrothermal pretreatment has been acknowledged as a strategic operation which impacts positively on the enzymatic saccharification by increasing the enzymatic susceptibility towards the pretreated lignocellulosic solid (Ruiz et al., 2021, 2020).

Research on enzymatic hydrolysis is essential not only from the biological aspect but also from the economic and environmental perspective. As reported in techno-economic analyses found in literature, the cellulolytic enzymes represent a significant cost value that is directly reflected on the ethanol final price (Larnaudie et al., 2019; Liu et al., 2016; Rijn et al., 2018). The enzyme cost contributes around 15% to the overall cost of an operating biorefinery, being the second largest contributor after feedstock (Boakye-Boaten et al., 2017). Moreover, life cycle assessment studies show that the enzyme dosage in a biorefinery process largely contributes to the global warming impact (GWI) varying from 2.8-16 g CO<sub>2</sub>eq/g enzyme, corresponding to 11-62% of the GWI of ethanol production (Papadaskalopoulou et al., 2019). These impacts and costs can be reduced by enhancing the use of enzymes and/or by recycling (Gomes et al., 2021, 2015). The economic viability of integrating a cellulases recycling system on bioethanol production has been studied and revealed a superior economic output, still, highly sensitive to the cost



of enzymes and ultrafiltration membranes (Aguilar et al., 2018).

The motive and challenge of second generation biorefinery to generate high-quality products through less pollution process that achieve industrial cost target drive researchers to consider technologies that improve the enzymatic hydrolysis, decrease the use of cellulolytic enzymes, and develop process configurations that boost the enzymatic efficiency (Aguilar et al., 2018; Oliveira et al., 2018; Pino et al., 2018; Singh et al., 2019). The benefit of enzyme immobilization for lignocellulosic bioconversion relies on the ease separation of the biocatalyst for its reuse, the storage stability as well as the stability gain in a wide range of temperatures and pH and against hydrolysate inhibitors (Abraham and Puri, 2020; Grewal et al., 2017; Qi et al., 2018). Still, the hydrolysis of real lignocellulosic substrates by immobilized enzyme cocktails faces specific challenges that only few works have addressed hindering its application in lignocellulose biorefineries (Zanusso et al., 2021).

Recently, several studies have demonstrated the successful cellulase immobilization onto different magnetic supports as magnetic graphene oxide, magnetic nanotubes, magnetic porous biochar, among many others (Mo et al., 2020; Paz-Cedeno et al., 2021; Sillu and Agnihotri, 2020). Magnetic supports hold the advantage of ease separation by applying an external magnetic field compared with other separation methods as filtration or centrifugation (Zang et al., 2014). Also, the separation operation can be done without interfering with the media, thus the contamination risk is decreased. However, there are still gaps to be filled about the immobilization of cellulase onto magnetic supports, mainly on the immobilization mechanism and the effect on the enzyme during the process, especially when enzyme cocktails are used, but also the applications on real substrate due to the challenge it implies. Corn cob processing green technologies such as autohydrolysis and enzyme saccharification are widely studied not only for its conversion to ethanol but also to added-value compounds such as xylitol and resveratrol (Aguilar-Reynosa et al., 2017; Baptista et al., 2020, 2018; Costa et al., 2021). Thus, the study and application of immobilized enzymes in hydrothermally pretreated corn cob is key for the advance of these valorization processes and will impact other lignocellulosic biomass-based processes. Also, leaning on the nature of corn cob being a dense and uniform lignocellulosic material with high energy content and low moisture, it can be considered as a model biomass (Anukam et al., 2017). In this work, as shown in Figure 3.1, a cellulases cocktail was immobilized on chitosan coated magnetic nanoparticles and the mechanism and reactions that took place are explained. Afterwards the physico-chemical and biological characterization of the immobilized cellulase was done to discern the behavior of the immobilized cellulase and its capability to be reused. Finally, an enzymatic hydrolysis assay using the immobilized cellulase on hydrothermally pretreated corn cob was carried out where free enzyme was used to compare

the glucose production and saccharification rate along the hydrolysis.

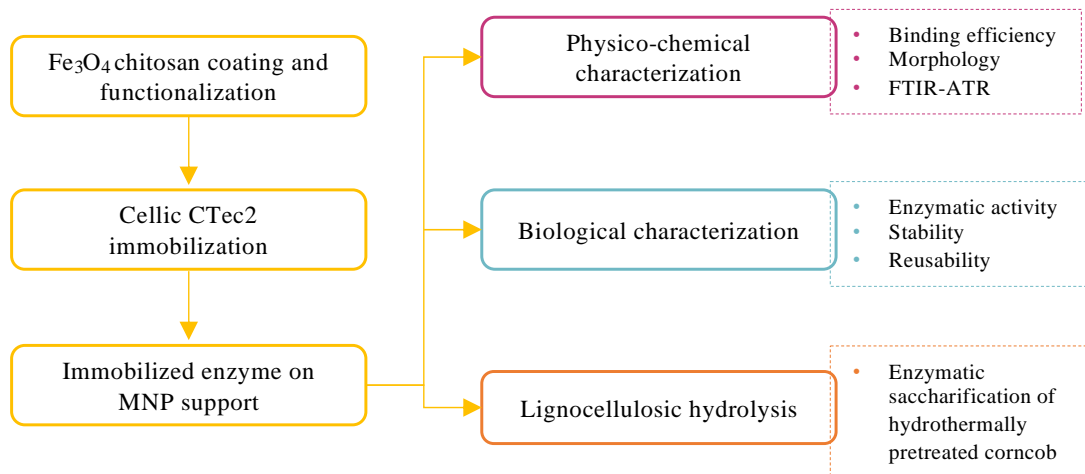


**Figure 3.1.** Schematic representation of the methodology followed in this chapter, characterization techniques used and the enzymatic hydrolysis.

## 3.2 EXPERIMENTAL METHODS

### 3.2.1 Chitosan coating and glutaraldehyde activation

Fe<sub>3</sub>O<sub>4</sub> magnetic nanoparticles (MNP) (50-100 nm; Sigma-Aldrich) were mixed in NaOH 1 M, vigorously shaken and sonicated. Then, a solution of 5 g/L of chitosan in acetic acid 1% (v/v) was prepared and stirred until chitosan was completely dissolved. The chitosan solution was added to the MNP suspension in a 1:1 ratio (v/v) so that the chitosan coated the Fe<sub>3</sub>O<sub>4</sub> nanoparticles. Afterward, the nanoparticles were magnetically separated and washed three times with ultrapure water. The chitosan coated MNP support was activated using glutaraldehyde (GA). For this, the support was added to a 2.5 % (v/v) solution of GA and incubated at 30 °C for 2 h at 150 rpm (Zang et al., 2014).

### 3.2.2 Cellulase cocktail immobilization

The activated MNP were magnetically separated and washed thrice with ultrapure water to remove unreacted GA. Subsequently, in conical tubes, 10 mg of activated MNP were mixed with a citrate buffer solution (0.1 M) containing 10 mg of cellulase cocktail protein per mL (Cellulase, enzyme blend [Cellic CTec2]; Sigma-Aldrich) and incubated at 30 °C for 2 h at 150 rpm (Zang et al., 2014). To test the enzyme-particle saturation, the same immobilization procedure was carried out but adding different enzyme loading (10, 50 and 100 mg of cellulase cocktail).

### **3.2.3 Physico-chemical characterization of MNP**

#### **3.2.3.1 FTIR-ATR characterization**

In order to confirm the immobilization of the cellulase cocktail onto the support through characteristic functional groups, Fourier transform infrared spectroscopy – attenuated total reflection (FTIR-ATR) (Bruker ALPHA II's) was performed. The spectra were recorded in a scanning range of 400-4000  $\text{cm}^{-1}$  (Hoarau et al., 2017). The functional groups related with the enzyme are amide I (C=O) and amide II (N-H and C-N).

#### **3.2.3.2 Microscopic morphology**

The microscopic morphology of bare nanoparticles ( $\text{Fe}_3\text{O}_4$ ),  $\text{Fe}_3\text{O}_4$  coated with chitosan and the immobilized cellulase was evaluated by transmission electron microscopy (TEM) using JEOL (JEM 2100 - HT – 80-200 kV LaB6 gun, JEOL Ltd, Japan) and scanning electron microscope (SEM) using a desktop scanning electron microscope (Phenom ProX with EDS detector [Phenom-World BV, Netherlands]). For TEM, the images were digital recorded using an UltraScan® 4000 CCD camera (Oneview, Gatan, USA). Samples were deposited onto grids coated with an ultrathin carbon film (400 mesh, approx. grid hole size of 2  $\mu\text{m}$ , PELCO®, TED PELLA INC., USA) and dried at room temperature for 24 h. Later micrographs of the samples were taken (Azevedo et al., 2020). For SEM, the immobilized cellulases were added to aluminum pin stubs with electrically conductive carbon adhesive tape (PLECO Tabs™) and dried for 24 h. Samples were imaged without coating.

### **3.2.4 Biological characterization of the immobilized cellulase cocktail**

#### **3.2.4.1 Binding efficiency**

The binding efficiency was calculated by subtracting the protein content in the supernatant after immobilization to the protein content of the solution added (Tan et al., 2018). The protein concentration content in the enzyme cocktail was determined according to the Bradford method (Bradford, 1976). The protein content of the crude cellulase cocktail was 62.5 mg/mL.

#### **3.2.4.2 Enzyme activity determination and acetic acid tolerance**

The FPU activity of cellulase enzyme was determined by the filter paper assay following the NREL protocol (NREL/TP-510-42628). The activity of the enzymatic cocktail was 120 FPU/mL. The above result

indicates the commercial enzymatic cocktail was in high quality and suitable for further immobilization experiments. In order to avoid the limitation of the immobilized enzyme to act on the paper string used in the common filter paper assay, as recommended by Qi et al. (2018), the immobilized enzyme activity was measured using microcrystalline cellulose (Avicel PH-101) under the same reaction conditions. In this modification, one unit (U) is defined as the amount of immobilized protein (in mg) on the support that releases 1  $\mu\text{mol}$  of equivalent glucose under assay conditions. Following the immediate separation of the immobilized enzyme using an external magnetic field, the released sugar was measured using DNS with glucose as standard (Miller, 1959). To test the tolerance of the immobilized enzyme in the presence of acetic acid, an hydrolysis using CMC 1% (w/v) as substrate, at 50 °C per 1 h, and 5 g/L of acetic acid was performed. The amount of immobilized enzyme was 5 mg of MNP support, and it was compared with free enzyme using the same correspondent amount in terms of protein (Qi et al., 2018). The glucose produced was measured using DNS with glucose as standard (Miller, 1959).

### **3.2.5 Storage stability and reusability of immobilized cellulase cocktail**

For the storage stability assay, the immobilized enzymes were stored at 4 °C for 30 days. Activity was measured on day 1 and after 30 days to determine the remaining activity. To test the reusability of the biocatalyst, several hydrolysis cycles were performed for 1 h at 50 °C using CMC 1% (w/v) as substrate. After each reaction cycle, the enzyme was separated using an external magnet, washed with buffer, and added to fresh substrate to start a new cycle (Asar et al., 2020). Glucose was measured using DNS with glucose as standard (Miller, 1959).

### **3.2.6 Hydrothermal pretreatment of corn cob**

Corn cob was provided from a producer of the north region of Portugal. Hydrothermal pretreatment conditions were selected based on previous work reported by Cunha et al. (2020a). Pretreatment was carried out using a 2 L stainless steel reactor (Parr Instruments Company) equipped with a PID temperature controller (Parr 4848 Reactor Controller). Corn cob pretreatment conditions were as follow: liquid-to-solid ratio of 4 (4 g distilled water/1 g of dry oven corn cob) in a non-isothermal regime with  $T_{\text{max}}=211$  °C equivalent to a severity of  $\log R_0 \approx 3.95$  (Overend and Chornet, 1987). The untreated corn cob composition was as follows: (g per 100 g of DW) 28.79 $\pm$ 1.45 of glucan, 29.63 $\pm$ 0.45 of xylan, 3.62 $\pm$ 0.13 or arabinan, 2.58 $\pm$ 0.05 of acetyl groups and 18.58 $\pm$ 0.87 of Klason lignin (Cunha et al., 2020a). The chemical composition of the corn cob solid fraction after pretreatment was determined

according to the National Renewable Energy Laboratory protocols (Sluiter et al., 2008) and the results were as follows: (g per 100 g of DW)  $61.17 \pm 0.39$  g of glucan,  $6.33 \pm 0.17$  g of xylan,  $19.74 \pm 0.26$  g of Klason lignin,  $0.29 \pm 0.00$  g of arabinan and  $0.56 \pm 0.21$  g of acetyl groups. This fraction was used as substrate in the enzymatic saccharification step using free (as control) and immobilized cellulase cocktail.

### 3.2.7 Enzymatic saccharification of hydrothermally pretreated corn cob

For the enzymatic kinetic assay, 20 mL of a 5% (w/v) suspension of pretreated corn cob was added to 50 mL Erlenmeyer flasks. Experiments were run in triplicate and incubated at 50 °C, 180 rpm, in citrate buffer 0.05 M (Aguilar-Reynosa et al., 2017). The enzyme loading was the same in terms of protein for the free and immobilized assays. The saccharification yield was calculated following the equation 3.1 (Ruiz et al., 2012):

$$\text{Saccharification yield (\%)} = \frac{[\text{Glucose}]}{1.111f[\text{Biomass}]} \cdot 100 \quad \text{eq. 3.1}$$

Where  $[\text{Glucose}]$  is glucose concentration (g/L), 1.111 is the conversion factor of cellulose to equivalent glucose,  $f$  is the cellulose fraction in dry biomass (g/g) and  $[\text{Biomass}]$  is dry biomass concentration at the beginning of the enzymatic saccharification (g/L). Samples were withdrawn each 24 h, centrifugated for 5 minutes and the supernatants were analyzed for glucose quantification using HPLC. For HPLC analyses, a Bio-Rad Aminex HPX-87H column was used operating at 60 °C with a flow rate of 0.6 mL/min and 0.005 M H<sub>2</sub>SO<sub>4</sub> as mobile phase coupled with a Knauer-IR refractive index detector.

To test the reusability using hydrothermally pretreated corncob, a concentration of 1% (w/v) was used to facilitate the magnetic recovery. Enzymatic hydrolysis was carried out at the same conditions of the kinetic assay. The reaction was kept during 48 h without sampling to avoid disturbing the homogenization of the reaction. After 48 h, the slurry was recuperated and magnetically separated. The immobilized enzyme was rinsed once with 0.05 M citrate buffer. Subsequently, the fresh substrate resuspended in buffer was added. The collected slurry after each batch was centrifugated for 5 minutes and the supernatant was stored for glucose quantification using HPLC at the same conditions of the kinetic assay.

### 3.2.8 Statistical analyses

A statistical analysis on the values of the glucose yield over each cycle where the immobilized enzyme was reused was carried out using a one-way ANOVA. Tukey pairwise comparison was used to determine the significance difference between cycles. Also, a t-test for the saccharification rate of corn cob using free and immobilized cellulase cocktail was applied to probe the significant difference between rates. Differences were considered statistically significance at  $p < 0.05$ . Minitab 16 software was used.

## 3.3 RESULTS AND DISCUSSION

### 3.3.1 Cellulase cocktail immobilization

The  $\text{Fe}_3\text{O}_4$  nanoparticles have gain interest in enzyme immobilization research due to advantageous properties as superparamagnetism and low toxicity.  $\text{Fe}_3\text{O}_4$  are usually coated or functionalized to provide functional groups that favor the bondage to the enzymes (Li et al., 2008). In this work, chitosan was used as polymeric shell and the immobilization procedure applied is presented in Figure 3.2. Chitosan was chosen due the amino groups that allow the enzyme to bond covalently providing a more stable biocatalyst compared with immobilization via adsorption. A chitosan solution of 5 g/L was first dissolved in 1% (v/v) acetic acid due to the solubility of chitosan on acidic solutions with pH lower than 6 (Wu et al., 2014). Higher concentrations of chitosan were tested (10 and 15 g/L, respectively) but the magnetic property of the MNP was drastically decreased as the chitosan shell created a considerable volume around the particle which difficult its magnetic separation. The decreased magnetic property was the parameter that led to use 5 g/L of chitosan solution. Similar results reported by Mo et al. (2020) lead them to use also lower chitosan concentrations though their argument was different. They reached higher immobilization yields (84.5%) when higher chitosan concentration was used assuming that more chitosan would lead to more functional group's availability. However, they showed that high enzyme loading resulted in low activity due to factors such as cellulase stack during the immobilization process which limits the enzyme diffusion during hydrolysis. Then, to avoid nanoparticles aggregation due to the strong dipole-dipole attraction of the MNP,  $\text{Fe}_3\text{O}_4$  was first dissolved and sonicated in a NaOH 1 M solution during 30 min. When the chitosan solution and the  $\text{Fe}_3\text{O}_4$  solution were mixed, the pH shifted to alkaline causing the precipitation of the chitosan on the surface of the negatively charged  $\text{Fe}_3\text{O}_4$ . The chitosan coating provides the amino groups for the further reaction with glutaraldehyde. Here, the glutaraldehyde reacts with the amino groups of the support (form the chitosan) to be converted into aldehydes group. Glutaraldehyde has the advantage of losing the chemical reactivity in a short period (days), thus providing

a stable enzyme-support complex (Boudrant et al., 2020). Subsequently, the enzyme solution is mixed with the activated support and the Schiff base linkage reaction occurs to form covalent bonds between the support and the enzyme (Zang et al., 2014). The Schiff reaction involves a covalent bond formation through the crosslinking of amine groups and aldehyde groups (Zhou et al., 2019).

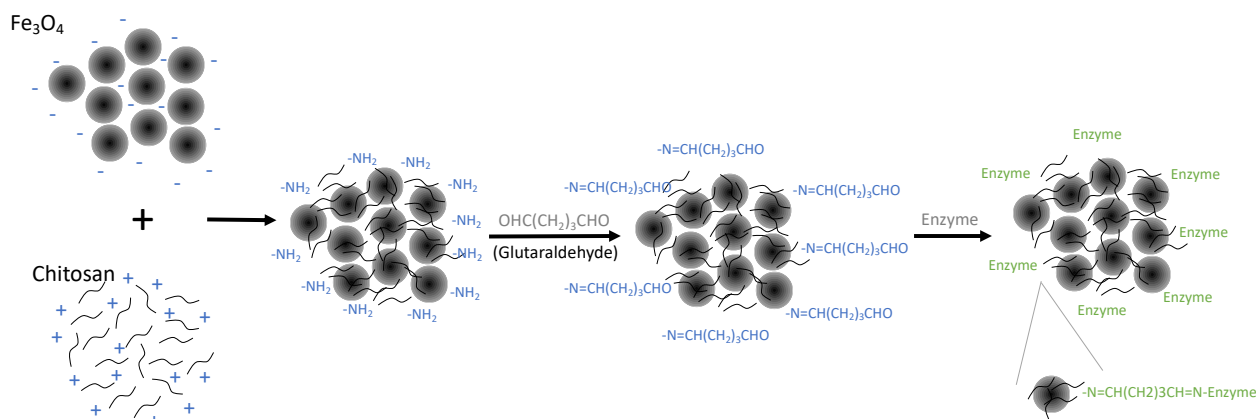


**Figure 3.2.** Schematic representation of cellulase immobilization using chitosan as coating agent and  $\text{Fe}_3\text{O}_4$  as magnetic support.

### 3.3.2 FTIR-ATR characterization

Infrared spectroscopy is an effective technique which relies on the capacity of most molecules to absorb light in the infrared region of the electromagnetic spectrum. This technique provides information of specific functional groups (Anderson and Voskerician, 2010). Hence, FTIR-ATR was used to determine characteristic functional groups present in the samples  $\text{Fe}_3\text{O}_4$ , chitosan, free enzyme,  $\text{Fe}_3\text{O}_4$  coated with chitosan and the immobilized cellulase complex. The spectra are shown in Figure 3.3. The characteristic Fe-O peak at  $542\text{ cm}^{-1}$ , corresponding to the vibration of the magnetic core (Hosseini et al., 2018) was observed in bare  $\text{Fe}_3\text{O}_4$ , the same Fe-O peak being observed in all samples containing the nanoparticles, i.e.,  $\text{Fe}_3\text{O}_4$  coated with chitosan and the immobilized enzyme on the support. The -C-O peak at  $1362\text{ cm}^{-1}$ , the peak associated to chitosan (Tan et al., 2018), was confirmed in  $\text{Fe}_3\text{O}_4$  coated with chitosan and the immobilized enzyme. Peaks at  $1632\text{ cm}^{-1}$  and  $1535\text{ cm}^{-1}$  representing the amide I (C=O stretching vibrations) and amide II (N-H bending and C-N stretching) of cellulase were identified in the immobilized cellulase complex, thus, confirming a successful enzyme attachment (Hosseini et al., 2018). Similar results were obtained by Paz-Cedeno et al. (2021) who immobilized Cellic CTec 2 onto graphene oxide magnetite (GO-MNP) and observed the same characteristic Fe-O peaks on samples containing  $\text{Fe}_3\text{O}_4$  along

with the characteristic N-H and C-N peaks allowing them to conclude on the success of the immobilization procedure.

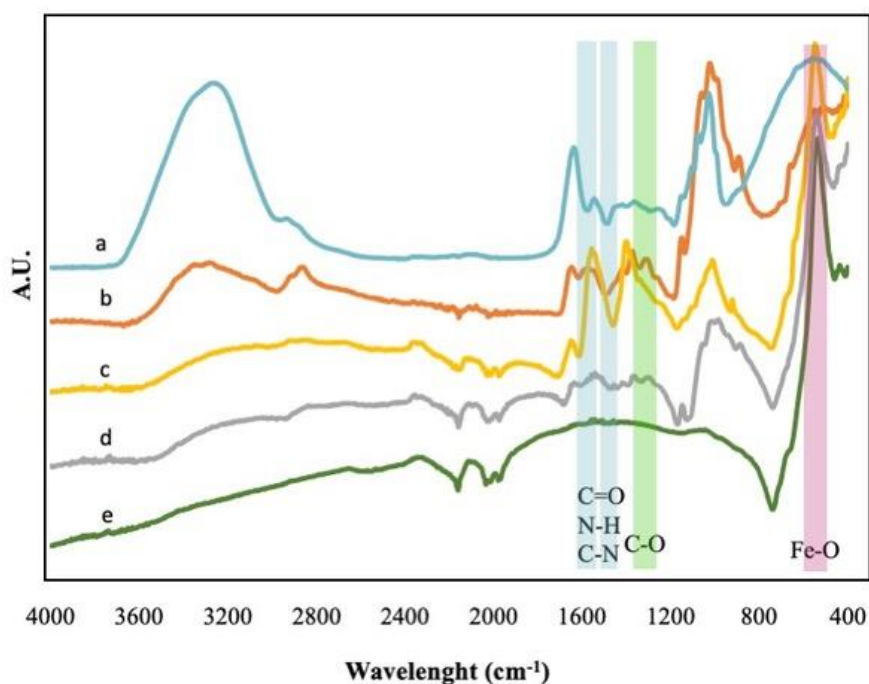


**Figure 3.3.** FTIR-ATR spectra a) free enzyme, b) chitosan, c) enzyme loaded on chitosan coated  $\text{Fe}_3\text{O}_4$ , d)  $\text{Fe}_3\text{O}_4$  chitosan coated, e)  $\text{Fe}_3\text{O}_4$

### 3.3.3 Microscopic morphology

The morphology of the magnetic nanoparticles ( $\text{Fe}_3\text{O}_4$ ),  $\text{Fe}_3\text{O}_4$  coated with chitosan and the immobilized cellulase were evaluated by transmission electron microscopy and scanning electron microscope. Figure 3.4 (a, b, c) shows the images obtained with TEM microscope. In Figure 3.4a,  $\text{Fe}_3\text{O}_4$  particles appear to be agglomerated, which is explained by the strong magnetic dipole-dipole attractions feature between particles and the drying process for the TEM sample preparation. When  $\text{Fe}_3\text{O}_4$  particles were coated with chitosan (Figure 3.4b), the nanoparticles display a grey shadow surrounding the particles due to the condensation of chitosan. Here, agglomeration was still noticeable. Tan et al. (2018) reported similar agglomeration phenomenon for their  $\text{Fe}_3\text{O}_4$  nanoparticles after coating with chitosan, even though chitosan is known to increase the repulsive forces between nanoparticles with the amino group. The agglomeration phenomena could also be related to the drying process of the samples prior the morphological analyses (Wang and Jiang, 2019). Figure 3.4c shows the enzyme loaded on the chitosan coated  $\text{Fe}_3\text{O}_4$  support where a denser layer around the surface could be noticed. Asar et al. (2020) also noticed the highly dense surface layer after enzyme immobilization on chitosan coated magnetic



graphene. However, after eight reuses of the immobilized enzyme, they observed a decrease on the density this layer surface probably associated to the enzyme leaching. Lastly, SEM microscope (Figure 3.4d) was used to observe the immobilized cellulase complex from a wide perspective. The image obtained using SEM showed a rough surface of the immobilized enzyme with different size agglomerates.

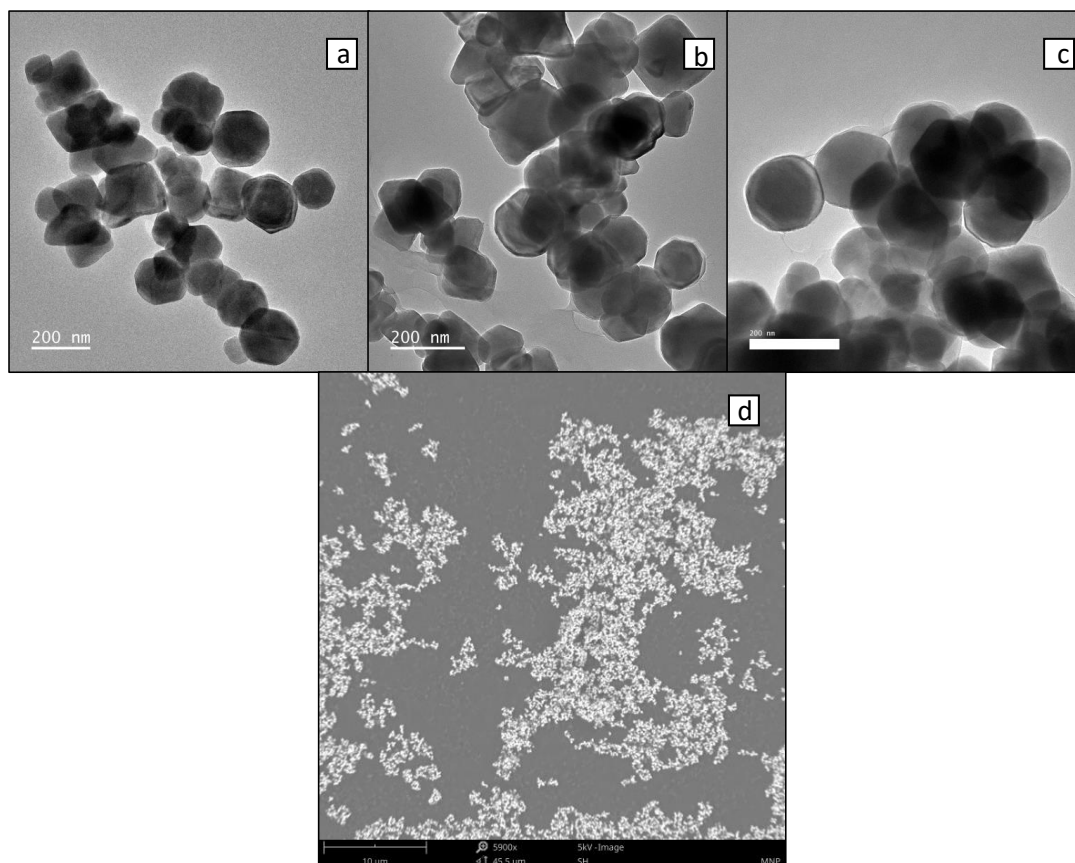


**Figure 3.4.** Spectroscopy images a) bare  $\text{Fe}_3\text{O}_4$ , b)  $\text{Fe}_3\text{O}_4$  coated with chitosan, c, d) enzyme loaded on chitosan coated  $\text{Fe}_3\text{O}_4$ ; TEM (a, b, c) SEM (d).

### 3.3.4 Binding efficiency, enzyme activity, and acetic acid tolerance

The wide range of methods used to measure and report enzyme activity hinders the possibility to make a precise comparison with what is reported in literature. Table 3.1 shows a summary of the results obtained in this work as well as the reported activities and corresponding units found in literature on cellulase immobilization. In this work, the amount of immobilized enzyme was  $65 \pm 6.02 \text{ mg}_{\text{protein}}/\text{g}_{\text{support}}$  with 70% binding efficiency. This value is within values reported by other authors where the cellulase binding efficiency varies from 40 to 90%, respectively (Alfrén and Høbley, 2014; Sillu and Agnihotri, 2020). For the immobilization procedure developed in this work, the enzyme activity of the MNP was determined to be  $20 \text{ U}/\text{g}_{\text{support}}$ . The binding efficiency parameter is related with the amount of enzyme

added as shown in Figure 3.5, higher enzyme efficiency (%) was achieved when 10 mg of enzyme were added and the lowest binding efficiency was achieved (~36%) when 100 mg of enzyme was loaded on the support. However, a higher enzyme loading does not obligatory means higher activity, as shown in Figure 3.6, the glucose yield did not even duplicate when particles with  $265 \pm 27.8 \text{ mg}_{\text{protein}}/\text{g}_{\text{support}}$  (corresponding to 100 mg of added enzyme) were used (Mo et al., 2020; Schnell et al., 2019). Considering the difficulty in comparing this result with values reported in the literature due to the different units used to quantify enzyme activity, the yield of glucose produced per gram of CMC was determined. The value obtained was 167.93 mg of glucose per g of CMC, which is similar to the yield 162.40 mg of glucose per g of CMC reported by Tan et al. (2018) using a hollow magnetic structure with cellulase immobilized inside the support. Table 3.1 shows some values obtained in previous reports that can resemble with the results obtained in this work, emphasizing on reports that used magnetic supports which is in essence an advantage for the proposed process.

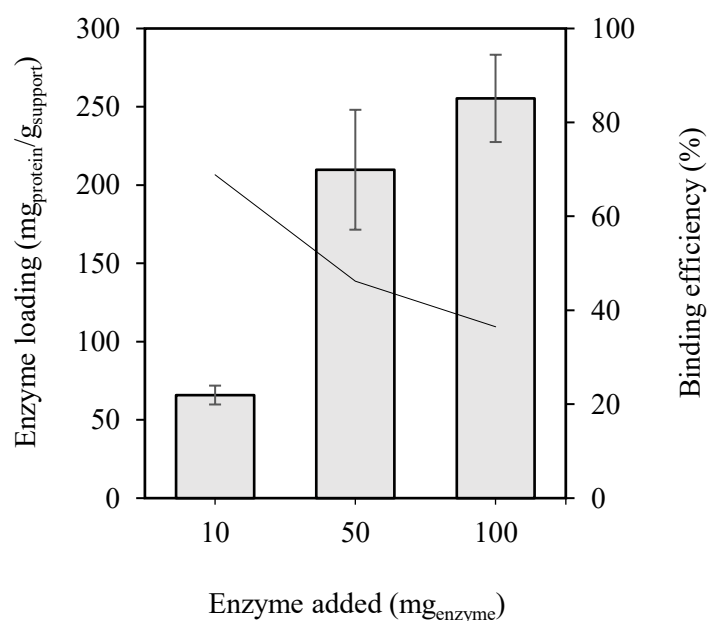


**Figure 3.5.** Chitosan coated magnetic nanoparticle saturation assay. Enzyme was added in 10, 50 and 100 mg<sub>enzyme</sub> and the enzyme loading, and binding efficiency were calculated. Enzyme loading is represented by bars, and the binding efficiency is represented by the continuous line.

Acetic acid is a by-product mainly found on the liquid fraction after the hydrothermal pretreatment. It is liberated from the hemicellulose and helps to provide an acidic condition during the pretreatment (Ko et al., 2015). Hodge et al. (2008) reported that the second most relevant enzyme inhibitor after sugars was acetic acid, decreasing the cellulose conversion up to 10%. Romani et al. (2014) reported that high concentrations of by-products from the pretreatment, namely, phenolic compounds,

furfural, and acetic acid have an inhibitory effect on cellulase. Due to the protective effect of immobilization, when 5 g/L of acetic acid were added to the hydrolysis, the immobilized enzyme reported an increase of 8.6% (from  $83.3 \pm 3.8$  to  $91.2 \pm 3.6$   $\text{g}_{\text{glucose}}/\text{g}_{\text{CMC}}$ ) in glucose production where the free enzyme decreased in 18.7% (from  $337.0 \pm 16.7$  to  $273.8 \pm 21.9$   $\text{g}_{\text{glucose}}/\text{g}_{\text{CMC}}$ ). This increased tolerance is related to the enzymes being covalent bonded to the support, which generates a steric hindrance that could impede the inhibitor compound to reach the enzyme active site (Qi et al., 2018). Qi et al. (2018) also reported better tolerance to vanillin and formic acid using immobilized cellulase. The acetic acid tolerance showed by the immobilized cellulase is promising for enzymatic hydrolysis where whole slurry (liquid and solid phase) is used.

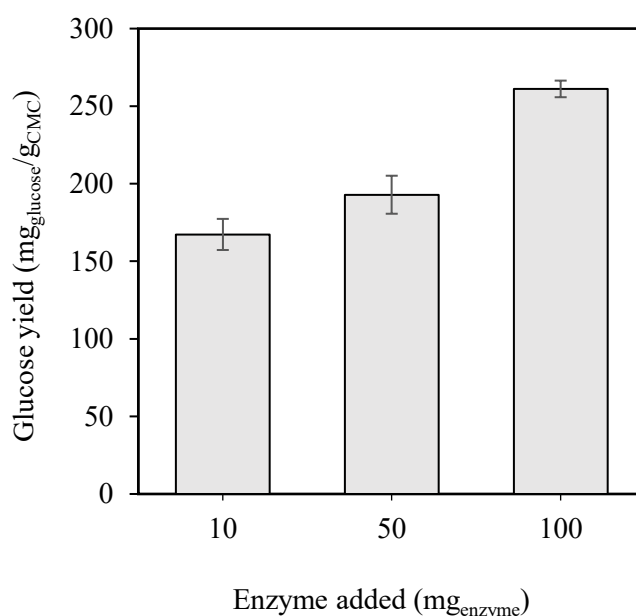


**Figure 3.6.** Glucose production using MNP at different enzyme loadings. The hydrolysis was performed at  $50^{\circ}\text{C}$ , during 1 h using CMC 1% (w/v) as substrate in 0.1 M citrate buffer at pH 4.8.

### 3.3.5 Storage stability

Immobilized enzyme was stored at  $4^{\circ}\text{C}$  for 30 days and the activity was measured at the end of that period. Relative to the activity at day 1, the immobilized enzyme maintained 80% of the initial activity and this lost in activity may be related to the enzyme modification caused by the packing effect or agglomeration during storage period (Hoarau et al., 2017; Sigurdardóttir et al., 2019; Wang and Jiang, 2019). Similar works reported 81.2% and 64% of retained activity after 20 and 45 days of storage, respectively, with a low loss activity trend compared with the free form (Asar et al., 2020; Sillu and Agnihotri, 2020). The importance of the storage stability, also called “shelf stability”, is relevant from the

point of view of manufacturing and practical applications, as it determines the long-term use of the enzyme complex.

### 3.3.6 Reusability of immobilized cellulase

The immobilized cellulase reusability was studied up to 13 cycles in batch operation using CMC as substrate. After each cycle of reaction, the immobilized enzyme was separated and resuspended with fresh substrate. As shown in Figure 3.7, immobilized cellulase maintained 44.8% of its relative activity after 13 utilization cycles compared to the first utilization. It can be observed a decrease of ~23% from the first to the second cycle, then the decrease in each cycle is less than 5%. The ANOVA analysis of the differences in enzyme activity between cycles showed statistical difference between them and the Tuckey pairwise comparison allowed to conclude that from the second cycle until the last one, no significant difference occurred. The significant activity difference in cycle 1 and 2 is attributed to the removed/leaked enzyme that was adsorbed on the support and not covalently bonded (Zang et al., 2014). The loss in activity after the second cycle can be also associated to factors as agglomeration behavior and/or to the natural deactivation of the enzyme rather than the leakage of the enzyme from the support, protein denaturation, and inhibition (Schnell et al., 2019; Sigurdardóttir et al., 2018). Asar et al. (2020) obtained similar results for cellulase immobilized on Fe<sub>3</sub>O<sub>4</sub>/graphene oxide nanocomposite reporting a retention of 49% of its relative activity after the 8<sup>th</sup> cycle. A study performed by Mariño et al. (2021) using immobilized cellulases onto amino functionalized magnetic beads reported that the residual activity of β-glucosidase was maintained in 62.7% after 6 cycles of 96 h. However, they used cellulose isolated from orange bagasse, thus having the advantage of being more similar to a commercial cellulose than to a lignocellulosic material. The immobilization technique plays an important role to determine the ability of enzyme to be reused. It is not straightforward that stronger bonding (as covalent) will be the most resistant bondage for reutilization. For example, Wang et al. (2013) tested adsorption as technique for cellulase onto PAMAM (a dendritic polymer with precise molecular weight) and reported after six cycles a retained activity of 41%. Although the retained activity decreased, they suggest that immobilization via adsorption tends to retain the enzyme activity better than covalent binding as the later might cause rigid bonds. These set of batch hydrolysis evidence the ability of the immobilized enzyme to be magnetically separated, recovered, and re-interact with fresh substrate. Also, a total of 1384.19 mg<sub>glucose</sub>/g<sub>CMC</sub> were obtained without adding any fresh enzyme during each cycle which is 8.2-fold the glucose obtained during a batch hydrolysis without reusing the enzyme.

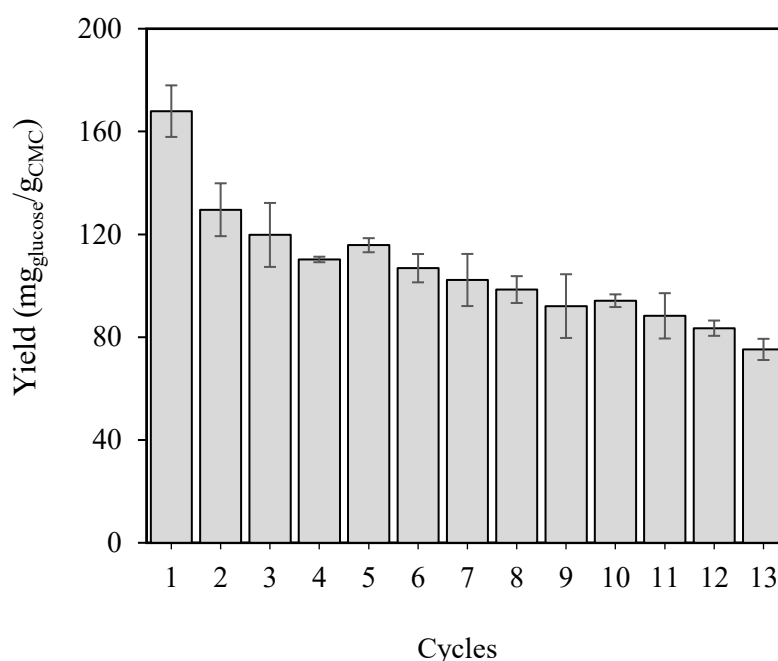


**Figure 3.7.** Reusability of cellulase immobilized on chitosan coated  $\text{Fe}_3\text{O}_4$  nanoparticles. The yield represents the mg of glucose produced per g of substrate (CMC) and the bars represent the number of cycles performed.

**Table 3.1** Overview of reported activity and yield of cellulase immobilized on different supports.

Support	Enzyme	Activity	Yield (mg glucose/ g <sub>substrate</sub> )	Enzyme load	Reference
Chitosan coated $\text{Fe}_3\text{O}_4$	Cellic CTec2	2.8 (g glucose/kg particles*min)	168	65 mg protein/g support	Present study
M-Cyanyric	Cellic CTec2	2.8 (g glucose/kg particles*min)	N/D	4.6 mg protein/g support	Alfrén and Hobley, 2014
M-PGL	Cellic CTec2	1.6 (g glucose/kg particles*min)	N/D	11.9 mg protein/g support	Alfrén and Hobley, 2014
Magnetic chitosan	Cellulase (Meiji Seika Farma Co.)	N/D	270	112.3 mg cellulase/g support	Zang et al., 2014
Magnetic chitosan	Cellulase (Meiji Seika Farma Co.)	N/D	162.40	202.63 mg cellulase/g support	Tan et al., 2018

**Table 3.1** Continued

<b>Support</b>	<b>Enzyme</b>	<b>Activity</b>	<b>Yield (mg glucose/g<sub>substrate</sub>)</b>	<b>Enzyme load</b>	<b>Reference</b>
Semi-oxidize magnetite	Cellulase from <i>Trichoderma longibrachiatum</i>	5.82 U/g	N/D	0.143 g/g	Schnell et al., 2019
Maghemite	Cellulase from <i>Trichoderma longibrachiatum</i>	5.17 U/g	N/D	0.230 g/g	Schnell et al., 2019
Magnetite	Cellulase from <i>Trichoderma longibrachiatum</i>	1.52 U/g	N/D	0.350 g/g	Schnell et al., 2019
Magnetic halloysite nanotube	Cellulase from <i>Aspergillus niger</i>	N/D	37.2	116.6 mg/g support	Sillu and Agnihotri, 2020
Chitosan magnetic porous biochar	Cellulase (pale yellow powder) (Meiji Seika Farma Co.)	N/D	330.9	80.5 mg cellulase/ g support	Mo et al., 2020

N/D: not defined

### 3.3.7 Enzymatic saccharification of pretreated corn cob using immobilization as strategy

The pretreated corn cob cellulose-rich fraction reached 61.17% of glucan content and was in accordance with the range of reported by other authors (Aguilar-Reynosa et al., 2017). Corn cob usually presents, after hydrothermal pretreatment, a deconstruction on compact fibers and a decreased particle size (Sun et al., 2021). Particularly, hydrothermal pretreatment modifies the cellulose fraction by increasing the surface area, reducing the depolymerization degree, and increasing the pore volume. Also, the hemicellulose is significantly removed which impacts positively on the enzymatic hydrolysis as the hemicellulose-derived sugars are inhibitors for cellulases (Song et al., 2021). These changes improve the cellulose digestibility during the enzymatic hydrolysis (Ruiz et al., 2020).

Enzymatic susceptibility is shown in Figure 3.8 where similar values of saccharification yield after 120 h, were obtained for free and immobilized enzyme. The higher glucose concentration obtained was 25.27 g/L for the free enzyme and 21.84 g/L for the immobilized enzyme, representing a saccharification

yield of 71.03% and 64.45%, respectively, after 120 h. Saccharification yields of 53.30% for free and 52.67% for immobilized cellulase onto magnetic nanoparticles after 72 h using pretreated rice straw hydrolysis and 60.64% for free and 56.34% for immobilized cellulase onto chitosan coated magnetic nanoparticles cellulose conversion hydrolyzing pretreated *Agave aroviensis* leaves were previously reported (Kaur et al., 2020; Sánchez-Ramírez et al., 2017). These reports confirm that the conversion yields are similar for both free and immobilized enzymes as also obtained in our work. Thus, comparable yields can be obtained using immobilized and free cellulase.

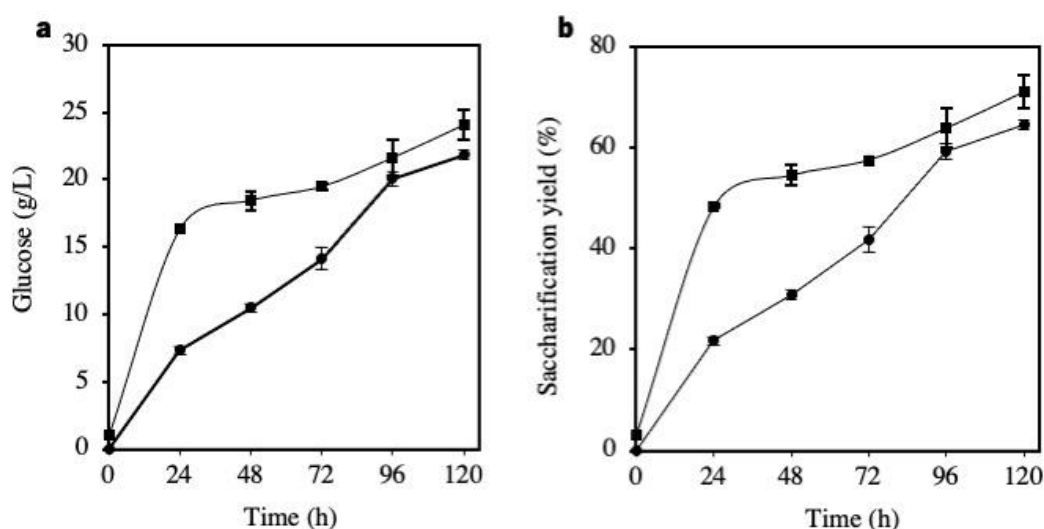


**Figure 3.8.** Enzymatic hydrolysis kinetic. Glucose production (a) and saccharification yield (b) of pretreated corn cob at a solid loading of 5% (w/v). ■ free enzyme, ● immobilized enzyme.

The saccharification productivity (g/L·h) at 24 h was 2.1 times faster for the free enzyme (Table 3.2). This can be attributed to diffusional limitations the immobilized enzyme faces at the initial hours of the reaction increasing the adversity to enter in contact with the active site of the immobilized enzyme (Jia et al., 2017; Kaur et al., 2020; Sánchez-Ramírez et al., 2017). Other authors reported that, with immobilized enzyme, the reaction media was less homogeneous than when free enzyme was used, which might also jeopardize the glucose yield (Zheng et al., 2013). Likewise, Pino et al. (2019) observed a decline on the glucose production rate when increasing the substrate loading and attributed this behavior to the increased viscosity of the cellulosic substrate which difficult the mixture. Ruiz et al. (2012) compared the initial saccharification rate of different substrates and observed higher rates when using pretreated substrates or easily available cellulose (as filter paper). It must be highlighted that, despite the reduced saccharification rates for the initial times, no statistic difference between the saccharification rate at 96 and 120 h for free and immobilized enzyme ( $p > 0.05$ ) was observed. Additionally, enzymatic

hydrolysis confronts diverse effects that can disturb the conversion efficiency regardless the enzymes being immobilized. For example, after hydrothermal pretreatment, most of the lignin remains on the solid, increasing the possibility of non-productive binding (Rahikainen et al., 2013; Singh et al., 2021; Song et al., 2021). Overall, these results confirm the usefulness of cellulases immobilization for pretreated LCM hydrolysis.

**Table 3.2** Saccharification rate of pretreated corn cob hydrolysis with 5% (w/v) loading using free and immobilized cellulase cocktail.

<b>Saccharification rate g/(L·h)</b>		
<b>Time (h)</b>	<b>Free</b>	<b>Immobilized</b>
24	$0.68 \pm 0.00$	$0.31 \pm 0.01$
96	$0.23 \pm 0.01$	$0.21 \pm 0.00$
120	$0.20 \pm 0.00$	$0.18 \pm 0.00$

The reusability of the immobilized cellulase was studied up to 3 cycles of 48 h. After each cycle, the immobilized cellulase was rinsed with buffer and fresh substrate was added. The immobilized catalyst was tested using 1% (w/v) of hydrothermally pretreated corn cob and achieved a saccharification yield of 91% after 48 h, meanwhile the second and third reuse batch attain 32 and 15%, respectively (Figure 3.9). When using real substrate and magnetically immobilized cellulase the problems arise mainly during the magnetic separation at the end of the reaction. It is common to lose enzyme capacity from the first to the second cycle due to the leaking of the enzyme that was absorbed (not bonded) on the support (Zang et al. 2014). However, an additional complication was noticed when using pretreated corn cob as some of the immobilized enzyme was strongly bonded to the remaining solids and the magnetic force applied was not strong enough to separate it. Paz-Cedeno et al. (2021) reported a conversion of 72% in the first cycle of pretreated sugarcane bagasse hydrolysis using immobilized enzyme, then the conversion decreased to 56, 43, 37, and 34%, respectively, during the following cycles. However, the concentration used of pretreated sugarcane bagasse was 0.1% (w/v) which might facilitate the separation and a progressive conversion decrease between cycles. Other studies reported a retained activity of cellulase immobilized on magnetic supports of 50% - 63% after four cycles using lignocellulosic biomass, but the solid loading concentration used was not mentioned (Jia et al., 2017; Kaur et al., 2020).



Two relevant features of this work, rarely addressed in literature, must be pointed out. The solid load used was 5% (w/v) and the saccharification of a real cellulose substrate. This is relevant as a higher amount of glucose is expected when increasing solid concentration although other difficulties arise as poor mass and heat transfer between the enzyme and the substrate may limit this effect (Pino et al., 2018). Although 5% (w/v) is not generally considered as high solid load, it is when considering immobilized cellulase. The solid load concentrations reported on the few examples of enzymatic hydrolysis of a pretreated lignocellulosic substrate using immobilized enzymes range from 0.1% to 6% (w/v) (Kaur et al., 2020; Kumar et al., 2017; Paz-Cedeno et al., 2021). Most of the cellulase immobilization works focus on the characterization of the support and the hydrolysis is exclusively performed on synthetic cellulose such as microcrystalline cellulose and carboxymethyl cellulose or isolated cellulose from pretreated residues (Asar et al., 2020; Mariño et al., 2021; Mo et al., 2020; Schnell et al., 2019; Sillu and Agnihotri, 2020; Tan et al., 2018). Thus, the data collected in this work, under particularly challenging conditions, contributes to advance the application of enzyme immobilization in real lignocellulosic substrates paving the way to the economic feasibility of lignocellulosic valorization processes.

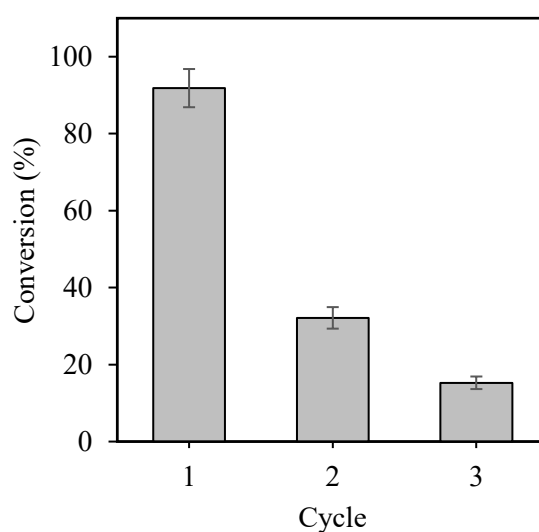


**Figure 3.9.** Reusability of immobilized cellulase using hydrothermally pretreated corn con at 1% (w/v) after 48 h.

### 3.4 CONCLUSIONS

The role of cellulolytic enzymes for lignocellulosic conversion represents a challenge due to the high enzyme costs. This work presented a description of the immobilization technique using magnetic support and its reusability. Also, the immobilized cellulase was successfully applied on the hydrolysis of a real lignocellulosic substrate, namely hydrothermally pretreated corn cob, and to the best of our

knowledge, this work represents one of the highest lignocellulosic solid loadings tested for enzyme immobilization. It is shown that the application of immobilized cellulolytic enzymes on magnetic support can be a promising technique to improve the enzymatic hydrolysis process as it holds advantages as easy enzyme recovery by applying an external magnetic field. Furthermore, reusability becomes an important advantage compared to free enzyme due to the straightforward recovery and possible application in continuous processes.

### 3.5 REFERENCES

- Abraham, R.E., Puri, M., 2020. Commercial application of lignocellulose-degrading enzymes in a biorefinery, in: Arora, N.K., Mishra, J., Mishra, V. (Eds.), *Microbial Enzymes: Roles and Applications in Industries*. Springer Singapore, Singapore, pp. 287–301. [https://doi.org/10.1007/978-981-15-1710-5\\_11](https://doi.org/10.1007/978-981-15-1710-5_11)
- Aguilar-Reynosa, A., Romani, A., Rodríguez-Jasso, R.M., Aguilar, C.N., Garrote, G., Ruiz, H.A., 2017. Comparison of microwave and conduction-convection heating autohydrolysis pretreatment for bioethanol production. *Bioresour. Technol.* 243, 273–283.
- Aguilar, D.L., Rodríguez-Jasso, R.M., Zanuso, E., Lara-Flores, A.A., Aguilar, C.N., Sanchez, A., Ruiz, H.A., 2018. Operational strategies for enzymatic hydrolysis in a biorefinery, in: Kumar, S., Sani, R. (Eds.), *Biorefining of biomass to biofuels. Biofuel and Biorefinery Technologies*. pp. 223–248. [https://doi.org/10.1007/978-3-319-67678-4\\_10](https://doi.org/10.1007/978-3-319-67678-4_10)
- Alfrén, J., Hobbey, T.J., 2014. Immobilization of cellulase mixtures on magnetic particles for hydrolysis of lignocellulose and ease of recycling. *Biomass and Bioenergy* 65, 72–78. <https://doi.org/10.1016/j.biombioe.2014.03.009>
- Anderson, J.M., Voskerician, G., 2010. The challenge of biocompatibility evaluation of biocomposites, in: Ambrosio, L. (Ed.), *Biomedical Composites*, Woodhead Publishing Series in Biomaterials. Woodhead Publishing, pp. 325–353. <https://doi.org/https://doi.org/10.1533/9781845697372.3.325>
- Anukam, A.I., Goso, B.P., Okoh, O.O., Mamphweli, S.N., 2017. Studies on characterization of corn cob for application in a gasification process for energy production. *J. Chem.* 2017, 6478389. <https://doi.org/10.1155/2017/6478389>
- Asar, M.F., Ahmad, N., Husain, Q., 2020. Chitosan modified Fe<sub>3</sub>O<sub>4</sub>/graphene oxide nanocomposite as a support for high yield and stable immobilization of cellulase: its application in the saccharification of microcrystalline cellulose. *Prep. Biochem. Biotechnol.* 50, 460–467. <https://doi.org/10.1080/10826068.2019.1706562>
- Azevedo, M.A., Cerqueira, M.A., Fuciños, P., Silva, B.F.B., Teixeira, J.A., Pastrana, L., 2020. Rhamnolipids-based nanostructured lipid carriers: Effect of lipid phase on physicochemical properties and stability. *Food Chem.* 128670. <https://doi.org/https://doi.org/10.1016/j.foodchem.2020.128670>
- Baptista, S.L., Carvalho, L.C., Romani, A., Domingues, L., 2020. Development of a sustainable bioprocess based on green technologies for xylitol production from corn cob. *Ind. Crops Prod.* 156, 112867. <https://doi.org/10.1016/j.indcrop.2020.112867>

- Baptista, S.L., Costa, C.E., Cunha, J.T., Soares, P.O., Domingues, L., 2021. Metabolic engineering of *Saccharomyces cerevisiae* for the production of top value chemicals from biorefinery carbohydrates. *Biotechnol. Adv.* 47, 107697. <https://doi.org/10.1016/j.biotechadv.2021.107697>
- Baptista, S.L., Cunha, J.T., Romani, A., Domingues, L., 2018. Xylitol production from lignocellulosic whole slurry corn cob by engineered industrial *Saccharomyces cerevisiae* PE-2. *Bioresour. Technol.* 267, 481–491. <https://doi.org/10.1016/j.biortech.2018.07.068>
- Barbosa, F.C., Silvello, M.A., Goldbeck, R., 2020. Cellulase and oxidative enzymes: new approaches, challenges and perspectives on cellulose degradation for bioethanol production. *Biotechnol. Lett.* 42, 875–884. <https://doi.org/10.1007/s10529-020-02875-4>
- Boakye-Boaten, N.A., Kurkalova, L., Xiu, S., Shahbazi, A., 2017. Techno-economic analysis for the biochemical conversion of *Miscanthus x giganteus* into bioethanol. *Biomass and Bioenergy* 98, 85–94. <https://doi.org/10.1016/j.biombioe.2017.01.017>
- Boudrant, J., Woodley, J.M., Fernandez-Lafuente, R., 2020. Parameters necessary to define an immobilized enzyme preparation. *Process Biochem.* 90, 66–80. <https://doi.org/10.1016/j.procbio.2019.11.026>
- Bradford, M., 1976. A rapid and sensitive method for the quantitation of microgram quantities of protein utilizing the principle of protein-dye binding. *Anal Biochem* 72, 248–254.
- Chen, J., Yuan, Z., Zanuso, E., Trajano, H.L., 2017. Response of biomass species to hydrothermal pretreatment, in: Ruiz, H., Hedegaard Thomsen, M., Trajano, H. (Eds.), *Hydrothermal Processing in Biorefineries*. Springer, Cham, Switzerland, pp. 95–140. [https://doi.org/10.1007/978-3-319-56457-9\\_4](https://doi.org/10.1007/978-3-319-56457-9_4)
- Costa, C.E., Møller-Hansen, I., Romani, A., Teixeira, J.A., Borodina, I., Domingues, L., 2021. Resveratrol production from hydrothermally pretreated eucalyptus wood using recombinant industrial *Saccharomyces cerevisiae* strains. *ACS Synth. Biol.* 10, 1895–1903. <https://doi.org/10.1021/acssynbio.1c00120>
- Cunha, J.T., Romani, A., Inokuma, K., Johansson, B., Hasunuma, T., Kondo, A., Domingues, L., 2020a. Consolidated bioprocessing of corn cob-derived hemicellulose: engineered industrial *Saccharomyces cerevisiae* as efficient whole cell biocatalysts. *Biotechnol. Biofuels* 13, 1–15. <https://doi.org/10.1186/s13068-020-01780-2>
- Cunha, J.T., Soares, P.O., Baptista, S.L., Costa, C.E., Domingues, L., 2020b. Engineered *Saccharomyces cerevisiae* for lignocellulosic valorization: a review and perspectives on bioethanol production. *Bioengineered* 11, 883–903. <https://doi.org/10.1080/21655979.2020.1801178>
- Gomes, D., Cunha, J., Zanuso, E., Teixeira, J., Domingues, L., 2021. Strategies towards reduction of cellulases consumption: Debottlenecking the economics of lignocellulosics valorization processes. *Polysaccharides* 2, 287–310. <https://doi.org/10.3390/polysaccharides2020020>
- Gomes, D., Rodrigues, A.C., Domingues, L., Gama, M., 2015. Cellulase recycling in biorefineries—is it possible? *Appl. Microbiol. Biotechnol.* 99, 4131–4143. <https://doi.org/10.1007/s00253-015-6535-z>
- Grewal, J., Ahmad, R., Khare, S.K., 2017. Development of cellulase-nanoconjugates with enhanced ionic liquid and thermal stability for in situ lignocellulose saccharification. *Bioresour. Technol.* 242, 236–243. <https://doi.org/10.1016/j.biortech.2017.04.007>
- Hoarau, M., Badiéyan, S., Marsh, E.N.G., 2017. Immobilized enzymes: Understanding enzyme-surface interactions at the molecular level. *Org. Biomol. Chem.* 15, 9539–9551.

<https://doi.org/10.1039/c7ob01880k>

- Hodge, D.B., Karim, M.N., Schell, D.J., McMillan, J.D., 2008. Soluble and insoluble solids contributions to high-solids enzymatic hydrolysis of lignocellulose. *Bioresour. Technol.* 99, 8940–8948. <https://doi.org/10.1016/j.biortech.2008.05.015>
- Hosseini, S.H., Hosseini, S.A., Zohreh, N., Yaghoubi, M., Pourjavadi, A., 2018. Covalent immobilization of cellulase using magnetic poly(ionic liquid) support: Improvement of the enzyme activity and stability. *J. Agric. Food Chem.* 66, 789–798. <https://doi.org/10.1021/acs.jafc.7b03922>
- Jia, J., Zhang, W., Yang, Z., Yang, X., Wang, N., Yu, X., 2017. Novel magnetic cross-linked cellulase aggregates with a potential application in lignocellulosic biomass bioconversion. *Molecules* 22, 269. <https://doi.org/10.3390/molecules22020269>
- Kaur, P., Taggar, M.S., Kalia, A., 2020. Characterization of magnetic nanoparticle-immobilized cellulases for enzymatic saccharification of rice straw. *Biomass Convers. Biorefinery* 11, 955–969. <https://doi.org/10.1007/s13399-020-00628-x>
- Ko, J.K., Um, Y., Park, Y.C., Seo, J.H., Kim, K.H., 2015. Compounds inhibiting the bioconversion of hydrothermally pretreated lignocellulose. *Appl. Microbiol. Biotechnol.* 99, 4201–4212. <https://doi.org/10.1007/s00253-015-6595-0>
- Kumar, A., Singh, S., Tiwari, R., Goel, R., Nain, L., 2017. Immobilization of indigenous holocellulase on iron oxide (Fe<sub>2</sub>O<sub>3</sub>) nanoparticles enhanced hydrolysis of alkali pretreated paddy straw. *Int. J. Biol. Macromol.* 96, 538–549. <https://doi.org/10.1016/j.ijbiomac.2016.11.109>
- Kumar, B., Bhardwaj, N., Agrawal, K., Chaturvedi, V., Verma, P., 2020. Current perspective on pretreatment technologies using lignocellulosic biomass: An emerging biorefinery concept. *Fuel Process. Technol.* 199, 106244. <https://doi.org/10.1016/j.fuproc.2019.106244>
- Larnaudie, V., Ferrari, M.D., Lareo, C., 2019. Techno-economic analysis of a liquid hot water pretreated switchgrass biorefinery: Effect of solids loading and enzyme dosage on enzymatic hydrolysis. *Biomass and Bioenergy* 130, 105394. <https://doi.org/10.1016/j.biombioe.2019.105394>
- Li, G. yin, Jiang, Y. ren, Huang, K. long, Ding, P., Chen, J., 2008. Preparation and properties of magnetic Fe<sub>3</sub>O<sub>4</sub>-chitosan nanoparticles. *J. Alloys Compd.* 466, 451–456. <https://doi.org/10.1016/j.jallcom.2007.11.100>
- Liu, G., Zhang, J., Bao, J., 2016. Cost evaluation of cellulase enzyme for industrial-scale cellulosic ethanol production based on rigorous Aspen Plus modeling. *Bioprocess Biosyst. Eng.* 39, 133–140. <https://doi.org/10.1007/s00449-015-1497-1>
- Mariño, M.A., Moretti, P., Tasic, L., 2021. Immobilized commercial cellulases onto amino-functionalized magnetic beads for biomass hydrolysis: enhanced stability by non-polar silanization. *Biomass Convers. Biorefinery*. <https://doi.org/10.1007/s13399-021-01798-y>
- Miller, G.L., 1959. Use of dinitrosalicylic acid reagent for determination of reducing sugar. *Anal. Chem.* 31, 426–428. <https://doi.org/10.1021/ac60147a030>
- Mo, H., Qiu, J., Yang, C., Zang, L., Sakai, E., 2020. Preparation and characterization of magnetic polyporous biochar for cellulase immobilization by physical adsorption. *Cellulose* 27, 4963–4973. <https://doi.org/10.1007/s10570-020-03125-6>
- Oliveira, C., Romani, A., Gomes, D., Cunha, J.T., Gama, F.M., Domingues, L., 2018. Recombinant family 3 carbohydrate-binding module as a new additive for enhanced enzymatic saccharification of whole slurry from autohydrolyzed *Eucalyptus globulus* wood. *Cellulose* 25, 2505–2514.

<https://doi.org/10.1007/s10570-018-1722-6>

- Overend, R.P., Chornet, E., 1987. Fractionation of lignocellulosics by steam-aqueous pretreatments. *Philos. Trans. R. Soc. London* 321, 523–536. <https://doi.org/https://doi.org/10.1098/rsta.1987.0029>
- Papadaskalopoulou, C., Sotiropoulos, A., Novacovic, J., Barabouti, E., Mai, S., Malamis, D., Kekos, D., Loizidou, M., 2019. Comparative life cycle assessment of a waste to ethanol biorefinery system versus conventional waste management methods. *Resour. Conserv. Recycl.* 149, 130–139. <https://doi.org/10.1016/j.resconrec.2019.05.006>
- Paz-Cedeno, F.R., Carceller, J.M., Iborra, S., Donato, R.K., Godoy, A.P., Veloso de Paula, A., Monti, R., Corma, A., Masarin, F., 2021. Magnetic graphene oxide as a platform for the immobilization of cellulases and xylanases: Ultrastructural characterization and assessment of lignocellulosic biomass hydrolysis. *Renew. Energy* 164, 491–501. <https://doi.org/10.1016/j.renene.2020.09.059>
- Pino, M.S., Rodríguez-Jasso, R.M., Michelin, M., Flores-Gallegos, A.C., Morales-Rodríguez, R., Teixeira, J.A., Ruiz, H.A., 2018. Bioreactor design for enzymatic hydrolysis of biomass under the biorefinery concept. *Chem. Eng. J.* 347, 119–136. <https://doi.org/10.1016/j.cej.2018.04.057>
- Pino, M.S., Rodríguez-Jasso, R.M., Michelin, M., Ruiz, H.A., 2019. Enhancement and modeling of enzymatic hydrolysis on cellulose from agave bagasse hydrothermally pretreated in a horizontal bioreactor. *Carbohydr. Polym.* 211, 349–359. <https://doi.org/10.1016/j.carbpol.2019.01.111>
- Qi, B., Luo, J., Wan, Y., 2018. Immobilization of cellulase on a core-shell structured metal-organic framework composites: Better inhibitors tolerance and easier recycling. *Bioresour. Technol.* 268, 577–582. <https://doi.org/10.1016/j.biortech.2018.07.115>
- Rahikainen, J.L., Martin-Sampedro, R., Heikkinen, H., Rovio, S., Marjamaa, K., Tamminen, T., Rojas, O.J., Kruus, K., 2013. Inhibitory effect of lignin during cellulose bioconversion: The effect of lignin chemistry on non-productive enzyme adsorption. *Bioresour. Technol.* 133, 270–278. <https://doi.org/10.1016/j.biortech.2013.01.075>
- Rijn, R. Van, Nieves, I.U., Shanmugam, K.T., Ingram, L.O., Vermerris, W., 2018. Techno-Economic evaluation of cellulosic ethanol production based on pilot biorefinery data: a case study of sweet sorghum bagasse processed via L+SScF. *Bioenergy Res.* 11, 414–425. <https://doi.org/https://doi.org/10.1007/s12155-018-9906-3>
- Romani, A., Ruiz, H.A., Pereira, F.B., Domingues, L., Teixeira, J.A., 2014. Effect of hemicellulose liquid phase on the enzymatic hydrolysis of autohydrolyzed *Eucalyptus globulus* wood. *Biomass Convers. Biorefinery* 4, 77–86. <https://doi.org/10.1007/s13399-013-0093-3>
- Ruiz, H.A., Conrad, M., Sun, S.-N., Sanchez, A., Rocha, G.J.M., Romani, A., Castro, E., Torres, A., Rodríguez-Jasso, R.M., Andrade, L.P., Smirnova, I., Sun, R.-C., Meyer, A.S., 2020. Engineering aspects of hydrothermal pretreatment: From batch to continuous operation, scale-up and pilot reactor under biorefinery concept. *Bioresour. Technol.* 299, 122685. <https://doi.org/10.1016/J.BIORTECH.2019.122685>
- Ruiz, H.A., Galbe, M., Garrote, G., Ramirez-Gutierrez, D.M., Ximenes, E., Sun, S.N., Lachos-Perez, D., Rodríguez-Jasso, R.M., Sun, R.C., Yang, B., Ladisch, M.R., 2021. Severity factor kinetic model as a strategic parameter of hydrothermal processing (steam explosion and liquid hot water) for biomass fractionation under biorefinery concept. *Bioresour. Technol.* 342. <https://doi.org/10.1016/j.biortech.2021.125961>
- Ruiz, H.A., Vicente, A.A., Teixeira, J.A., 2012. Kinetic modeling of enzymatic saccharification using wheat

- straw pretreated under autohydrolysis and organosolv process. *Ind. Crops Prod.* 36, 100–107. <https://doi.org/10.1016/j.indcrop.2011.08.014>
- Sánchez-Ramírez, J., Martínez-Hernández, J.L., Segura-Ceniceros, P., López, G., Saade, H., Medina-Morales, M.A., Ramos-González, R., Aguilar, C.N., Ilyina, A., 2017. Cellulases immobilization on chitosan-coated magnetic nanoparticles: application for *Agave Atrovirens* lignocellulosic biomass hydrolysis. *Bioprocess Biosyst. Eng.* 40, 9–22. <https://doi.org/10.1007/s00449-016-1670-1>
- Schnell, F., Kube, M., Berensmeier, S., Schwaminger, S.P., 2019. Magnetic recovery of cellulase from cellulose substrates with bare iron oxide nanoparticles. *ChemNanoMA* 5, 422–426. <https://doi.org/10.1002/cnma.201800658>
- Sigurdardóttir, S.B., Lehmann, J., Grivel, J., Zhang, W., Kaiser, A., Pinelo, M., 2019. Alcohol dehydrogenase on inorganic powders: Zeta potential and particle agglomeration as main factors determining activity during immobilization. *Colloids Surfaces B Biointerfaces* 175, 136–142. <https://doi.org/https://doi.org/10.1016/j.colsurfb.2018.11.080>
- Sigurdardóttir, S.B., Lehmann, J., Ovtar, S., Grivel, J.-C., Della Negra, M., Kaiser, A., Pinelo, M., 2018. Enzyme immobilization on inorganic surfaces for membrane reactor applications: mass transfer challenges, enzyme leakage and reuse of materials. *Adv. Synth. Catal.* 360, 2578–2607. <https://doi.org/10.1002/adsc.201800307>
- Sillu, D., Agnihotri, S., 2020. Cellulase immobilization onto magnetic halloysite nanotubes: Enhanced enzyme activity and stability with high cellulose saccharification. *ACS Sustain. Chem. Eng.* 8, 900–913. <https://doi.org/10.1021/acssuschemeng.9b05400>
- Singh, A., Rodríguez-Jasso, R.M., Saxena, R., Cerda, R.B., Singhanía, R.R., Ruiz, H.A., 2021. Subcritical water pretreatment for agave bagasse fractionation from tequila production and enzymatic susceptibility. *Bioresour. Technol.* 338, 125536. <https://doi.org/https://doi.org/10.1016/j.biortech.2021.125536>
- Singh, A., Rodríguez Jasso, R.M., Gonzalez-Gloria, K.D., Rosales, M., Belmares Cerda, R., Aguilar, C.N., Singhanía, R.R., Ruiz, H.A., 2019. The enzyme biorefinery platform for advanced biofuels production. *Bioresour. Technol. Reports* 7, 100257. <https://doi.org/10.1016/j.biteb.2019.100257>
- Sluiter, A., Hames, B., Ruiz, R., Scarlata, C., Sluiter, J., Templeton, D., Crocker, D., 2008. Determination of structural carbohydrates and lignin in biomass - NREL/TP-510-42618. *Lab. Anal. Proced.* 17.
- Song, B., Lin, R., Lam, C.H., Wu, H., Tsui, T.H., Yu, Y., 2021. Recent advances and challenges of interdisciplinary biomass valorization by integrating hydrothermal and biological techniques. *Renew. Sustain. Energy Rev.* 135, 110370. <https://doi.org/10.1016/j.rser.2020.110370>
- Sun, Q., Chen, W.J., Pang, B., Sun, Z., Lam, S.S., Sonne, C., Yuan, T.Q., 2021. Ultrastructural change in lignocellulosic biomass during hydrothermal pretreatment. *Bioresour. Technol.* 341, 125807. <https://doi.org/10.1016/j.biortech.2021.125807>
- Tan, L., Tan, Z., Feng, H., Qiu, J., 2018. Cellulose as a template to fabricate a cellulase-immobilized composite with high bioactivity and reusability. *New J. Chem.* 42, 1665–1672. <https://doi.org/10.1039/C7NJ03271D>
- Wang, D., Jiang, W., 2019. Preparation of chitosan-based nanoparticles for enzyme immobilization. *Int. J. Biol. Macromol.* 126, 1125–1132. <https://doi.org/10.1016/j.ijbiomac.2018.12.243>
- Wang, S., Su, P., Ding, F., Yang, Y., 2013. Immobilization of cellulase on polyamidoamine dendrimer-grafted silica. *J. Mol. Catal. B Enzym.* 89, 35–40. <https://doi.org/10.1016/j.molcatb.2012.12.011>

- Wu, Q.-X., Lin, D.-Q., Yao, S.-J., 2014. Design of chitosan and its water soluble derivatives-based drug carriers with polyelectrolyte complexes. *Mar. Drugs* 12, 6236–6253. <https://doi.org/10.3390/md12126236>
- Zang, L., Qiu, J., Wu, X., Zhang, W., Sakai, E., Wei, Y., 2014. Preparation of magnetic chitosan nanoparticles as support for cellulase immobilization. *Ind. Eng. Chem. Res.* 53, 3448–3454. <https://doi.org/10.1021/ie404072s>
- Zanuso, E., Gomes, D.G., Ruiz, H.A., Teixeira, J.A., Domingues, L., 2021. Enzyme immobilization as a strategy towards efficient and sustainable lignocellulosic biomass conversion into chemicals and biofuels: Current status and perspectives. *Sustain. Energy Fuels* 5, 4233–4247. <https://doi.org/10.1039/d1se00747e>
- Zanuso, E., Lara-Flores, A.A., Aguilar, D.L., Velazquez-Lucio, J., Aguilar, C.N., Rodriguez-Jasso, R.M., Ruiz, H.A., 2017. Kinetic modeling, operational conditions, and biorefinery products from hemicellulose: Depolymerization and solubilization during hydrothermal processing, in: Ruiz, H., Hedegaard Thomsen, M., Trajano, H. (Eds.), *Hydrothermal Processing in Biorefineries*. [https://doi.org/10.1007/978-3-319-56457-9\\_5](https://doi.org/10.1007/978-3-319-56457-9_5)
- Zheng, P., Wang, J., Lu, C., Xu, Y., Sun, Z., 2013. Immobilized  $\beta$ -glucosidase on magnetic chitosan microspheres for hydrolysis of straw cellulose. *Process Biochem.* 48, 683–687. <https://doi.org/10.1016/j.procbio.2013.02.027>
- Zhou, M., Ju, X., Zhou, Z., Yan, L., Chen, J., Yao, X., Xu, X., Li, L.Z., 2019. Development of an immobilized cellulase system based on metal-organic frameworks for improving ionic liquid tolerance and in situ saccharification of bagasse. *ACS Sustain. Chem. Eng.* 7, 19185–19193. <https://doi.org/10.1021/acssuschemeng.9b05175>

## CHAPTER IV

---

### Oscillatory flow bioreactor assessment for enzymatic hydrolysis of lignocellulosic biomass

**The work reported on this chapter is published in:**

Zanuso, E., Ruiz, H.A., Domingues, L., Teixeira, J.A. *Submitted for publication*. Oscillatory flow bioreactor operating at high loadings for enzymatic hydrolysis of lignocellulosic biomass



## **ABSTRACT**

Bioreactors technology applied to enzymatic hydrolysis has been studied to overcome the main limitation of enzymatic hydrolysis which is the cost of enzymes. The bioreactor design should satisfy the major restraints of the enzymatic hydrolysis process which in general encompass poor mass and heat transfer, challenging rheological conditions, and enzyme inhibition. In this chapter is presented the application of an oscillatory flow reactor (OFR) for lignocellulosic biomass enzymatic hydrolysis at high solids loading. OFR consists of a tubular reactor with periodical constrictions where vortices are created due to the oscillating flow determined by frequency and amplitude conditions. This can be favorable for enzymatic hydrolysis as efficient mixtures can be accomplished at low shear rates. In this work, high solid loadings 18% (w/v) and low enzyme dosage was studied to determine the conditions of amplitude (2 – 6 mm) and frequency (2 – 4 Hz) that best fit the process and their influence in OFR. The conditions tested demonstrated a positive effect on the process, where at an amplitude of 6 mm and frequency of 4 Hz, an increment in productivity was observed, respecting the other conditions tested. Then, the fed-batch strategy was tested achieving a solid loading of 25% (w/v) and a saccharification yield of 97%. This novel contribution using OFR at high solids loading is crucial as advances in lignocellulosic biotransformation technology are still in demand to achieve efficient and economically feasible processes.

## 4.1 INTRODUCTION

Biochemical platform conversion of lignocellulosic biomass involves a multistep process to generate a sugar platform that can be further converted into a wide range of biofuels, namely bioethanol (Cunha et al., 2020b) and chemicals (Baptista et al., 2021). Two crucial steps of this process are: i) pretreatment: to deal with the recalcitrance of the material and render it to the action of enzymes and, ii) enzymatic hydrolysis: to break down the polysaccharides into fermentable sugars (Kumar et al., 2019). Pretreatment aims to modify the composition and structure of the lignocellulosic biomass and enhance the enzyme accessibility to the cellulose, relocate the lignin, and depolymerize and solubilize the hemicellulose (Kumar et al., 2020). Some examples of pretreatment methods include acid, alkali, ionic liquids, organosolv, deep eutectic solvents, hydrothermal processing (steam explosion, liquid hot water), and ammonia fiber explosion. Hydrothermal pretreatment uses water as solvent at temperatures in the range of 150 – 230 °C and pressure of 4.8 – 28 bar (approx.). Under these conditions, water molecules changes to H<sub>3</sub>O<sup>+</sup> and OH<sup>-</sup> ions acting as catalyzer which alter the lignocellulosic chemical bonds (Ruiz et al., 2020; Sun et al., 2021). Also, hydrothermal pretreatment conditions dissolve the acetyl group, present in the hemicellulose, into acetic acid. The acidic conditions gained by the formation of acetic acid benefit the breakdown of the cellulose-hemicellulose-matrix bonds. Thus, under subcritical conditions, water acts as an efficient polar solvent comparable with other polar solvents such as methanol or ethanol (Sarker et al., 2021).

Enzymatic hydrolysis is a heterogeneous reaction that uses mainly cellulases cocktail as soluble catalyst under mild conditions and low energy consumption (Zanuso et al., 2021). The most studied cellulase cocktail is comprised of endo-glucanase, exo-glucanase and  $\beta$ - glucosidase which work coactively to convert cellulose into a sugar platform of fermentable monomeric sugars as glucose (Singh et al., 2019). This can be easily achieved when substrate loading is < 6 - 10% (w/v) (depending on the capacity of water retention of the material) the reaction-diffusion limitations are lessened due to the availability of “free” water. A different reaction scheme is observed when high solid loadings are employed.

High solid enzymatic hydrolysis (HSEH) generally occurs at dry solid loading > 12 - 15% (w/v) where the water availability is very limited at the beginning of the reaction. The advantages of operating at high solid loadings are the reduction in operational cycles, lower energy consumption and higher sugar concentration which impact positively on the process economics and efficiency (Shiva et al., 2022). HSEH adversity relies on factors such as high viscosity, low diffusion, low mass transfer, and difficulty to perform

rheological characterization of the slurry (Lu et al., 2021). Viscosity varies from substrate to substrate as it is related to the porosity of the material, thus, higher porosity increases the water absorbability capacity affecting the viscosity (Battista et al., 2018). The porosity variations rise more complications in the process as the need for substrate-specific solutions. The approaches followed to minimize those problems comprise viscosity reduction by pre-hydrolysis, bioreactor designs, and fed-batch feeding (Da Silva et al., 2020).

A novel reactor to be applied in the enzymatic hydrolysis process is the oscillatory flow reactor (OFR). The OFR (also known as oscillatory baffled reactor; OBR) consists of a tubular reactor with equally spaced baffles subjected to an oscillatory motion (Stonestreet and Harvey, 2002). The OFR's unique features are the vortices created inside the reactor due to the baffles and periodically reversed flow which increases the radial mixing in the tube as shown in Figure 4.1 (Reis et al., 2005). When applying oscillation to a smooth tube, no benefit is observed as the behavior is similar to a plug flow reactor, however, the difference in OFR is the baffled tube so when oscillation is applied, vortices are formed. Thus, the mixing in OFR can be controlled very precisely in a wide range of mixing conditions (Ni et al., 2003). The motion inside the space between each baffle creates a well-mixed region resulting in a uniform mixing along the column considered to behave as a series of stirred tanks (Masngut et al., 2010). OFR has been applied for liquid-liquid, solid-liquid, and gas-liquid reactions thanks to the specific features that can offer heat and mass transfer improvement, well-controlled and homogeneous mixture, and compact setups (Bianchi et al., 2020). This reactor technology has been applied in disciplines such as medicinal chemistry (Hwang et al., 2017), protein crystallization (Castro et al., 2016), transesterification (Eze and Harvey, 2018), photochemical transformation (Debrouwer et al., 2020), and biodiesel production (Harvey et al., 2003) among others.

In bioprocesses, OFR becomes an interesting bioreactor alternative as efficient mixing can be achieved with low shear stress for the biocatalyst compared with STBR where the impellers can cause high shear stress leading to enzyme deactivation (Afedzi et al., 2022; Da Silva et al., 2020). The authors Ikwebe and Harvey (2020) whose study explored the shear effect of OFR and STBR for ethanol production from cassava reported up to 63% shear reduction, especially on the enzymes, as they observed higher deactivation on the STBR than the OFR. The shear reduction was reflected in the 20-25% higher ethanol concentrations than in STBR when using 5% and 10% (w/v) cassava loading, respectively. Despite ethanol production from cassava being considered as 1st generation biorefinery, this study demonstrates the potential of OFR for biorefinery intensification processes. Regarding cellulose conversion, in another study using microcrystalline cellulose at 2.5% (w/v), Ikwebe and Harvey (2015) performed a comparative power

density analysis where they achieved higher conversion in OFR than in STR at all the power densities tested. It was also reported by Abbot et al. (2014) a theoretical 94.99% decrease in power requirement for  $\alpha$ -cellulose maximum conversion when using OFR instead of STR. Also, a preliminary report from Buchmaier et al. (2019) using  $\alpha$ -cellulose as substrate and comparing OFR and STBR reported a 6.7% higher glucose concentration in OFR while using only 7% of the STBR power density ( $W/m^3$ ). These are promising results that evidence the OFR's potential to obtain similar or higher conversion rates than other reactor configurations while decreasing energy consumption. Considering the importance of enzymatic hydrolysis at high solid loading and the OFR features, this work aimed to assess the performance of the oscillatory flow bioreactor for the enzymatic hydrolysis on the corn cob biomass hydrothermally pretreated hence filling a gap of knowledge regarding the use of OFR for lignocellulosic bioconversion. An experimental design was proposed to evaluate the operational conditions of the reactor, namely, frequency and amplitude. In addition, fed-batch strategies were also tested to overcome mixture problems and achieve operation at the challenging condition of 25% (w/v) solid loading.

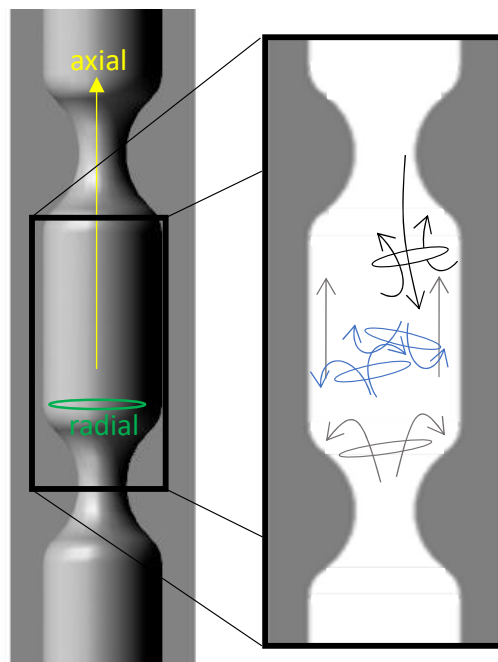


**Figure 4.1** Schematic representation of vortices created inside OFR. Rings and arrows were added for visualization of the angles phase. Gray) beginning of the cycle; blue) before flow reversing; black) after flow reversing. (Adapted and modified from [Reis et al., 2005]).

## 4.2 EXPERIMENTAL METHODS

### 4.2.1 Hydrothermal pretreatment of corn cob

Corn cob was collected from the north region of Portugal and milled to a particle size < 10 mm. Hydrothermal pretreatment was carried out under a non-isothermal regime at a severity factor ( $\log R_o$ ) of 3.95. The severity factor correlates with the temperature and time of the hydrothermal reaction following the equation 4.1 and 4.2:

$$\log R_o = \log [R_{o \text{ Heating}} + R_{o \text{ Cooling}}] \quad \text{eq. 4.1}$$

$$\log R_o = \left[ \int_0^{t_{MAX}} \frac{T(t)-100}{\omega} dt + \int_{t_{MAX}}^{t_F} \frac{T'(t)-100}{\omega} dt \right] \quad \text{eq. 4.2}$$

This equation is usually applied for the non-isothermal heating regimen where  $T(t)$  is the temperature in the heating and cooling stages,  $t$  represents time, and  $\omega$  is the empirical parameter (14.75) that corresponds to the activation energy of the glycosidic bond cleavages of carbohydrates (Ruiz et al., 2021). At a  $T_{max}=211$  °C, a  $\log R_o$  of 3.95 was calculated. The equipment used to carry out the hydrothermal pretreatment was a 2 L stainless steel reactor (Parr Instruments Company) equipped with a PID temperature controller (Parr 4848 Reactor Controller). 4 g of distilled water were added per 1 g of dry oven corn cob. The reactor was filled and heated to the desired temperature (211 °C) at a heating rate of 11.4 °C/min. The chemical composition of the corn cob (untreated and treated) was determined according to the National Renewable Energy Laboratory protocols (Sluiter et al., 2008). The slurry was separated using a vacuum system to obtain a liquid and a solid fraction. The solid fraction was washed with distilled water, dried at 35 °C for 24 h, and used as substrate in the experiments. Biomass moisture was considered in the balance in the process.

### 4.2.2 Oscillatory flow reactor bioreactor configuration for enzymatic hydrolysis

The experiments were performed using an oscillatory flow reactor consisting of a single jacketed tube with a total volume of 150 mL of built-in glass. The inner diameter of the reactor is 2.2 cm and has a 57 cm height providing a total volume (including the oscillation chamber) of 150 mL. The reactor was operated vertically as shown in Figure 4.2. A linear motor device (Festo) was used to provide oscillations

with a piston. The motor provides amplitudes in the range of 0-20 mm and frequencies oscillation in the range of 1-8 Hz. The oscillatory motor device was controlled digitally. The temperature was controlled by circulating controlled temperature water through the tube's jacket. The pretreated corn cob was supplied from the top of the reactor using a funnel, then, samples were withdrawn from the sampling port located at the bottom of the reactor using a 5 mL syringe.

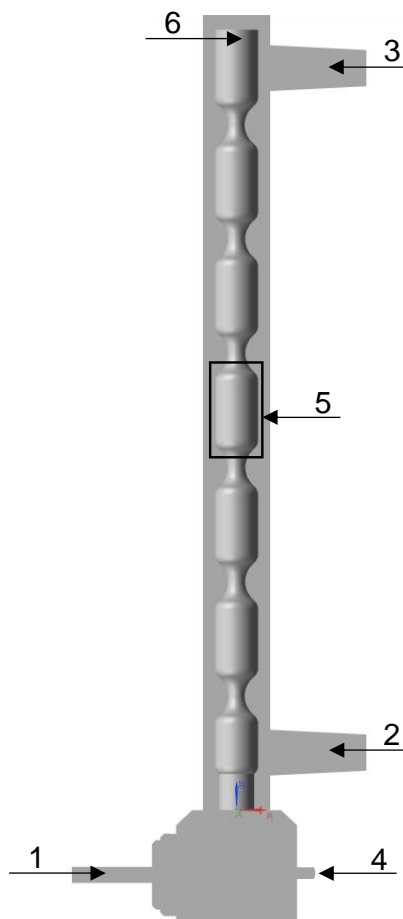


**Figure 4.2.** Schematic representation of the OFR used in this work. 1) oscillatory device and chamber; 2) heating fluid inlet; 3) heating fluid outlet, 4) sampling port, 5) baffles with smooth periodic constrictions, 6) solids inlet.

### 4.2.3 Analytical methods

Glucose was quantified by HPLC (Shimadzu, LC 2060C, Japan) using BioRad Aminex HPX-87H column (300 x 7.8 mm) at 60 °C using a mobile phase of sulfuric acid at 5 mM and a flow rate of 0.6 mL/min. The chromatogram intensity was detected using a high-sensitivity refractive index detector (Shimadzu, RID 20A, Japan) with pure glucose as standard.

#### 4.2.4 Enzymatic hydrolysis

The experiments were carried out for 20 h with a solid loading of 18% (w/v) of the pretreated corn cob, citrate buffer 0.05 M (pH 4.8), 0.2% (w/v) sodium azide was added to prevent microbial growth, and the necessary amount of deionized water was calculated to make a total volume of 80 mL. The temperature was set up at 50 °C. The enzyme used was Cellic CTec2 (Cellulase, enzyme blend; Sigma-Aldrich) at 10 FPU/g substrate for all experiments. The enzyme activity was determined by the filter paper assay following the NREL protocol (NREL/TP-510-42628) where the activity was 143 FPU/mL. At the end of each experiment, the slurry obtained was drained out of the reactor, centrifuged for 5 minutes and the supernatant was stored at -24 °C for further HPLC analysis. Then, the reactor was cleaned before each experiment with a chlorine solution and rinsed 3 times with ultrapure water. The saccharification yield was calculated using the following equation (eq. 4.3) (Ruiz et al., 2012):

$$\text{Saccharification yield (\%)} = \frac{[\text{Glucose}]}{1.111f[\text{Biomass}]} \cdot 100 \quad \text{eq. 4.3}$$

Where [Glucose] is glucose concentration (g/L), 1.111 is the conversion factor of cellulose to equivalent glucose, f is the cellulose fraction in dry biomass (g/g) and [Biomass] is dry biomass concentration at the beginning of the enzymatic saccharification (g/L). Productivity was calculated by dividing the glucose concentration at the determined time (hours).

#### 4.2.5 Preliminary experiments in OFR

Preliminary experiments using hydrothermally pretreated corn cob were carried out to estimate the behavior of the hydrolysis and optimize the procedure to load the solids into the reactor. Then to facilitate the loading, a comparison of solids between dry and of wet was carried out. Samples were withdrawn at 4, 6, 8, and 12 h. Enzymatic hydrolysis experiments were carried out at 5% (w/v) at the lowest and highest operational values of frequency (2 and 4 Hz) and amplitude (2 and 6 mm). For all the preliminary experiments the glucose produced was analyzed using HPLC after 24 h by draining the whole slurry, centrifugating for 5 minutes and recovering the supernatant for analytical analysis. For this set of experiments, the enzyme loading was 20 FPU/mL to provide favorable enzymatic conditions in a 0.05 M citrate buffer (pH 4.8) at 50 °C.

### 4.2.6 Experimental design

A full factorial experimental design was used to evaluate the influence of two factors, frequency (Hz) and amplitude (mm) on glucose production (g/L). The center point was set halfway between the levels of each factor with a duplicate to estimate the error. Solid loading was maintained at 18% (w/v) as it was the maximum loading where no clogging was observed at the beginning of the reaction in the OFR. Statistica v. 7 software was used for the ANOVA statistical analysis to compare the experiment differences in the oscillation conditions tested with a 95% confidence level and a Tukey pairwise comparison was used to determine if there were differences between each condition tested.

### 4.2.7 Fed-batch strategy for enzymatic hydrolysis

A set of experiments were run in a fed-batch where the final solid loading concentration was 25 % (w/v). Three strategies were tested as shown in Table 4.1. The different feeding times are identified by FB 1-3. The total enzyme requirement was added at the beginning of the reaction with an enzyme loading of 10 FPU/g substrate. The oscillation conditions used were selected according to the best condition obtained in batch operation.

**Table 4.1** HSEH fed-batch mode conditions.

Fed-batch	Time (h)					
	Feeding time and loading (% w/v)					
	0	4	6	8	12	24
FB1	6.25	6.25		6.25	6.25	
FB2	8.3		8.3		8.3	
FB3	18					7

## 4.3 RESULTS AND DISCUSSION

### 4.3.1 Chemical composition of untreated and hydrothermally pretreated corn cob

The untreated corn cob chemical composition obtained as g per 100 g of dry weight was glucan  $32.86 \pm 1.38$  g, xylan  $31.82 \pm 2.16$  g, arabinan  $2.45 \pm 0.18$  g, acetyl group  $1.12 \pm 0.06$  g, lignin  $14.08 \pm 0.41$  g. Hydrothermal pretreatment induces structural changes in the lignocellulosic biomass which increase cellulose accessibility. These changes include the break-up of cell fibers and mainly the



solubilization and depolymerization of the hemicellulose into the liquid fraction (Sun et al., 2021). After the hydrothermal pretreatment, the chemical composition obtained was as follows: glucan  $62.27 \pm 2.21$  g, xylan  $15.03 \pm 0.48$  g, arabinan not detected, acetyl group not detected, and lignin  $22.52 \pm 1.85$  g. These results are in accordance with what has been previously reported (Cunha et al., 2020a). The increase in glucan content after pretreatment is related to the fractionation of the biomass where the hemicellulose is solubilized into the liquid phase, remaining a cellulose rich solid (Ruiz et al., 2020). Moreover, corn cob was chosen due to its nature as dense and uniform material being used as a lignocellulosic model material (Anukam et al., 2017).

### 4.3.2 Preliminary experiments

A first approach to test the use of OFR was carried out with a solid load of 5% (w/v) to avoid high viscosity slurries and restricted free water (obstacles faced when operating at high solid loading). The reactions were carried out during 24 h and the final glucose was measured. The concentrations obtained (Figure 4.3) were 24.36, 29.86, 31.31, and 32.42 g/L, respectively, representing a conversion of 69, 85, 89, and 92%, respectively. The main objective of these assessment was to observe the solids performance inside the reactor to avoid clogging when loading the OFR. The behavior of higher conversion rates at the higher frequency tested is related to the flow velocity required to achieve particles suspension (Reis et al., 2005). The flow velocity at these conditions is lower due to the particles not being agglomerated, hence, suspension was easier at high frequencies. However, the fact that exceed enzyme was added, could hinder the real behavior of the reactor.

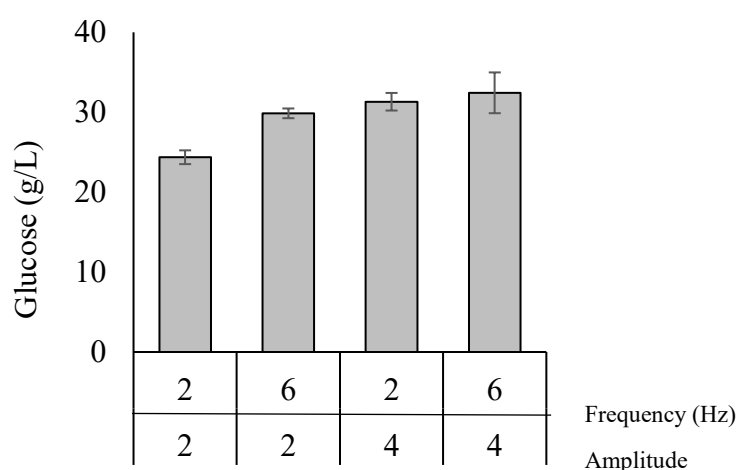


**Figure 4.3.** Preliminary enzymatic hydrolysis assay using 5% (w/v) hydrothermally pretreated corn cob during 24 h, at 50°C at different oscillatory conditions of amplitude and frequency.

According to National Renewable Energy Laboratory (Selig et al., 2008), using air dried material can cause interference with the maximum conversion due to the pore collapse that might occur in the microstructure of the material. But operating wet material with this reactor configuration was laborious and the moisture environment could not be controlled during the loading of the reactor. The dry solids enzymatic hydrolysis behavior (Figure 4.4) was not depressed in comparison with wet solids. This can be related to several facts as the material being dried at mild conditions (35 °C) and that the pore collapse might be an issue when testing solids for enzymatic susceptibility, but for high solids loading it is a minor factor (Sharma and Horn, 2016). Also, for this reactor configuration, solids were first loaded then the liquid media (including the enzyme) was added which facilitated the particles suspension in the reactor.

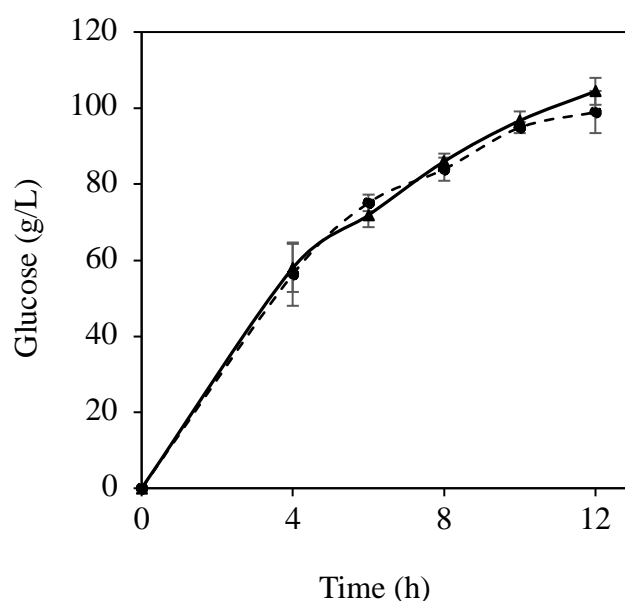


**Figure 4.4.** Glucose production comparison in OFR using wet and dry substrate at 18% (w/v) and 20 FPU/mL. Wet solids (dotted line) dry solids (continuous line).

#### 4.3.3 OFR configuration for enzymatic hydrolysis

In enzymatic hydrolysis processes, OFR can be advantageous compared to STBR as the later relies on mechanical stirring which can cause stress and deactivation of the enzyme. Table 4.2 shows results for different bioreactor configurations for high solid loading, being clear that in STBR the impeller selection is of great importance to achieve an efficient mixture at high solids load. This work demonstrates the use of OFR for HSEH where no impellers are needed as the mixture is achieved through oscillation. Impeller geometry plays a great role in the mixing conditions as studied by Battista et al. (2019) where they tested small diameter impellers with a diameter of 90 mm and more complex impellers with diameters of 140

mm. They reported that a small diameter impeller did not achieve mixing when 20% (w/w) of wheat straw in batch mode operation was added, whereas tall impellers with higher diameter blades guaranteed sufficient mixing at 80 rpm being the double helicoidal impeller the one that performed the best, allowing radial and axial flows to all the mass of the reaction medium. Du et al. (2014) compared a horizontally rotated bioreactor (HRR) based on the mixing principle of gravity and free fall and a vertical stirred tank bioreactor (VSTR) with a helical impeller. Using pretreated corn stover at 25% (w/w), and after 15 h, the material was well liquified in the HRR but still in a solid state in the VSTR. The authors related the slow liquefaction in the VSTR to the impossibility of the impeller to rotate at the beginning of the reaction, whereas the HRR had a mixing speed of 100 rpm. The OFR potential is clear as it can be observed in Table 4.2, the time to reach 81% conversion yield at 18% (w/v) solid loading of hydrothermally pretreated corn cob is 2.4 faster than using STR at 20% (w/w) using wheat straw alkali pretreated (Ludwig et al., 2014).

OFR uses oscillation to cause mixing in each inter-baffle zone which can be easily controlled by changing the oscillation conditions (Ejim et al., 2017). Also, the reactor used in this work was designed with smooth periodic constrictions. In OFR, constrictions can be single or multi-orifice baffles, and with smooth periodic constrictions. A patent about OFR with oscillatory periodic constrictions was published in 2015 where the authors also propose the wide application of OFR (Ferreira et al., 2015). The advantage of a smooth periodic constriction relies on the decrease of “high shear zones” as compared with sharp edges baffles and the smoothness of the constriction prevents particles from sedimentation (McGlone et al., 2015).

Ejim et al. (2017) compared the impact of smooth versus sharp edge baffles using a suspension of PVC particles (10% w/w) and conclude that smooth periodic constrictions require lower oscillation amplitude to achieve a full suspension. In general, OFR limitations that have been reported include particle density limits and a threshold for solid concentration. However, the advantages overcome those restraints as OFR are acclaimed for the favorable handling of slurries, heat, and mass transfer improvements, and linear scalability (McGlone et al., 2015). OFR scale-up is considered to be straight-forward by maintaining the dimensionless parameters that dictate the fluid mechanical conditions, namely the oscillatory Reynolds number ( $Re_o$ ) and the Strouhal number ( $St$ ), and the geometric features of the reactor design as the baffle spacing ( $L$ ) and the baffle orifice open area ( $S$ ) (Ahmed et al., 2017; Bianchi et al., 2020; Stonestreet and Harvey, 2002). However, the biggest challenge of OFR scaling up relies on the efficient mechanical device capable of providing oscillations at a large scale (Ikwebe and Harvey, 2015).

**Table 4.2** Different bioreactor configuration for HSEH.

Substrate	Pretreatment	Solid loading	Bioreactor configuration	Conversion yield (%)	Reference
Corn cob	Hydrothermal	18% (w/v)	Oscillatory flow reactor with smooth periodic constrictions	81% after 20 h	This work
Agave bagasse	Hydrothermal	25% (w/v)	Horizontal with peg-mixer impeller	98% after 72 h	Pino et al., 2019
Corn stover	Diluted acid and steam pretreatment	25% (w/w)	Horizontal rotated reactor with impeller	~ 65%	Du et al., 2014
Wheat straw	Alkali	20 % (w/w)	STR with segmented helical stirrer	76% after 48 h	Ludwig et al., 2014
Beechwood	Organosolv	30 % (w/w)	STR with segmented helical stirrer	72% after 48 h	Ludwig et al., 2014
Agave bagasse	Ethanosolv	30 % (w/w)	Mini-bioreactors with peg-mixer impeller	70% after 24 h	Caspeta et al., 2014
Wheat straw	Hydrothermal	40 % (w/w)	Horizontally rotated drum divided in 5 chambers with 3 paddlers each	35% after 96 h	Jørgensen et al., 2007

#### 4.3.4 Enzymatic hydrolysis at low enzyme load in OFR

For this set of enzymatic hydrolysis runs a solid loading of 18% (w/v) was chosen as the maximum loading where the corn cob and the limited liquid of the reaction could be mixed in the OFR at the beginning of the reaction. The enzyme loading was 10 FPU/mL to evaluate the capacity of the OFR. In OFR, particles are considered in suspension when the velocity of the fluid (in opposite direction) suppresses the terminal velocity of the particle (Cruz et al., 2021). When working at high LCM loading, solids are packed at the onset of the reaction as the water is entrapped in the cell walls of the corn cob (Pino et al., 2019). However, just after a few minutes, the oscillation started, and the suspension of the solid phase was observed in the OFR. The glucose concentration and saccharification yield at the end of each experiment are shown in Table 4.3. The highest glucose concentration was 100.53 g/L representing

a conversion yield of 81% and a productivity of 5 g/(L·h) with a frequency of 4 Hz and amplitude of 6 mm. At the lowest amplitude tested (2 mm) the lowest saccharification rates were obtained reflected in a decrease of 24% - 34% in productivity. Also, the increase in productivity is an indicator that the operational parameters in OFR maximize the process efficiency under the specific conditions tested, mostly related to an improvement in mass transfer (Siddiqui et al., 2022). This is in accordance with what is reported in literature where low oscillatory velocities cause particles to move slow and non-uniform solid suspension can occur, causing sedimentation at the bottom of the reactor (Bianchi et al., 2020). Reis et al. (2005) tested the conditions to suspend ion exchange resins particles at a concentration of 16% (w/v) and small diameter polyamine particles at 15% (w/v) and reported that the optimal well-mixed conditions were 12.1 Hz and 4 mm.

**Table 4.3** OFR frequency and amplitude experimental conditions and corresponding, glucose production, and saccharification yield for 18% solid loading (w/v).

<b>Solid loading (% w/v)</b>	<b>Frequency (Hz)</b>	<b>Amplitude (mm)</b>	<b>Glucose (g/L)</b>	<b>Saccharification yield (%)</b>	<b>Productivity (g/(L·h))</b>
18	2	2	69.94 ± 4.95	56.41	3.50 ± 0.24
	4	2	65.73 ± 3.30	53.01	3.29 ± 0.16
	2	6	76.56 ± 0.03	61.75	3.83 ± 0.00
	4	6	100.53 ± 5.64	81.08	5.03 ± 0.28
	3	4	76.29 ± 6.12	61.53	3.8 ± 0.30

From the ANOVA analysis it was verified that each of the conditions tested are statistically different corresponding to a  $p$ value = 0.004 and an  $F$ value of 16.91. Then, the Tukey pairwise comparison showed that the condition of 4 Hz and 6 mm is the only statistically significant condition at a 95% confidence that differs from the other treatments. To observe the effect of frequency and amplitude on the process, the main effect plot was used. As shown in Figure 4.3, the line is not horizontal, thus, both frequency and amplitude have a positive effect on the process, meaning that the higher levels of frequency and amplitude tested led to higher glucose production. This is in accordance with reported studies where increases in amplitude lead to higher axial dispersion and higher radial mixings are associated with

increased frequencies (Reis et al., 2004). These results also validate the conclusion of Reis et al. (2004) that amplitude has a stronger effect on the mixing rather than frequency.

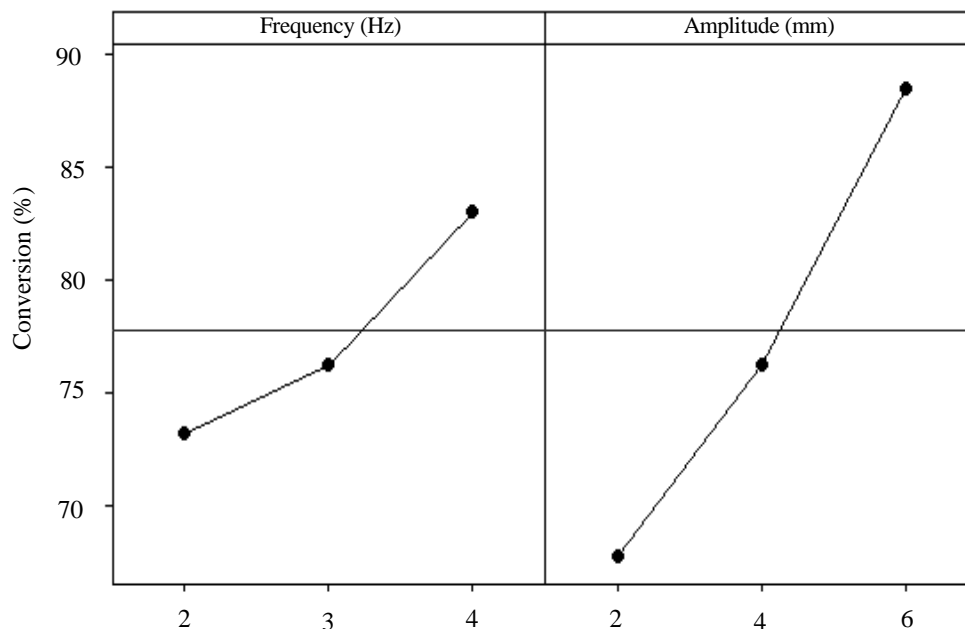


**Figure 4.5.** Main effect plot for glucose (g/L) showing the positive impact of frequency and amplitude on the process.

#### 4.3.5 Fed-batch strategy in OFR

Fed-batch mode was used as a strategy to reduce the initial mixture reaction limitations when operating at high solid loading. This strategy has been studied for lignocellulosic substrate to maintain low levels of viscosity while gradually increasing the cumulative substrate (Du et al., 2017; Pino et al., 2019). Three feeding strategies were tested, and the feed times are shown in Table 4.1. The maximum hydrothermally pretreated corn cob load tested was 25% (w/v) for all the experiments and the oscillation conditions were 4 Hz of frequency and 6 mm of amplitude (based on the best result obtained in the batch assessment). The first strategy tested (FB1) consisting of 4 feedings in the first 12 h of reaction, was performed in the OFR and compared with traditional flask incubator shaking at 150 rpm. Figure 4.6 shows the fed-batch kinetics of both OFR and flask. At 24 h, an improvement of 28% in terms of cellulose conversion could be noticed in the OFR, and the overall reaction performed better in the OFR than in the shaking flasks. This improvement can be related to the good mixture achieved in the OFR which favors the solid-enzyme contact and the low shear conditions which improves enzyme access to the substrate (Bianchi et al., 2020; Ikwebe and Harvey, 2015). Based on the improvement observed, two more

strategies (FB2 and FB3) were tested in the OFR to reduce the feeding times. The kinetics of glucose production and saccharification conversion are shown in Figure 4.7. The FB2 and FB3 reached 170 and 162 g/L of glucose, respectively, representing 97 and 93% cellulose to glucose conversion, respectively. The FB2 and FB3 strategies achieved higher conversion compared with the FB1 strategy (75.54%). The lower conversion in FB1 could be explained by the loss of enzymatic activity during the initial phase of the reaction due to the higher enzyme ratio added and the fact that the enzyme could have reached its maximum non-productive bonding with lignin as the total enzyme required was added since the beginning (dos Santos et al., 2019; Du et al., 2017). Thus, due to the higher accumulation of enzymes added initially, the hydrolysis capacity of the enzyme could have been reduced by inhibition when the substrate was added over time (Alias et al., 2021). It is interesting to highlight that the saccharification rate at 24 h was similar in the three scenarios tested, even when 7% (w/v) of the solids were still to be added for the FB3. This result is opposed the reported by Cai et al. (2021) where their best fed-batch strategy using acidic pretreated corn cob was the addition of low amounts of solids every 5 h; with this strategy 84.4% cellulose conversion was obtained after 96 h with a global solid load of 25% (w/v). On the other hand, Pino et al. (Pino et al., 2019) studied the fed-batch strategy in two feds starting with 20% (w/v) and adding 10% (w/v) at 12 h. They reported a cellulose conversion improvement regarding the batch assay. Also, Gong et al. (2020) mentioned that it is beneficial for the fed-batch process to feed early, as long as there is no interference with the mixture. By early feeding the hydrolysis reaction time can be reduced and there is less risk of enzyme deactivation. Hence, the fed-batch is a good strategy to overcome viscosity, insufficient free water, and mixture problems but feeding points should be carefully considered as it was observed that feeding intervals are a factor that causes a decrease in enzyme efficiency.

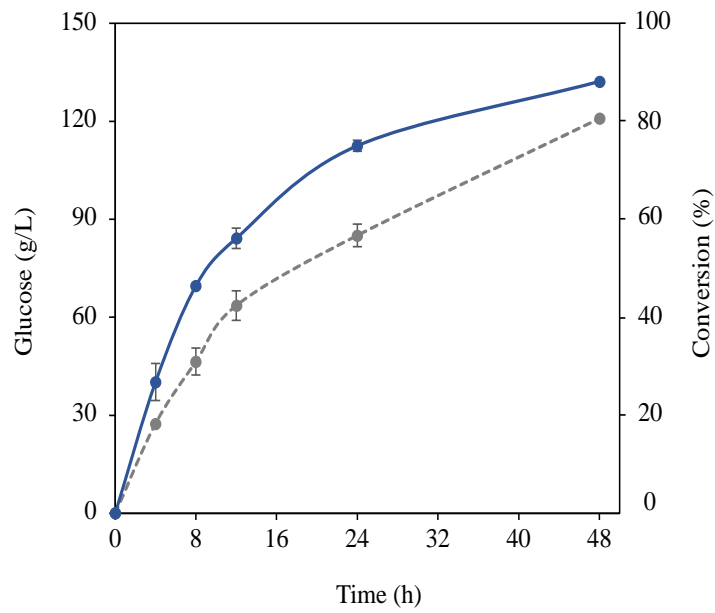


**Figure 4.6.** Fed-batch kinetic in OFR (blue, continued line) and flask (gray, dotted line) using 25% (w/v) hydrothermally pretreated corn cob.

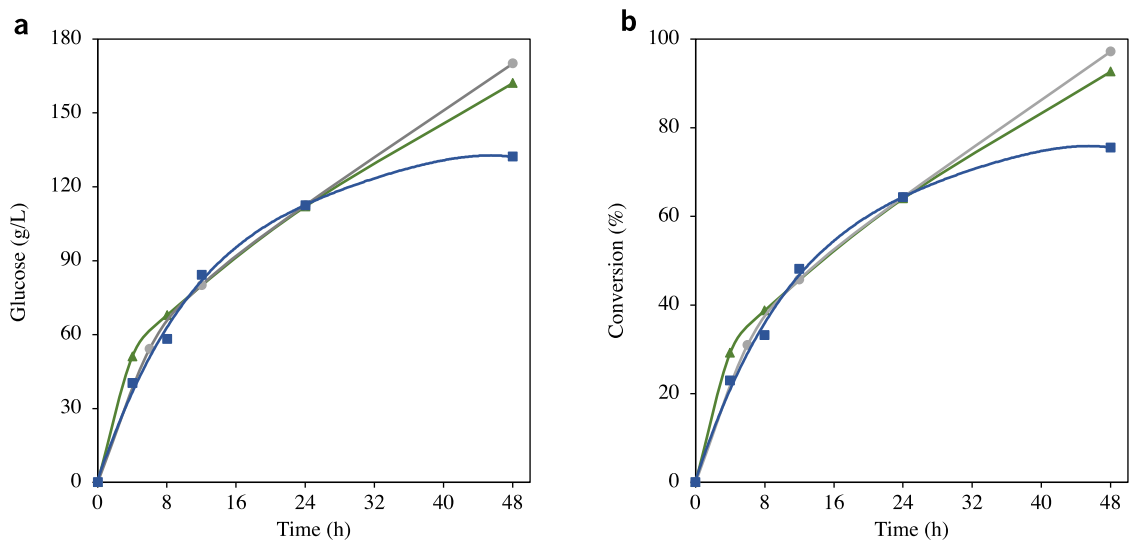


**Figure 4.7.** Glucose production (a) and conversion (b) of HSEH kinetics in OFR by fed batch strategy. FB1 (■ blue), FB2 (● gray), FB3 (▲ green).

#### 4.4 CONCLUSIONS

With this study, OFR applications were broadened and the operating parameters of OFR that influence HSEH were evaluated. It was validated that both frequency and amplitude have an effect on the process and that OFR can achieve an efficient mixture in complex rheological conditions. Moreover, the fed-batch strategy in OFR for high solids loading and low enzyme addition showed promising results



by improving the overall reaction yield. Further investigations in macroscopic mass and heat transfer, scale-up, and energy consumption should be conducted for OFR performance using lignocellulosic substrate at high solid loading.

#### 4.5 REFERENCES

- Abbott, M.S.R., Valente Perez, G., Harvey, A.P., Theodorou, M.K., 2014. Reduced power consumption compared to a traditional stirred tank reactor (STR) for enzymatic saccharification of alpha-cellulose using oscillatory baffled reactor (OBR) technology. *Chem. Eng. Res. Des.* 92, 1969–1975. <https://doi.org/10.1016/j.cherd.2014.01.020>
- Afedzi, A.E.K., Rattanaporn, K., Parakulsuksatid, P., 2022. Impeller selection for mixing high-solids lignocellulosic biomass in stirred tank bioreactor for ethanol production. *Bioresour. Technol. Reports* 17, 100935. <https://doi.org/10.1016/j.biteb.2021.100935>
- Ahmed, S.M.R., Phan, A.N., Harvey, A.P., 2017. Scale-up of oscillatory helical baffled reactors based on residence time distribution. *Chem. Eng. Technol.* 40, 907–914. <https://doi.org/10.1002/ceat.201600480>
- Alias, N.H., Abd-Aziz, S., Phang, L.Y., Ibrahim, M.F., 2021. Enzymatic saccharification with sequential-substrate feeding and sequential-enzymes loading to enhance fermentable sugar production from sago hampas. *Processes* 9. <https://doi.org/10.3390/pr9030535>
- Anukam, A.I., Goso, B.P., Okoh, O.O., Mamphweli, S.N., 2017. Studies on characterization of corn cob for application in a gasification process for energy production. *J. Chem.* 2017, 6478389. <https://doi.org/10.1155/2017/6478389>
- Baptista, S.L., Costa, C.E., Cunha, J.T., Soares, P.O., Domingues, L., 2021. Metabolic engineering of *Saccharomyces cerevisiae* for the production of top value chemicals from biorefinery carbohydrates. *Biotechnol. Adv.* 47, 107697. <https://doi.org/10.1016/j.biotechadv.2021.107697>
- Battista, F., Gomez Almendros, M., Rousset, R., Boivineau, S., Bouillon, P.A., 2018. Enzymatic hydrolysis at high dry matter content: The influence of the substrates' physical properties and of loading strategies on mixing and energetic consumption. *Bioresour. Technol.* 250, 191–196. <https://doi.org/10.1016/j.biortech.2017.11.049>
- Battista, F., Gomez Almendros, M., Rousset, R., Bouillon, P.A., 2019. Enzymatic hydrolysis at high lignocellulosic content: Optimization of the mixing system geometry and of a fed-batch strategy to increase glucose concentration. *Renew. Energy* 131, 152–158. <https://doi.org/10.1016/j.renene.2018.07.038>
- Bianchi, P., Williams, J.D., Kappe, C.O., 2020. Oscillatory flow reactors for synthetic chemistry applications. *J. Flow Chem.* 10, 475–490. <https://doi.org/10.1007/s41981-020-00105-6>
- Buchmaier, J., Brunner, C., Griesbacher, U., Phan, A., Harvey, A., Krishna Gudimanchi, R., Nidetzky, B., Muster, B., 2019. Oscillatory flow bioreactor (OFB) applied in enzymatic hydrolysis at high solid loadings. *Chem. Biochem. Eng. Q.* 33, 459–470.

- Cai, X., Hu, C.H., Wang, J., Zeng, X.H., Luo, J.X., Li, M., Liu, Z.Q., Zheng, Y.G., 2021. Efficient high-solids enzymatic hydrolysis of corncobs by an acidic pretreatment and a fed-batch feeding mode. *Bioresour. Technol.* 326, 124768. <https://doi.org/10.1016/j.biortech.2021.124768>
- Caspeta, L., Caro-Bermúdez, M.A., Ponce-Noyola, T., Martinez, A., 2014. Enzymatic hydrolysis at high-solids loadings for the conversion of agave bagasse to fuel ethanol. *Appl. Energy* 113, 277–286. <https://doi.org/10.1016/j.apenergy.2013.07.036>
- Castro, F., Ferreira, A., Teixeira, J.A., Rocha, F., 2016. Protein crystallization as a process step in a novel meso oscillatory flow reactor: study of lysozyme phase behavior. *Cryst. Growth Des.* 16, 3748–3755. <https://doi.org/10.1021/acs.cgd.6b00262>
- Cruz, P.C., Silva, C.R., Rocha, F.A., Ferreira, A.M., 2021. Mixing performance of planar oscillatory flow reactors with liquid solutions and solid suspensions. *Ind. Eng. Chem. Res.* 60, 2663–2676. <https://doi.org/10.1021/acs.iecr.0c04991>
- Cunha, J.T., Romani, A., Inokuma, K., Johansson, B., Hasunuma, T., Kondo, A., Domingues, L., 2020a. Consolidated bioprocessing of corn cob-derived hemicellulose: engineered industrial *Saccharomyces cerevisiae* as efficient whole cell biocatalysts. *Biotechnol. Biofuels* 13, 1–15. <https://doi.org/10.1186/s13068-020-01780-2>
- Cunha, J.T., Soares, P.O., Baptista, S.L., Costa, C.E., Domingues, L., 2020b. Engineered *Saccharomyces cerevisiae* for lignocellulosic valorization: a review and perspectives on bioethanol production. *Bioengineered* 11, 883–903. <https://doi.org/10.1080/21655979.2020.1801178>
- Da Silva, A.S.A., Espinheira, R.P., Teixeira, R.S.S., De Souza, M.F., Ferreira-Leitão, V., Bon, E.P.S., 2020. Constraints and advances in high-solids enzymatic hydrolysis of lignocellulosic biomass: A critical review. *Biotechnol. Biofuels* 13, 1–28. <https://doi.org/10.1186/s13068-020-01697-w>
- Debrouwer, W., Kimpe, W., Dangreau, R., Huvaere, K., Gemoets, H.P.L., Mottaghi, M., Kuhn, S., Van Aken, K., 2020. Ir/Ni Photoredox dual catalysis with heterogeneous base enabled by an oscillatory plug flow photoreactor. *Org. Process Res. Dev.* 24, 2319–2325. <https://doi.org/10.1021/acs.oprd.0c00150>
- dos Santos, A.C., Ximenes, E., Kim, Y., Ladisch, M.R., 2019. Lignin–enzyme interactions in the hydrolysis of lignocellulosic biomass. *Trends Biotechnol.* 37, 518–531. <https://doi.org/10.1016/j.tibtech.2018.10.010>
- Du, J., Cao, Y., Liu, G., Zhao, J., Li, X., Qu, Y., 2017. Identifying and overcoming the effect of mass transfer limitation on decreased yield in enzymatic hydrolysis of lignocellulose at high solid concentrations. *Bioresour. Technol.* 229, 88–95. <https://doi.org/10.1016/j.biortech.2017.01.011>
- Du, J., Zhang, F., Li, Y., Zhang, H., Liang, J., Zheng, H., Huang, H., 2014. Enzymatic liquefaction and saccharification of pretreated corn stover at high-solids concentrations in a horizontal rotating bioreactor. *Bioprocess Biosyst. Eng.* 37, 173–181. <https://doi.org/10.1007/s00449-013-0983-6>
- Ejim, L.N., Yerdelen, S., McGlone, T., Onyemelukwe, I., Johnston, B., Florence, A.J., Reis, N.M., 2017. A factorial approach to understanding the effect of inner geometry of baffled meso-scale tubes on solids suspension and axial dispersion in continuous, oscillatory liquid–solid plug flows. *Chem. Eng. J.* 308, 669–682. <https://doi.org/10.1016/j.cej.2016.09.013>

- Eze, V.C., Harvey, A.P., 2018. Continuous reactive coupling of glycerol and acetone – A strategy for triglyceride transesterification and in-situ valorisation of glycerol by-product. *Chem. Eng. J.* 347, 41–51. <https://doi.org/10.1016/j.cej.2018.04.078>
- Ferreira, A., Rocha, F., Teixeira, J.A., Vicente, A.A., 2015. Apparatus for mixing based on oscillatory flow reactors provided with smooth periodic constrictions. *WO/2015/056156*.
- Gong, Z., Wang, X., Yuan, W., Wang, Y., Zhou, W., Wang, G., Liu, Y., 2020. Fed-batch enzymatic hydrolysis of alkaline organosolv-pretreated corn stover facilitating high concentrations and yields of fermentable sugars for microbial lipid production. *Biotechnol. Biofuels* 13, 1–15. <https://doi.org/10.1186/s13068-019-1639-9>
- Harvey, A.P., Mackley, M.R., Seliger, T., 2003. Process intensification of biodiesel production using a continuous oscillatory flow reactor. *J. Chem. Technol. Biotechnol.* 78, 338–341. <https://doi.org/10.1002/jctb.782>
- Hwang, Y.J., Coley, C.W., Abolhasani, M., Marzinzik, A.L., Koch, G., Spanka, C., Lehmann, H., Jensen, K.F., 2017. A segmented flow platform for on-demand medicinal chemistry and compound synthesis in oscillating droplets. *Chem. Commun.* 53, 6649–6652. <https://doi.org/10.1039/c7cc03584e>
- Ikwebe, J., Harvey, A.P., 2020. Fuel ethanol production from cassava (*Manihot esculenta* Crantz) in an oscillatory baffled reactor. *Biofuels* 11, 451–457. <https://doi.org/10.1080/17597269.2017.1370886>
- Ikwebe, J., Harvey, A.P., 2015. Enzymatic saccharification of cellulose: A study of mixing and agitation in an oscillatory baffled reactor and a stirred tank reactor. *Biofuels* 6, 203–208. <https://doi.org/10.1080/17597269.2015.1078560>
- Jørgensen, H., Vibe-Pedersen, J., Larsen, J., Felby, C., 2007. Liquefaction of lignocellulose at high-solids concentrations. *Biotechnol. Bioeng.* 96, 862–870. <https://doi.org/10.1002/bit.21115>
- Kumar, B., Bhardwaj, N., Agrawal, K., Chaturvedi, V., Verma, P., 2020. Current perspective on pretreatment technologies using lignocellulosic biomass: An emerging biorefinery concept. *Fuel Process. Technol.* 199, 106244. <https://doi.org/10.1016/j.fuproc.2019.106244>
- Kumar, G., Dharmaraja, J., Arvindnarayan, S., Shoban, S., Bakonyi, P., Dattatray Saratale, G., Nemestóthy, N., Bélafi-Bakó, K., Yoon, J.-J., Kim, S.-H., 2019. A comprehensive review on thermochemical, biological, biochemical and hybrid conversion methods of bio-derived lignocellulosic molecules into renewable fuels. *Fuel* 251, 352–367. <https://doi.org/10.1016/j.fuel.2019.04.049>
- Lu, M., He, D., Li, J., Han, L., Xiao, W., 2021. Rheological characterization of ball-milled corn stover with different fragmentation scales at high-solids loading. *Ind. Crops Prod.* 167, 113517. <https://doi.org/10.1016/j.indcrop.2021.113517>
- Ludwig, D., Michael, B., Hirth, T., Rupp, S., Zibek, S., 2014. High solids enzymatic hydrolysis of pretreated lignocellulosic materials with a powerful stirrer concept. *Appl. Biochem. Biotechnol.* 172, 1699–1713. <https://doi.org/10.1007/s12010-013-0607-2>
- Masngut, N., Harvey, A.P., Ikwebe, J., 2010. Potential uses of oscillatory baffled reactors for biofuel production. *Biofuels* 1, 605–619. <https://doi.org/10.4155/bfs.10.38>
- McGlone, T., Briggs, N.E.B., Clark, C.A., Brown, C.J., Sefcik, J., Florence, A.J., 2015. Oscillatory flow reactors (OFRs) for continuous manufacturing and crystallization. *Org. Process Res. Dev.* 19, 1186–1202. <https://doi.org/10.1021/acs.oprd.5b00225>

- Ni, X., Mackley, M.R., Harvey, A.P., Stonestreet, P., Baird, M.H.I., Rama Rao, N. V., 2003. Mixing through oscillations and pulsations -A guide to achieving process enhancements in the chemical and process industries. *Chem. Eng. Res. Des.* 81, 373–383. <https://doi.org/10.1205/02638760360596928>
- Pino, M.S., Rodríguez-Jasso, R.M., Michelin, M., Ruiz, H.A., 2019. Enhancement and modeling of enzymatic hydrolysis on cellulose from agave bagasse hydrothermally pretreated in a horizontal bioreactor. *Carbohydr. Polym.* 211, 349–359. <https://doi.org/10.1016/j.carbpol.2019.01.111>
- Reis, N., Harvey, A.P., Mackley, M.R., Vicente, A.A., Teixeira, J.A., 2005. Fluid mechanics and design aspects of a novel oscillatory flow screening mesoreactor. *Chem. Eng. Res. Des.* 83, 357–371. <https://doi.org/10.1205/cherd.03401>
- Reis, N., Vicente, A.A., Teixeira, J.A., Mackley, M.R., 2004. Residence times and mixing of a novel continuous oscillatory flow screening reactor. *Chem. Eng. Sci.* 59, 4967–4974. <https://doi.org/10.1016/j.ces.2004.09.013>
- Ruiz, H.A., Conrad, M., Sun, S.-N., Sanchez, A., Rocha, G.J.M., Romani, A., Castro, E., Torres, A., Rodríguez-Jasso, R.M., Andrade, L.P., Smirnova, I., Sun, R.-C., Meyer, A.S., 2020. Engineering aspects of hydrothermal pretreatment: From batch to continuous operation, scale-up and pilot reactor under biorefinery concept. *Bioresour. Technol.* 299, 122685. <https://doi.org/10.1016/J.BIORTECH.2019.122685>
- Ruiz, H.A., Galbe, M., Garrote, G., Ramirez-Gutierrez, D.M., Ximenes, E., Sun, S.N., Lachos-Perez, D., Rodríguez-Jasso, R.M., Sun, R.C., Yang, B., Ladisch, M.R., 2021. Severity factor kinetic model as a strategic parameter of hydrothermal processing (steam explosion and liquid hot water) for biomass fractionation under biorefinery concept. *Bioresour. Technol.* 342. <https://doi.org/10.1016/j.biortech.2021.125961>
- Ruiz, H.A., Vicente, A.A., Teixeira, J.A., 2012. Kinetic modeling of enzymatic saccharification using wheat straw pretreated under autohydrolysis and organosolv process. *Ind. Crops Prod.* 36, 100–107. <https://doi.org/10.1016/j.indcrop.2011.08.014>
- Sarker, T.R., Pattnaik, F., Nanda, S., Dalai, A.K., Meda, V., Naik, S., 2021. Hydrothermal pretreatment technologies for lignocellulosic biomass: A review of steam explosion and subcritical water hydrolysis. *Chemosphere* 284, 131372. <https://doi.org/10.1016/j.chemosphere.2021.131372>
- Selig, M., Weiss, N., Ji, Y., 2008. Enzymatic saccharification of lignocellulosic biomass. NERL/TP-510-42629. Natl. Renew. Energy Lab. Golden, CO.
- Sharma, S., Horn, S.J., 2016. Enzymatic saccharification of brown seaweed for production of fermentable sugars. *Bioresour. Technol.* 213, 155–161. <https://doi.org/https://doi.org/10.1016/j.biortech.2016.02.090>
- Shiva, Climent Barba, F., Rodríguez-Jasso, R.M., Sukumaran, R.K., Ruiz, H.A., 2022. High-solids loading processing for an integrated lignocellulosic biorefinery: Effects of transport phenomena and rheology – A review. *Bioresour. Technol.* 127044. <https://doi.org/10.1016/j.biortech.2022.127044>
- Siddiqui, K.S., Ertan, H., Poljak, A., Bridge, W.J., 2022. Evaluating enzymatic productivity—The missing link to enzyme utility. *Int. J. Mol. Sci.* 23, 6908. <https://doi.org/10.3390/ijms23136908>
- Singh, A., Rodríguez Jasso, R.M., Gonzalez-Gloria, K.D., Rosales, M., Belmares Cerda, R., Aguilar, C.N., Singhania, R.R., Ruiz, H.A., 2019. The enzyme biorefinery platform for advanced biofuels

- production. *Bioresour. Technol. Reports* 7, 100257.  
<https://doi.org/10.1016/j.biteb.2019.100257>
- Sluiter, A., Hames, B., Ruiz, R., Scarlata, C., Sluiter, J., Templeton, D., Crocker, D., 2008. Determination of structural carbohydrates and lignin in Biomass - NREL/TP-510-42618. *Lab. Anal. Proced.* 17.
- Stonestreet, P., Harvey, A.P., 2002. A mixing-based design methodology for continuous oscillatory flow reactors. *Chem. Eng. Res. Des.* 80, 31–44. <https://doi.org/10.1205/026387602753393204>
- Sun, Q., Chen, W.J., Pang, B., Sun, Z., Lam, S.S., Sonne, C., Yuan, T.Q., 2021. Ultrastructural change in lignocellulosic biomass during hydrothermal pretreatment. *Bioresour. Technol.* 341, 125807. <https://doi.org/10.1016/j.biortech.2021.125807>
- Zanuso, E., Gomes, D.G., Ruiz, H.A., Teixeira, J.A., Domingues, L., 2021. Enzyme immobilization as a strategy towards efficient and sustainable lignocellulosic biomass conversion into chemicals and biofuels: Current status and perspectives. *Sustain. Energy Fuels* 5, 4233–4247. <https://doi.org/10.1039/d1se00747e>

## **CHAPTER V**

---

Conclusions and future perspectives

## 5.1 CONCLUSIONS

Sugar – glucose – is a simple molecule that serves as the primary substrate to many biological fermentation processes that, in lignocellulosic biorefineries, could produce a broad of products at both, large volume, as liquid transportation fuels, and low volume but high-value compounds as specific chemicals. Biorefineries are the direction we must follow to use renewable carbon and get away from petrol-derived products. Bioprocess engineering research is essential to support biorefineries. The aim of this thesis was to contribute to sustainable biomass processing, namely, the enzymatic hydrolysis of lignocellulosic biomass via strategies such as enzyme immobilization and bioreactor operations. Under this scope, several subjects were explored, analyzed, and studied following the biorefinery concept. This chapter addresses the summary of the main conclusions from the work presented.

Although countless advances in cellulase production and research to reduce costs and improve bioprocesses, as of today, cellulases are still generally expensive, affecting the economics of the biorefinery process. Other than being expensive, cellulases, are highly sensitive and prone to be affected by factors such as inhibition and denaturation. Enzyme immobilization was studied as a strategy to reduce the enzyme loading in the enzymatic hydrolysis process. The magnetic properties of  $\text{Fe}_3\text{O}_4$  nanoparticles made this support attractive for easy enzyme reuse by applying an external magnetic field. By coating  $\text{Fe}_3\text{O}_4$  nanoparticles with chitosan, functional groups were provided to the support that attained an immobilized biocatalyst load of  $65 \text{ mg}_{\text{protein}}/\text{g}_{\text{support}}$ . Before testing the immobilized cellulase, it was important to corroborate the immobilization by techniques such as microscopy and FTIR-ATR. The successfully immobilized cellulase maintained 43% of its initial activity after 13 reusing cycles using carboxymethyl cellulose as substrate. This proved that the enzyme was capable to re-start the hydrolysis when the fresh substrate was added. Also, the 13 reusing cycles represented an 8.2-fold glucose production than when the enzyme was not reused. The analysis of the immobilized cellulase cocktail using 5% (w/v) of hydrothermally pretreated corn cob resulted in a saccharification yield of 64% after 120 h, confirming that the immobilized enzyme was active with real substrate. Recognizing the need to use high solid loading, it must be highlighted that the used value of 5% (w/v) of pretreated corn cob is among the highest loading reported in the literature regarding immobilized cellulase.

Given the complexity of enzymatic hydrolysis, bioprocess engineering plays an important role in the equipment development and products manufacturing. An alternative strategy to assess the enzymatic hydrolysis was tackled by exploring the oscillatory flow reactor (OFR) as strategic bioreactor configuration. Oscillatory flow reactor is known to improve mass and heat transfer (major parameters that affect the

enzymatic hydrolysis). However, an added challenge was imposed as nowadays it is imperative to work at high solid loadings in order to achieve higher sugar concentrations, reduce operational cycles, and decrease water consumption. Moreover, regarding bioethanol production, glucose concentrations above ~80 g/L are recommended to achieve ethanol titers higher than 4% (w/v) through microbial fermentation which is considered to benefit distillation by diminishing the energy demand (Raj et al., 2022). By taking all into account, the OFR batch operation assessment achieved a maximum solid loading of 18% (w/v) attaining 81% cellulose-to-glucose conversion in 20 h at low enzyme dosage using hydrothermally pretreated corn cob representing a glucose concentration of 100 g/L. Both amplitude and frequency have a positive effect on the process, the highest conditions tested of amplitude (6 mm) and frequency (4 Hz) tested allowed the highest value of productivity of 5.03 g/(L·h), between 24-34% higher than the other conditions tested. Then, by adopting the fed batch strategy into the OFR, a maximum solid loading of 25% (w/v) was achieved reaching saccharification yields of 97% after 48 h. These results are highly positive as they expand the application horizon of OFR and demonstrate the feasibility of high solid loadings operation in alternative reactor configurations.

## 5.2 FUTURE PERSPECTIVES

Based on the results obtained in this work, some considerations to improve and ideas of further steps are mentioned next. Even though enzyme immobilization has been widely studied, there are still areas to explore and research on the biorefinery concept. The cellulase immobilization should be characterized and tested under the paradigm of second-generation biorefinery. For example, the immobilized enzyme tolerance should be tested against compounds derived from the pretreatment of lignocellulosic biomass that are known to be inhibitors of cellulase such as xylooligomers, lignin compounds, acetic acid, and glucose (Haven and Jørgensen, 2013; Qi et al., 2018; Qing et al., 2010; Ruiz et al., 2012). Also, optimized ratios to combine immobilized and free enzymes in order to compensate for the loss in activity when reusing the immobilized enzyme could decrease the enzyme input throughout the process. Likewise, improvements on the enzyme binding onto magnetic nanoparticles can be considered as future work using technologies such as protein-engineering functional materials employing tag mediated protein immobilization strategies (Freitas et al., 2022). From an operational point of view, studies in bioreactor design can optimize the magnetic field used to recover the immobilized enzyme and enhance reusability as the development of a reactor coupled with a controlled magnetic system (Al-Qodah et al., 2015).



Regarding the second enzymatic hydrolysis strategy approached in this work, the oscillatory flow reactor opens a vast research area when carrying out enzymatic saccharification of lignocellulosic biomass. For instance, the use of other lignocellulosic materials should be tested to gather information about the performance of the OFR in different rheological circumstances. From a process engineering orientation, improvements on the reactor design in terms of process control and real time monitoring can boost the application of OFR in bioprocesses as enzymatic hydrolysis, bioconversion/fermentation, and continuous operations (Furlong et al., 2020). For example, a future perspective is the possibility to use OFR in fermentation processes where agitation and aeration plays an important role on the microorganism performance, thus OFR could provide specific mixture conditions along the process (Costa et al., 2022). Additionally in high solid loadings enzymatic hydrolysis, by accurately monitoring the reaction progress, for example by measuring the decrease in viscosity throughout time, the optimum fed-time can be predicted facilitating the solid loadings. From a long-term standpoint and taking the advantage that the OFR scale-up is considered to be straightforward, the reactor design could be optimized for this complex process using simulation tools and computational fluid dynamics (Gaona et al., 2021) To conclude, economic and energetic efficiency analyses should take place for the application of OFR in biorefineries industries to attain the optimized conversion yield at the minimum energy consumption (Ahmed et al., 2017; Shiva et al., 2022).

To conclude, there is still plenty of research areas to discover and question in order to achieve a biobased economy and accomplish the must needed detachment from fossil fuels in the near future. Through this work, alternative enzymatic hydrolysis strategies were explored to bring knowledge, awareness, and open key points for possible future research.

### 5.3 REFERENCES

- Ahmed, S.M.R., Phan, A.N., Harvey, A.P., 2017. Scale-up of oscillatory helical baffled reactors based on residence time distribution. *Chem. Eng. Technol.* 40, 907–914. <https://doi.org/10.1002/ceat.201600480>
- Al-Qodah, Z., Al-Shannag, M., Assirey, E., Orfali, W., Bani-Melhem, K., Alananbeh, K., Bouquellah, N., 2015. Characteristics of a novel low density cell-immobilized magnetic supports in liquid magnetically stabilized beds. *Biochem. Eng. J.* 97, 40–49. <https://doi.org/10.1016/j.bej.2015.01.004>
- Costa, C.E., Romani, A., Teixeira, J.A., Domingues, L., 2022. Resveratrol production for the valorisation of lactose-rich wastes by engineered industrial *Saccharomyces cerevisiae*. *Bioresour. Technol.* 359, 127463. <https://doi.org/10.1016/j.biortech.2022.127463>

- Freitas, A.I., Domingues, L., Aguiar, T.Q., 2022. Tag-mediated single-step purification and immobilization of recombinant proteins toward protein-engineered advanced materials. *J. Adv. Res.* 36, 249–264. <https://doi.org/10.1016/j.jare.2021.06.010>
- Furlong, V.B., Corrêa, L.J., Lima, F. V., Giordano, R.C., Ribeiro, M.P.A., 2020. Estimation of biomass enzymatic hydrolysis state in stirred tank reactor through moving horizon algorithms with fixed and dynamic fuzzy weights. *Processes* 8. <https://doi.org/10.3390/PR8040407>
- Gaona, A., Lawryshyn Y., Saville, B.A., 2021. High-solids enzymatic hydrolysis of biomass: Hydrodynamics and reaction kinetics integration via numerical modeling. *Phys. Fluids* 33, 037107. <https://doi.org/10.1063/5.0036138>
- Haven, M.Ø., Jørgensen, H., 2013. Adsorption of  $\beta$ -glucosidases in two commercial preparations onto pretreated biomass and lignin. *Biotechnol. Biofuels* 6, 1–14. <https://doi.org/10.1186/1754-6834-6-165>
- Qi, B., Luo, J., Wan, Y., 2018. Immobilization of cellulase on a core-shell structured metal-organic framework composites: Better inhibitors tolerance and easier recycling. *Bioresour. Technol.* 268, 577–582. <https://doi.org/10.1016/j.biortech.2018.07.115>
- Qing, Q., Yang, B., Wyman, C.E., 2010. Xylooligomers are strong inhibitors of cellulose hydrolysis by enzymes. *Bioresour. Technol.* 101, 9624–9630. <https://doi.org/10.1016/j.biortech.2010.06.137>
- Raj, T., Chandrasekhar, K., Kumar, A.N., Banu, J.R., Yoon, J-J., Bhatia, S.K., Yang, Y-H., Varjani, S., Kim, S-H., 2022. Recent advances in commercial biorefineries for lignocellulosic ethanol production: Current status, challenges and future perspectives. *Bioresour. Technol.* 334, 126292. <https://doi.org/10.1016/j.biortech.2021.126292>
- Ruiz, H.A., Vicente, A.A., Teixeira, J.A., 2012. Kinetic modeling of enzymatic saccharification using wheat straw pretreated under autohydrolysis and organosolv process. *Ind. Crops Prod.* 36, 100–107. <https://doi.org/10.1016/j.indcrop.2011.08.014>
- Shiva, Rodríguez-Jasso, R.M., Rosero-Chasoy, G., López-Sandin, I., Morais, A.R.C., Ruiz, H.A., 2022. Enzymatic hydrolysis, kinetic modeling of hemicellulose fraction, and energy efficiency of autohydrolysis pretreatment using agave bagasse. *BioEnergy Res.* <https://doi.org/10.1007/s12155-022-10442-0>